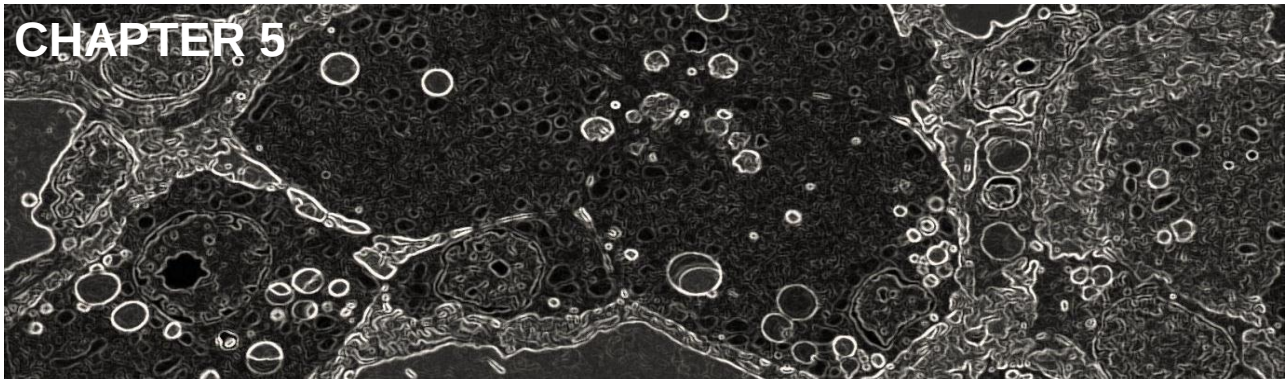

TRANSMISSION ELECTRON MICROSCOPY OF THE LIVER

5.1 INTRODUCTION

In addition to textbooks, for example, Ross *et al.* (2003), that discuss the electron microscopy of the human liver, its ultrastructure is also dealt with in great depth by Phillips *et al.* (1987) as well as by Goldblatt & Gunning in a brief review in 1984. The fine structure of the liver of other mammalian species is covered extensively in the literature (Wisse & Knook 1977; De Leeuw *et al.* 1990; McCuskey & McCuskey 1990; Van Bezooijen 1990; Baratta *et al.* 2009). Some publications compare the electron microscopical aspects of liver cells of various species, including reptiles (Beresford & Henninger 1986; Kalashnikova 1996; Schaffner 1998). The liver of the Nile crocodile was not specifically investigated by these authors. Goldblatt *et al.* (1987) and Henninger (1982) gave short descriptions of the ultrastructure of the newt liver and the box turtle respectively. The West African crocodile *Osteolaemus tetraspis* liver was explored ultrastructurally by Storch *et al.* in 1989. There is an obvious paucity of literature dealing with the ultrastructure of the crocodilian liver and the present study will therefore rely on the descriptions in other vertebrates for evaluation.

5.2 MATERIALS AND METHODS

After removal of the liver from the body cavity the portal vein was connected to a perfusion apparatus (Chapter 4, Fig. 4.3) and perfused with a 0.5% heparin sodium (5000 IU/ml) saline solution, using the peristaltic pump at 80 ml/min, to remove the blood from the sinusoids. The heparin solution was replaced with 2.5% glutaraldehyde in Millonig's buffer (pH 7.4, 0.13 M) and perfused for approximately 20 minutes until a pale discoloration of the liver tissue indicated successful perfusion (Chapter 4, Fig. 4.4).

Small samples taken in parallel to the histology tissue blocks (namely 9 areas/liver lobe, 5 right liver lobes) were diced into 1mm^3 tissue blocks and immersion-fixed in 2.5% glutaraldehyde in Millonig's phosphate buffer (pH 7.2) for at least 24 hours. The tissue blocks were then rinsed in Millonig's buffer, post-fixed in 1% osmium tetroxide in the same buffer for a minimum of one hour, rinsed again and dehydrated through a series of graded ethanols before infiltrating with propylene oxide and epoxy resin (TAAB 812 resin, TAAB Laboratories, England) (Bozzola & Russell 1992). The isthmus tissue failed to perfuse in areas and a cross-sectional tissue block (n=5) of this area was therefore also immersion-fixed in 10% acqueous buffered formalin and fixed for a minimum of 24 hours before dissecting into smaller blocks and processing into epoxy resin.

Toluidine blue stained (Hayat 2000) 0.35 micron semi-thin resin sections (n=66) were assessed light microscopically for the selection of optimally perfused areas (sinusoids not disrupted or collapsed) for ultrastructural examination. Ultra-thin (50-90 nm) sections (Reichert-Jung Ultramicrotome) were collected onto copper grids (n=132) and stained with Reynold's lead citrate and an acqueous saturated solution of uranyl acetate (Hayat 2000).

5.3 IMAGE CAPTURING & PROCESSING

The ultrastructure of the resident liver cells with their organelles, bile canaliculi, sinusoidal spaces and connective tissue in 80 grids were examined with a Philips CM 10 transmission electron microscope (FEI, Eindhoven, Netherlands) operated at 80 kV. A Megaview III side-mounted digital camera was used to capture the images and iTEM software (Olympus Soft Imaging System GMBH) to adjust the brightness and contrast.

5.4 RESULTS

The ultrastructural findings in the liver of the juvenile Nile crocodile reflected the light microscopy results (Chapter 4): a parenchyma with hepatocytes, and non-parenchymal cells, namely endothelial, Kupffer and stellate cells, with a connective stromal component, were present. Blood cells, for example, pit cells, lymphocytes, plasma cells, eosinophils and thrombocytes were seen. The isthmus contained the same components as the liver tissue proper.

5.4.1 Parenchyma

Hepatocytes

Hepatocytes were arranged in the form of tubular cell cords. In transverse section the cords were composed of approximately five hepatocytes arranged around a bile canaliculus (Fig. 5.1) while in longitudinal section they appeared as a two-cell-thick plate between which the bile canaliculus was sometimes observed. The four individual cell sides of a hepatocyte as seen in both the transverse and longitudinal sections were in contact basally with a sinusoidal wall, laterally with two adjacent hepatocytes and apically with a bile canaliculus. The hepatocyte surface facing the sinusoid was lined by microvilli that presented in the space of Disse - the hepatocytes were therefore not in direct contact with the sinusoidal wall. The cross-sectional tubular cell arrangement showed hepatocytes converging to form a central bile canaliculus (Fig. 5.1). In this instance the hepatocyte side facing the sinusoid was dome-shaped. Pinocytotic vesicles between the microvilli were apparent (Fig. 5.2). The lateral cell membranes of the hepatocytes, a distance away from the canaliculi, sometimes exhibited occasional desmosomes (Fig. 5.4) and microvilli. The basal lamina surrounding groups of hepatocytes, as demonstrated with the PAS-D reaction (Chapter 4), was absent ultrastructurally. A basal lamina was however found lining the hepatocytes on the side directly adjacent to Glisson's capsule (Fig. 5.3).

Nucleus – Generally one, round, eccentrically placed nucleus was present close to the sinusoidal lumen (Fig. 5.1). Occasional bi-nucleated cells were found (Fig. 5.6). Heterochromatin masses were displayed throughout the nucleus as well as forming a definite rim along the nuclear envelope. The nucleus was enclosed by a typical double membraned nuclear envelope. Prominent nucleoli (Fig. 5.5), mostly one per nucleus, were seen. The nucleoli were large with no limiting membrane and were mostly positioned off-centre in the nuclei. They had rough edges and some displayed a combination of electron-dense and lightly contrasted material occasionally surrounding an open space. No nuclear inclusions were noted.

Endoplasmic Reticulum – The granular endoplasmic reticulum (GER) presented as matching membrane pairs dotted with ribosomes and was present between the other cytoplasmic constituents. GER membranes also appeared in parallel with the lateral plasma membranes and often surrounded mitochondria (Fig. 5.7). Nude membraned

vesicles (i.e. without ribosomes) representing smooth endoplasmic reticulum (SER) were also found in the cytoplasm.

Mitochondria – Several mitochondria surrounded by a double membrane, with the inner membrane forming the cristae, were seen in the hepatocytes. The mitochondrial matrix contained electron-dense granules (Figs. 5.7 & 5.8). There was a polar orientation of the mitochondria in some hepatocytes with most of the mitochondria converging towards the bile canaliculi.

Peroxisomes – A few scattered, spherical, single-membrane-bound peroxisomes with amorphous contents of medium electron density were seen (Fig. 5.8). These organelles were indistinct and smaller than mitochondria and a nucleoid or marginal plate could not be identified.

Lysosomes – Lysosomes limited by a single membrane were present in the cytoplasm, mostly at the peribiliary pole of the hepatocytes. The lysosomes contained hemosiderin granules (Fig. 5.9) and slit-like spaces indicating the presence of cholesterol esters (Fig. 5.10).

Golgi – The accepted description of this organelle as parallel, curved, flattened saccules of cisternae with bulbous ends applied to the Golgi apparatus (Fig. 5.14). This structure was frequently found in the pericanalicular cytoplasm.

Cytoskeleton – Microtubules and microfilaments (Fig. 5.14) were seen in the cytoplasm.

Glycogen – Monoparticulate glycogen particles (beta or single glycogen particles) and glycogen rosettes (alpha or clusters of electron dense monoparticulate glycogen particles) (Fig. 5.8) were abundant throughout the cytosol except in areas where lipid droplets and lysosomes dominated.

Lipid – Variable numbers of lipid droplets that varied in size (Fig. 5.1) were present and were concentrated at the sinusoidal pole in some hepatocytes. The lipid droplets were virtually electron-lucent and not surrounded by a membrane.

Centrioles – These structures were seen at the pericanalicular pole in a few hepatocytes (Fig. 5.13).

Pigments - Loose lying cytoplasmic melanin granules were occasionally seen (Fig. 5.11). Prominent membranous concretions with morphological features typical of bile pigment were also noticed (Fig. 5.12).

Other inclusions - Cytoplasmic electron opaque slit-like areas (Fig. 5.10), indicating cholesterol esters, were found near the bile canaliculi.

Due to their position in relation to the hepatocytes the **bile canaliculi** will be discussed under this heading. In transverse section they appeared as small spaces forming a 'lumen' lined by hepatocyte plasma membranes displaying scanty microvilli protruding into the space (Fig. 5.13). Longitudinal sections of cords of hepatocytes showed elongated bile canaliculi (Fig. 5.15). Junctional complexes between neighbouring hepatocytes sealed off the canalicular spaces (Fig. 5.14).

5.4.2 Non-parenchymal Component

The angular **sinusoids** (Figs. 5.16 & 5.17) found between groups of hepatocytes were lined by endothelial cells. Kupffer cells could sometimes be found lining the spaces and stellate cells were resident in the subendothelial tissue. A few blood cells also occupied the sinusoidal lumen. No basal lamina was seen around the sinusoids, but the space of Disse (Fig. 5.18) containing the basal microvilli of the hepatocytes was present between the endothelial cells and groups of hepatocytes. Normal collagen fibrils and long-spacing collagen fibrils were noted in the space of Disse (Figs. 5.20 & 5.21).

Endothelial cells

Lining the sinusoids were flat endothelial cells with thin nuclei and long cytoplasmic extensions (Figs. 5.16 & 5.17). Very active endothelial cells were more bulky in appearance. This lining was sometimes interrupted by Kupffer cell cytoplasmic protrusions or Kupffer cells forming part of the lining (Figs. 5.17 & 5.31). Fenestrated cytoplasmic extensions and gaps between neighbouring endothelial cells were seen (Fig. 5.18). Overlapping cell extensions with tight junctions were noticed in a few instances (Fig. 5.19). The endothelial cell nuclei sometimes nestled in the recess between neighbouring hepatocyte groups (Fig. 5.22) and nucleoli were present. The endothelial cell cytoplasm was packed with pinocytotic vesicles that included bristle-coated pinocytotic vesicles. The

formation of invaginations of the cell membrane that close and break off to form pinocytotic vesicles in the cytoplasm were evident (Fig. 5.23). Many prominent lysosomes with electron-dense contents (Figs. 5.20 & 5.21), a few mitochondria and inconspicuous strands of GER were also observed in the cytoplasm.

Kupffer cells

The Kupffer cells were large pleomorphic pigmented cells that formed part of the sinusoidal lining (Fig. 5.17 & 5.31), but also protruded into the sinusoidal lumen (Figs. 5.24 & 5.25), sometimes spanning the lumen (Fig. 5.36). They often inserted between hepatocyte groups forming bridges between adjacent sinusoids or were located in the space of Disse (Fig. 5.26 & 5.27) and were also frequently noted as part of the hepatocyte cell cords (Figs. 5.28 & 5.29). The Kupffer cells themselves did not form groups, but were seen as isolated cells in the areas mentioned. Their surfaces were irregular due to the presence of filipodia and lamellapodia. No junctions were present between Kupffer and endothelial cells, but close contact and penetration through fenestrae were seen in some instances (Figs. 5.25 & 5.30). Kupffer cells were also seen interacting with pit cells (Fig. 5.62) and were found close to some hepatic stellate cells in Disse's space (Fig. 5.27). Kupffer cell nuclei were irregular, conforming to the very large phagosomes and inclusions by having indentations and being pushed to an eccentric position in the cytoplasm (Figs. 5.28 & 5.29).

Clusters of melanin granules admixed with an electron-dense fine granular component (hemosiderin) and other electron-lucent fragments (ceroid) were found in large phagosomes (Figs. 5.32 & 5.33). Melanin granules were also present in the sinusoidal luminal Kupffer cells (Fig. 5.31). Typical lipofuscin granules consisting of an electron-dense component mixed with lipid were absent from these compound inclusions. Engulfment of apoptotic or dying white blood cells, red blood cells, thrombocytes and cellular debris was evident (Figs. 5.34, 5.35 & 5.36).

Conspicuous cytoplasmic organelles that consisted of elongated, parallel tubular structures (Fig. 5.26) bound by a single membrane and containing electron-dense filamentous or crystalline material (depending on the sectioning plane) were seen (Fig. 5.39 to Fig. 5.42). For the purpose of the present study this structure will be called 'tubulosomes'. There was a clear zone visible between the filamentous or crystalline

interiors and the limiting membranes. The tubulosomes were usually grouped together displaying longitudinal, transverse or oblique profiles, but were also sometimes separated into smaller groups around phagosomes (Fig. 5.37). They were occasionally found close to mitochondria where they seemed to originate from the mitochondria (Fig. 5.38). In cross sections of the tubulosomes the contents displayed circular, angular and divided contours (Figs. 5.39, 5.40, 5.41 & 5.42). The width of the tubulosomes varied from 77 nm to 192 nm with the longest one being observed measuring 6.5 µm. A few appeared curved. The tubulosomes were also present in the pigmented cells forming part of the hepatocyte groups.

Scanty cytoplasmic lipid droplets (Fig. 5.25) were observed and mitochondria (some with dilated cristae), Golgi, GER, SER and microtubules were also present throughout the cytoplasm.

Stellate cells

Stellate cells with long cytoplasmic extensions were seen lying in the space of Disse (Figs. 5.43 & 5.44). They were in close contact with endothelial cells, Kupffer cells and hepatocytes, sometimes touching the endothelial cells (Fig. 5.46). Usually one or two prominent, non-membrane bound lipid droplets were present that often indented the nucleus giving it an angular shape (Figs. 5.45 & 5.46). Cytoplasmic filaments, microtubules, coated and pinocytotic vesicles were observed (Figs. 5.47 & 5.48). Pairs of centrioles were often noted with some forming ciliary basal bodies (Fig. 5.49). The cytoplasm also contained a few small mitochondria, insignificant GER, Golgi, glycogen and sparse mulltivesicular bodies (Fig. 5.47). A cytoplasmic structure with the periodicity of long-spacing collagen (Fig. 5.48), similar to that found in Disse's space, was seen. Collagen fibrils and long-spacing collagen fibrils were also found in close association with the cytoplasm.

Other cells, also with subendothelial extensions and occupying the same position as stellate cells, exhibited myofibroblastic features (Figs. 5.50 & 5.51). They contained filaments forming subplasmalemmal densities (Figs. 5.54 & 5.55) and a few cells also displayed dilated granular endoplasmic reticulum (Fig. 5.56). Pinocytotic vesicles and microtubules were evident (Figs. 5.54 & 5.55). No lipid droplets were seen in these cells.

Stellate cells and myofibroblastic cells were often found occupying the same recess (Fig. 5.51) with the latter also touching the endothelial and Kupffer cells (Figs. 5.52 & 5.53).

Blood cells

Pit cells

A few cells known as pit cells, resembling a larger version of lymphocytes in shape and the presence of pseudopodia, were seen in the sinusoids (Fig. 5.57). They contained many small membrane-bound electron dense granules (Figs. 5.57 & 5.58) of approximately the same size (0.11-0.18 µm) and electron-density. They also exhibited an indented eccentric nucleus (Fig. 5.57) and a few larger membrane-bound clear vesicles (>0.2 µm) (Fig. 5.60) that sometimes contained electron-dense material (Fig. 5.58). Cytoplasmic collections of intermediate filaments (Fig. 5.59), as well as mitochondria, Golgi, a few multivesicular bodies (Fig. 5.60), single endocytotic vesicles and lipid droplets (Fig. 5.60) were present. They were often located in close contact with endothelial and Kupffer cells (Figs. 5.61 & 5.62).

Other blood cells

Typical plasma cells, thrombocytes, lymphocytes and eosinophils (Figs. 5.63, 5.64 & 5.65) were present in the sinusoidal spaces.

Intercalated cells

A few cells (Figs. 5.66 & 5.67), resembling lymphocytes, with an electron-lucent cytoplasm and sparse organelles (mainly mitochondria) were seen in the space of Disse and occasionally between hepatocytes.

5.4.3 Connective Tissue Stroma

Glisson's capsule consisted of an outer mesothelial lining supported by a thick collagenous layer that contained fibroblasts (Fig. 5.68). Prominent **fibrous trabeculae** (Fig. 5.69) were unmistakable between the hepatocyte groups, as was a collagenous framework around the portal triads containing fibroblasts. The black reticular fibres, demonstrated by light microscopy (Gordon & Sweets' stain, Chapter 4), appeared in the

space of Disse as sparse threads with a wider periodicity (Figs. 5.70 & 5.71) than normal collagen fibrils.

Nerves

Intrahepatic **nerves** were rare (Figs. 5.72 & 5.73) and consisted of unmyelinated axons enclosed in a basal lamina. Neurosecretory granules, mitochondria, lysosomes and microtubules were observed.

Portal tract

The portal triad consisted of branches of a **portal vein**, **hepatic artery** and **bile duct** (Figs. 5.74 & 5.75). **Lymphatic** vessels sometimes accompanied the triads. The structure of the blood and lymphatic vessels were generic. Cuboidal biliary cells with basal nuclei lined the bile ducts that were surrounded by a continuous basal lamina (Figs. 5.76 & 5.78). Apart from the usual cytoplasmic organelles, prominent intermediate filaments (Fig. 5.80) and interdigitations between the lateral membranes (Fig. 5.78) were noted. Concretions of bile pigment were demonstrated in certain biliary cells (Fig. 5.79). Apical surfaces presented with junctional complexes between neighbouring cells and projected microvilli and cilia into the ductal lumen (Fig. 5.77). Macrophages, lymphocytes, plasma cells and fibroblasts resided in the supporting collagenous framework. Collections of lymphocytes were occasionally seen in the portal areas (Figs. 5.81 & 5.82).

5.4.4 Isthmus

The ultrastructural make-up of the isthmus revealed the same elements found in the liver tissue proper. Despite the difficulty to discern the different components in areas due to incomplete perfusion fixation, the tubular nature of the hepatocyte groups interspersed by sinusoidal spaces could still be recognised (Fig. 5.83). The fine structure of the hepatocytes, endothelial cells, Kupffer cells, stellate cells, myofibroblastic blood cells, portal triads and collagenous trabeculae (Fig. 5.84 to Fig. 5.94) were identical to that found in the right liver lobes. Stellate cells seemed to be fewer in number and pit cells were not recognised. The isthmus deviated from the norm by the presence of hepatocytic cellular material being present in the sinusoidal spaces (Figs. 5.89, 5.91 & 5.92).

5.5 DISCUSSION

5.5.1 Parenchymal component

Hepatocytes

Descriptions of reptilian hepatocytes in the literature agree with the current findings in the juvenile Nile crocodile liver of large, polygonal cells arranged in either two-cell-thick plates (longitudinal section) or gland-like tubules (cross section) that also branched and anastomosed (Goldblatt *et al.*1987; Storch *et al.* 1989, Schaffner 1998; Starck *et al.* 2007).

Hepatocyte nuclei are round to oval (some are pleomorphic) in the liver of humans and in some reptilians (Phillips *et al.* 1987; Schaffner 1998; www.pathologyoutlines.com) as opposed to the uniformly round nuclear shape seen in this study. Nuclear features of the Nile crocodile hepatocytes, such as the marginal rim of heterochromatin with chromatin masses distributed throughout the nucleus and the presence of a double nuclear membrane, agrees with the findings in other reptiles (Storch *et al.* 1989; Schaffner 1998).

The morphology of the nucleolus in this study concurs with Schaffner's (1998) finding in reptiles that the nucleoli consist of electron-dense material mixed with pale areas. Two types of nucleoli, namely, open and compact nucleoli are described by Ghadially (1988) and the morphology of the nucleoli in the current study appears to fall between these two descriptions.

The Nile crocodile hepatocytes displayed scanty lateral microvillous projections. Lateral surfaces of hepatocytes in humans did not have microvilli (Phillips *et al*. 1987), but Fried (2008) found adjacent hepatocytes to be linked by 'projections' in vertebrates. Schaffner (1998) commented on lateral cell membrane 'peg & groove arrangements' in reptiles, while Phillips *et al.* (1987) found no microvilli on the lateral surfaces in the vertebrates they studied.

The peribiliary pink staining structures seen in the hepatocytes with the light microscope (Chapter 4) were confirmed ultrastructurally as mitochondria and hemosiderin granules and the large brown inclusions as bile pigment.

The combined presence of lipid droplets and glycogen accounted for the frothy appearance of the hepatocytes in histological preparations. Prominent lipid droplets of

varying sizes and quantities were present in the Nile crocodile hepatocytes. Extensive lipid accumulation is pathologic in mammalian livers, but fatty infiltration in crocodiles should not always be regarded as abnormal (Divers & Cooper 2000; Starck *et al.* 2007). Frequent feeding and underexercise during captivity, as well as other causes, for example, toxins (Schaffner 1998; Divers & Cooper 2000), contribute to lipid accumulation.

Peroxisomes in vertebrates commonly contain a nucleoid or crystalline inclusions or a marginal plate (Phillips *et al.* 1987; Schaffner 1998; Fried 2008). The peroxisomes in the present study had an amorphous interior of medium electron-density with no inclusions, comparable to the findings in the West African crocodile (Storch *et al.* 1989).

Bile canaliculi only existed at the apical borders between groups of hepatocytes in this study, in contrast to their location between the lateral membranes of hepatocytes in mammals. This observation concurs with the findings of a central shared canalicular lumen in the hepatocyte tubules of reptiles, including crocodilians, and testudines (Storch *et al.* 1989; Schaffner 1998; Moura *et al.* 2009).

The PAS-positive (Chapter 4) boundaries indicating the presence of a basal lamina around the groups of hepatocytes in the current study was not confirmed by electron microscopy. Storch *et al.* (1989) hypothesised that the PAS positive ‘basal lamina’ in the West African crocodile was due to the presence of collagen fibrils in the space of Disse. Perhaps the long-spacing collagen fibrils found in this location in the Nile crocodile liver accounts for the PAS positivity seen. Tanuma (1987) and Goldblatt *et al.* (1987) mentioned a basal lamina covering the basal surfaces of the hepatocytes in the turtle and newt respectively.

5.5.2 Non-parenchymal component

Sinusoids

The current study established that the angular sinusoids were lined by fenestrated endothelial cells with Kupffer cells sometimes forming part of this lining. Elias (1955) was of the opinion that the sinusoids of vertebrates were lined by potential phagocytes that do not span the lumen. Basement membranes were absent around sinusoids (De Leeuw *et al.* 1990; Fried 2008) as was supported by the findings of this study. Ghoddusi & Kelly (2004) reported that in chickens the endothelial cells were supported by a basement

membrane and Wisse *et al.* (1996) found fragments of subendothelial basal lamina-like material in rats.

Endothelial cells

Liver endothelial cells have a variety of functions including a filtration function allowing the two-way diffusion of substances and a pronounced endocytic capability (Kmieć 2001). This is also reflected in the current study by their ultrastructural morphology illustrating the presence of cytoplasmic fenestrations as well as numerous pinocytotic vesicles and prominent lysosomes. A basement membrane supporting the endothelial cells of the sinusoids is absent in most vertebrates, as in the juvenile Nile crocodile. This differs from the findings of Ghoddusi & Kelly (2004) that the chicken liver endothelium is supported by a basement membrane. Storch *et al.* (1989) described the endothelial cell processes of the West African crocodile as forming up to three layers, although they conceded that stellate cell projections may have been involved – this may also be ascribed to the tissue sectioning plane. The sinusoidal endothelium of the Nile crocodile liver exhibited only a single layer of endothelial cell processes.

Kupffer cells

The literature states that Kupffer cells are macrophages that form part of the reticuloendothelial system and reside in liver sinusoids (www.pathologyoutlines.com). They play a pivotal role in host defence by eliminating toxins and foreign substances (McCuskey & McCuskey 1990; Naito *et al.* 2004) and also remove effete and apoptotic red and white blood cells (Dini *et al.* 2002). They degrade hemoglobin to form hemosiderin (Kumar & Kiernan 2010) and bilirubin (www.pathologyoutlines.com).

Several publications (Junqueira *et al.* 1975; Wisse & Knook 1977; Phillips *et al.* 1987; Wisse et al 1996; Schaffner 1998; Ross *et al.* 2003; Ghoddusi & Kelly 2004) describe the position of Kupffer cells as being inside the sinusoidal lumen, part of the sinusoidal lining, embedded in the endothelial lining, situated as intraluminal macrophages or as fixed cells. Elias (1955) mentioned that the sinusoids were lined by potential phagocytes that never bridge the lumen. The Kupffer cells in the juvenile Nile crocodile liver did not reflect these findings as they were found in several positions and not only in the sinusoidal spaces. They can therefore be considered as highly mobile and not fixed cells.

The large phagosomes seen in the present study contained ceroid in addition to other pigments (Chapter 4, Light microscopy). Typical lipofuscin granules were not observed with the electron microscope which may be due to the age of the Nile crocodiles used, as it is an age related pigment (Yin 1996). Yin (1996) also stated that ceroid consisted of degraded cellular material and accumulated rapidly in secondary lysosomes throughout life and Kumar & Kiernan (2010) described ceroid as a type of lipofuscin – the present study therefore concludes that the PAS and PAS-D pink positivity (Chapter 4) found in the compound granules of the Kupffer cells was due to the presence of ceroid and not lipofuscin.

Two other pigments, namely, melanin and hemosiderin co-existed in the Kupffer cells in the present study. It has been established that the Kupffer cells of reptiles and amphibians synthesize melanin (Henninger & Beresford 1990; Kalashnikova 1992; Corsaro *et al.* 2000; Sichel *et al*. 2002). Iron (hemosiderin from breakdown of hemoglobin) catalyzes the formation of free radicals and the melanin traps these superoxide radicals (Beresford 1987; Sichel 2002; McClellan *et al.* 2006). The hypothesis of Henninger & Beresford (1990) that the production of melanin is a defence mechanism in response to possibly harmful iron may be an acceptable explanation for their co-existence in the Kupffer cells of the juvenile Nile crocodile as well.

Corsaro *et al.* (2000) described two types of Kupffer cells in amphibian livers – a small type with almost no melanin granules and a larger type that synthesizes melanin and is filled with melanin granules - the authors thought this to be a developmental stage of the Kupffer cells. The small type of Kupffer cell was not seen in the current study with only relatively large Kupffer cells containing numerous melanin granules being present in the different locations.

Lipid droplets were present in the Kupffer cells in this study, as well as in Kupffer cells of the lizard (Taira & Mutoh 1981), but McCuskey & McCuskey (1990) found no lipid in their study of mammals.

Several of the mentioned publications refer to vermiform processes formed by the Kupffer cell cytoplasm, but none were found in the Kupffer cells of the Nile crocodile liver.

No comparable structures to the conspicuous tubular cytoplasmic organelles ('tubulosomes') with filamentous/crystalline interiors found in the Kupffer cells of the juvenile Nile crocodile could be traced in the literature. Storch *et al.* 1989 mentioned the presence of small membrane-bound vesicles of unknown origin in the West African crocodile Kupffer cell – however, no images were published to illustrate them. Boler (1969) described the ultrastructure of cytosomes in canine Kupffer cells, but these were larger than the tubulosomes, spherical in form and contained tubular structures. The proposed hypotheses are that these organelles are specialised lysosomes dedicated to the breakdown of phagosome contents or are perhaps involved in melanin synthesis or may be responsible for cell mobility. A combination of these functions is also plausible. Mitochondria are often closely associated with other organelles (Ghadially 1988) that require adenosine triphosphate (Lehninger 1965, in Ghadially 1988) for energy transfer, which may explain the close relationship between the tubulosomes and the mitochondria in this study.

Schaffner (1998) mentioned a second pigmented macrophage in a perisinusoidal location in reptiles and Jacobson (2007) called them melanomacrophages. The present study found the same ultrastructural features, including the tubular structures, in the 'pigmented' cells in all the mentioned locations, i.e. in the sinusoids, perisinusoidal and as part of the groups of hepatocytes, and therefore deducts that these cells are all Kupffer cells.

Stellate cells

The hepatic stellate cells were previously also known as Ito cells, fat-storing cells, lipocytes, vitamin A-rich cells, perisinusoidal cells and interstitial cells (Flisiak 1997; Kmieć 2001; Sato *et al.* 2003; Senoo *et al.* 2010). Wisse *et al.* (1996), Dudas *et al.* (2009) and Sato *et al.* (2003) refer to them as the pericytes of liver sinusoids. According to the literature these cells exist in either the quiescent state as the storage cell of vitamin A, or are activated to become myofibroblast-like cells during liver injury in which case they lose their vitamin A component (Schaffner 1998; Kmieć 2001; Sato *et al.* 2003; Dudas *et al.* 2009; Senoo *et al.* 2010). They also play a role in the contractability of the sinusoids and produce extracellular matrix components (Sato *et al.* 2003).

The stellate cells in the present study have the same general ultrastructural features and location as those mentioned in the cited literature above. However, these cells differ in

some respects from published accounts in the literature. Cytoplasmic projections of stellate cells in the livers of two lizard species were found in the sinusoidal spaces (De Brito Gitirana 1988). No stellate cell processes were seen protruding into the spaces in the current study. The cells were however in close apposition to the endothelial cell cytoplasm, as was also noted by Sato *et al.* (2003), sometimes touching the endothelial cells.

De Brito Gitirana (1988) and Senoo *et al.* (2010) mention a well-developed GER – only a few GER strands were noticed in this study. Taira & Mutoh (1981) also found prominent GER in the lizard and the snake, but not in the turtle that they investigated.

Lipid droplets were sparse in the stellate cells studied in the lizard with most of the cells being devoid of lipid inclusions (De Brito Gitirana 1988) – almost all the stellate cells in the Nile crocodile liver exhibited lipid droplets with only a few cells not containing them. Storch *et al.* (1989) identified numerous lipid droplets in stellate cells of the West African crocodile. In contrast, only one or two, and at the most four large droplets, were seen in the Nile crocodile. Beresford & Henninger (1986) concluded that variable numbers and sizes of lipid droplets are present in the different reptile species. Wake (1974, in Geerts *et al.* 1990) distinguishes between two types of lipid droplets found in rat stellate cells, namely, membrane bound Type I and non-membrane bound Type II – only the latter was present in this study.

Wisse & Knook (1977) found the single cilium of the rat stellate cell projecting into the sinusoidal lumen – the current study showed that this structure was only present in the space of Disse. Tobe *et al.* (1985) established a '9+0' microtubular arrangement in the ciliary ultrastructure of the single cilium in human hepatic stellate cells and concluded that these cilia were immotile which would conform with the sensory or chemoreceptor function ascribed to single cilia in other locations (Ross *et al.* 2003).

Senoo *et al.* (2010) in a review article of hepatic stellate cells regarded multivesicular bodies as essential 'for the development of vitamin A containing lipid droplets'. Storch *et al.* (1989) consistently found multivesicular bodies in the stellate cells of the West African crocodile – this organelle was infrequently observed in the present study.

Most of the cited literature agrees that hepatic stellate cells store vitamin A and transform into fibroblasts or myofibroblastic cells under certain circumstances and are responsible for

the upkeep of the collagenous and reticular network around the sinusoids. Tanuma (1987) did not elude to this in his electron microscopy study of the turtle sinusoidal wall – he however described the existence of smooth muscle cells, in addition to stellate cells, as another subset of perisinusoidal cells. The present study showed cells with the combined features of smooth muscle cells and fibroblasts (Ghadially 1988) occupying the same position as stellate cells, sometimes accompanying the stellate cells. The fact that both cell types are present simultaneously in the same location leads to the conclusion that these may in fact be two separate cell populations, with the myofibroblastic cell regulating sinusoidal blood flow and being responsible for maintaining the extracellular matrix. Another scenario would be that these two cells are present in the same location due to separate stages of differentiation from stellate into myofibroblastic cell occurring in the same area.

Pit cells

Pit cells, also known as liver-specific natural killer cells (Luo *et al.* 2000; Kmieć 2001), were first described in 1976 (Wisse *et al.*1976, in Luo *et al.* 2000 & Nakatani *et al.* 2004). The name derives from the spherical dense cytoplasmic granules that are comparable to grape seeds (‘pit’ means seed). Phillips *et al.* (1987) described them as a variant of circulating lymphocytes.

Their function as natural killer cells was revealed by Kaneda *et al.* (1983, in Luo *et al.* 2000 & Nakatani *et al.* 2004). Pit cells are cytotoxic and destroy target cells by inducing necrosis and /or apoptosis (Luo *et al.* 2000) and are ideally located in the sinusoids as the first line of defence in the liver. Pit cell functions are apparently controlled by Kupffer cells Vanderkerken *et al.* (1995, in Wisse *et al.* 1996).

The ultrastructure of the pit cells described in this study is analogous to those in the literature. However, the larger vesicles with electron-dense contents differ from the rod-cored vesicles described by Bouwens *et al.* (1987), Nakatani *et al.* (2004) and Luo *et al.* (2000), in that they appear to be larger and do not have the distinctive internal rod bridging the diameter of the vesicle. Wisse *et al.* (1996) stated that pit cells lack pinocytotic activity, but single pinocytotic vesicles were demonstrated in this study.

Intercalated cells

Ghoddusi & Kelly (2004) described cells in the chicken liver that were mostly devoid of organelles and appeared between hepatocytes and in the space of Disse and called them intercalated cells. The authors eluded to the possibility that this cell may be the avian counterpart of the pit cell – the cells however lacked the electron-dense membrane-bound granules. Purton (1976, in Ghoddusi & Kelly 2004) referred to these immature mesenchymal cells as extrasinusoidal macrophages. The equivalent cell was described in the West African crocodile as free phagocytes (Storch *et al.* 1989). No evidence of phagocytosis was found in the intercalated cells of the present study – perhaps they are lymphocytes or the tissue equivalent of pit cells that have possibly degranulated.

5.5.3 Connective tissue stroma

A basal lamina was absent around hepatocyte groups in this study despite the PAS-D positive reaction for basal lamina demonstrated in figure 4.16 B (Chapter 4). However, the collagen fibres in the same figure also stained a pink colour - perhaps the pink borders partially surrounding some of the hepatocyte tubules, were the reticular fibres (collagen type III) ultrastructurally illustrated to be present. The long-spacing collagen fibres seen in the space of Disse are most probably reticular fibres.

The fine structural features found in the portal tracts of the current study correlates with that described in mammals and reptiles (Phillips *et al.*1987; Schaffner 1998). The presence of accumulations of lymphoid cells in the portal tracts of Nile crocodile liver were however not referred to by these authors. Kanesada (1956a, in Beresford & Henninger 1986) mentioned the presence of lymphoid tissue in the tortoise liver. Lymphocytes are immunocompetent cells that are distributed in connective tissue for immunological surveillance (Ross *et al.* 2003) and this may account for their occurrence in this region. The presence of a few lymphocytes and fibroblasts were mentioned by Goldbaltt & Gunning (1984), but they also noted that other inflammatory cells were generally absent - plasma cells are antibody-producing cells and were a regular occurrence in the portal tracts in this study. Perhaps the presence of lymphoid tissue in the portal tract area of the liver of farmed juvenile Nile crocodiles is part of the normal defensive system against antigens in the young crocodile – livers of farmed adult crocodiles, as well as those of wild

crocodiles, need to be examined for the presence of lymphoid tissue in the portal tract region to determine whether this is a unique feature of the livers of juvenile Nile crocodiles.

5.5.4 Isthmus

The ultrastructural results reflected the histology findings that the isthmus consisted of the full complement of liver tissue. However, the isthmus deviated in respect of the presence of hepatocytic cellular material in the sinusoidal spaces. A possible reason may be the failure of the isthmus to perfuse properly and the cellular material therefore not being washed out of the sinusoids. Kalashnikova (1996) terms this shedding of hepatocyte cytoplasmic fragments into the sinusoids of avian, reptilian and mammalian livers ‘clasmatosis’, the purpose being either the elimination of redundant cellular waste, or to provide the body with essential substances.

5.5 REFERENCES

BARATTA, J.L., NGO, A., LOPEZ, B., KASABWALLA, N., LONGMUIR, K.L. & ROBERTSON, R.T. 2009. Cellular organization of normal mouse liver: a histological, quantitative immunocytochemical, and fine structural analysis. *Histochemistry Cellular Biology,* 131: 713-726.

BERESFORD, W.A. 1987. Some light microscopic histology of the liver in *Caiman crocodilus*. *The Anatomical Record,* 218: 16A.

BERESFORD, W.A. & HENNINGER, J.M. 1986. A tabular comparative histology of the liver. *Archivum Histologicum Japonicum,* 49: 267-281.

BOLER, R.K. 1969. Fine structure of canine Kupffer cells and their microtubule-containing cytosomes. *The Anatomical Record,* 164: 483-496.

BOUWENS, L., REMELS, L., BEAKELAND, M., VAN BOSSUYT, H. & WISSE, E. 1987. Large granular lymphocytes or “Pit cells” from rat liver: isolation, ultrastructural characterization and natural killer activity. *European Journal of Immunology,* 17: 37-42.

BOZZOLA, J.J. & RUSSELL, L.D. 1992. *Electron microscopy: principles and techniques for biologists.* Jones and Bartlett Publishers, Massachusets.

CORSARO, C., SCALIA, M., LEOTTA, N., MONDIO, F. & SICHEL, G. 2000. Characterisation of Kupffer cells in some Amphibia. *Journal of Anatomy,* 196: 249-261.

DE LEEUW, A.M., BROUWER, A. & KNOOK, D.L. 1990. Sinusoidal endothelial cells of the liver: fine structure and function in relation to age. *Journal of Electron Microscopy Technique,* 14: 218-236.

DE BRITO GITIRANA, L. 1988. The fine structure of the fat-storing cell (Ito cell) in the liver of some reptiles. *Zeitschrift Mikroskopish- Anatomische Forschung,* 102: 143-149.

DINI, L., PAGLIARA, P. & CARLA, E.C. 2002. Phagocytosis of apoptotic cells by liver: a morphological study. *Microscopy Research and Technique*, 57: 530–540.

DIVERS, S.J. & COOPER, J.E. 2000. Reptile Hepatic Lipidosis. *Seminars in Avian and Exotic Pet Medicine,* 9: 153-164.

DUDAS, J., MANSUROGLU, T., BATUSIC, D. & RAMADORI, G. 2009. Thy-1 is expressed in myofibroblasts but not found in hepatic stellate cells following liver injury. *Histochemistry and Cell Biology,* 131:115–127.

ELIAS, H. 1955. Liver morphology. *Biological Reviews,* 30: 263-310.

FLISIAK, R. 1997. Role of Ito cells in the liver function. *Polish Journal of Pathology,* 48: 139-145.

FRIED, G.H. 2008. Liver, in *AccessScience.* © McGraw-Hill Companies. http://www.accessscience.com

GEERTS, A., BOUWENS, L. & WISSE, E. 1990. Ultrastructure and function of hepatic fat-storing and pit cells. *Journal of Electron Microscopy Technique,* 14: 247-256.

GHADIALLY, F.N. 1988. *Ultrastructural pathology of the cell and matrix.* Butterworths, London.

GHODDUSI, M. & KELLY, W.R. 2004. Ultrastructure of *in situ* perfusion-fixed avian liver, with special reference to structure of the sinusoids. *Microscopy Research and Technique,* 65:101–111.

GOLDBLATT, P.J. & GUNNING, W.T. 1984. Ultrastructure of the liver and biliary tract in health and disease. *Annals of Clinical and Laboratory Science,* 14: 159-167.

GOLDBLATT, P.J., HAMPTON, J.A., DIDIO, L.N., SKEEL, K.A. & KLAUNIG, J.E. 1987. Morphologic and histochemical analysis of the Newt (*Notophthalmus viridescens*) liver. *The Anatomical Record,* 217: 328-338.

HAYAT, M.A. 2000. *Principles and techniques of electron microscopy: biological applications.* Cambridge University Press, Cambridge, UK.

HENNINGER, J.M. 1982. Histology of the liver in the box turtle. *The Anatomical Record,* 202: 79A.

HENNINGER, J.M. & BERESFORD, W. A. 1990. Is it coincidence that iron and melanin coexist in hepatic and other melanomacrophages? *Histology and Histopathology,* 5: 457-459.

JACOBSON, E.R. 2007. Overview of reptile biology, anatomy, and histology, in *Infectious diseases and pathology of reptiles,* edited by E.R. Jacobson. CRC Press, Taylor & Francis Group, 6000 Broken Sound Parkway NW, Suite 300, Boca Raton, FL 33487-2742, pp.1-130.

JUNQUEIRA, L.C., CARNEIRO, J & CONTOPOULUS, A.N. 1975. *Basic histology.* Lange Medical Publications, Canada.

KALASHNIKOVA, M.M. 1992. Erythrophagocytosis and pigmented cells of the amphibian liver. *Byulleten' Éksperimental'noi Biologii i Meditsiny,* 113: 82-84.

KALASHNIKOVA, M.M. 1996. Liver cells in a comparative morphological series of animals: ultrastructural features and their significance. *Bulletin of Experimental Biology and Medicine,* 121: 543-548.

KMIEĆ , Z. 2001. Cooperation of liver cells in health and disease. *Advanced Anatomy, Embryology and Cellular Biology,* 161: 1-151.

KUMAR, G.L. & KIERNAN, J.A. 2010. *Education guide: Special stains and H & E.* Dako North America, California. www.dako.com.

LUO, D.Z., VERMIJLEN, D., AHISHALI, B., TRIANTIS, V., PLAKOUTSI, G., BRAET, F., VANDERKERKEN, K. & WISSE, E. 2000. On the cell biology of pit cells, the liver-specific NK cells. *World Journal of Gastroenterology,* 6: 1-11.

MCCLELLAN-GREEN, P., CELANDER, M. & OBERDÖRSTER, E. 2006. Hepatic, renal and adrenal toxicology, in *Toxicology of reptiles,* edited by S.C. Gardner & E. Oberdörster. CRC Press, Taylor & Francis Group, 6000 Broken Sound Parkway NW, Suite 300, Boca Raton, FL 33487-2742, pp.123-148.

MCCUSKEY, R.S. & MCCUSKEY, P.A. 1990. Fine structure and function of Kupffer cells. *Journal of Electron Microscopy Technique,* 14: 237-246.

NAITO, M., HASEGAWA, G., EBE, Y. & YAMAMOTO, T. 2004. Differentiation and function of Kupffer cells. *Medical Electron Microscopy,* 37:16–28.

NAKATANI, K., KANEDA, K., SEKI, S. & NAKAJIMA, Y. 2004. Pit cells as liver-associated natural killer cells: morphology and function. *Medical Electron Microscopy,* 37: 29–36.

PHILLIPS, M.J., POUCELL, S., PATTERSON, J & VALENCIA, P. 1987. *The liver: an atlas and text of ultrastructural pathology.* Raven Press, New York.

ROSS, M.H., KAYE, G.I. & PAWLINA, W. 2003. *Histology: a text and atlas.* Lippincott Williams & Wilkens, USA.

SATO, M. SUZUKI, S. & SENOO, H. 2003. Hepatic stellate cells: unique characteristics in cell biology and phenotype. *Cell Structure and Function,* 28: 105-112.

SCHAFFNER, F. 1998. The hepatic system, in *Biology of reptilia: volume 19, Morphology G: Visceral organs,* edited by C. Gans & A.B. Gaunt. Society for the Study of Amphibians and Reptiles, Missouri, pp. 485-531.

SENOO, H., YOSHIKAWA, K., MORII, M., MIURA, M., IMAI, K. & MEZAKI, Y. 2010. Hepatic stellate cell (vitamin A-storing cell) and its relative – past, present and future. *Cell Biology International,* 34: 1247–1272.

SICHEL, G., SCALIA, M. & CORSARO, C. 2002. Amphibia Kupffer cells. *Microscopy Research and Technique,* 57:477–490.

STARCK, M.J., CRUZ-NETO, A.P. & ABE, A.S. 2007. Physiological and morphological responses to feeding in broad-nosed caiman (*Caiman latirostris*). *The Journal of Experimental Biology,* 210: 2033-2045.

STORCH, V., BRAUNBECK, T. & WAITKUWAIT, W.E. 1989. The liver of the West African crocodile *Osteolaemus tetraspis.* An ultrastructural study. *Submicroscopical Cytology and Pathology,* 21: 317-327.

TAIRA, K. & MUTOH, H. 1981. Comparative ultrastructural study of the Ito cells in the liver of some reptiles. *Archivum Histologicum Japonicum,* 44: 373-384.

TANUMA, Y. 1987. Electron microscopic study on the hepatic sinusoidal wall of the soft-shelled turtle (*Amyda japonica*) with special remarks on the smooth muscle cells. *Archivum Histologicum Japonicum,* 50: 251-272.

TOBE, K., TSUCHIYA, T., ITOSHIMA, T., NAGASHIMA, H. & KOBAYASHI, T. 1985. Electron microscopy of fat-storing cells in liver diseases with special reference to cilia and cytoplasmic cholesterol crystals. *Archivum Histologicum Japonicum,* 48: 435-441.

VAN BEZOOIJEN, C.F A. 1990. Morphology, ultrastructure and function of hepatocytes during liver drug metabolism. *Journal of Electron Microscopy Technique,* 14: 152-174.

WISSE, E. & KNOOK, D.L. 1977. *Kupffer cells and other liver sinusoidal cells.* Elsevier, Amsterdam, Netherlands.

WISSE, E., BRAET, F., LUO, D., DE ZANGER, R., JANS, D., CRABBÉ, E. & VERMOESEN, A. 1996. Structure and function of sinusoidal lining cells in the liver. *Toxicologic Pathology,* 24: 100-111.

YIN, D. 1996. Biochemical basis of lipofuscin, ceroid, and age pigment-like fluorophores. *Free Radical Biology and Medicine,* 21: 871-888.

WWW Site reference:

www.pathologyoutlines.com

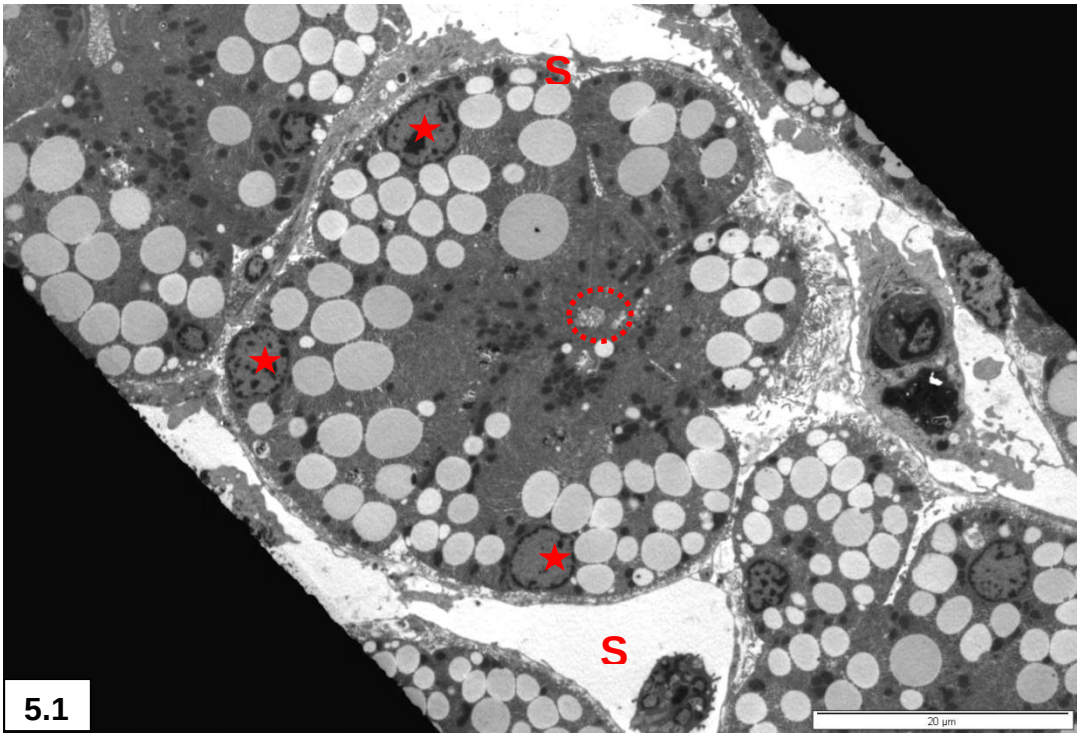

Figure 5.1: Cross-sectional cord of hepatocytes converging to form a central bile canaliculis (dashed circle). The cell membranes of each hepatocyte are in contact basally with a sinusoidal wall, laterally with adjacent hepatocytes and apically with a bile canaliculus. Note eccentric basal nuclei (stars) and the dome-shaped basal surface of the hepatocytes facing the sinusoids (**S**). Lipid droplets are evident.

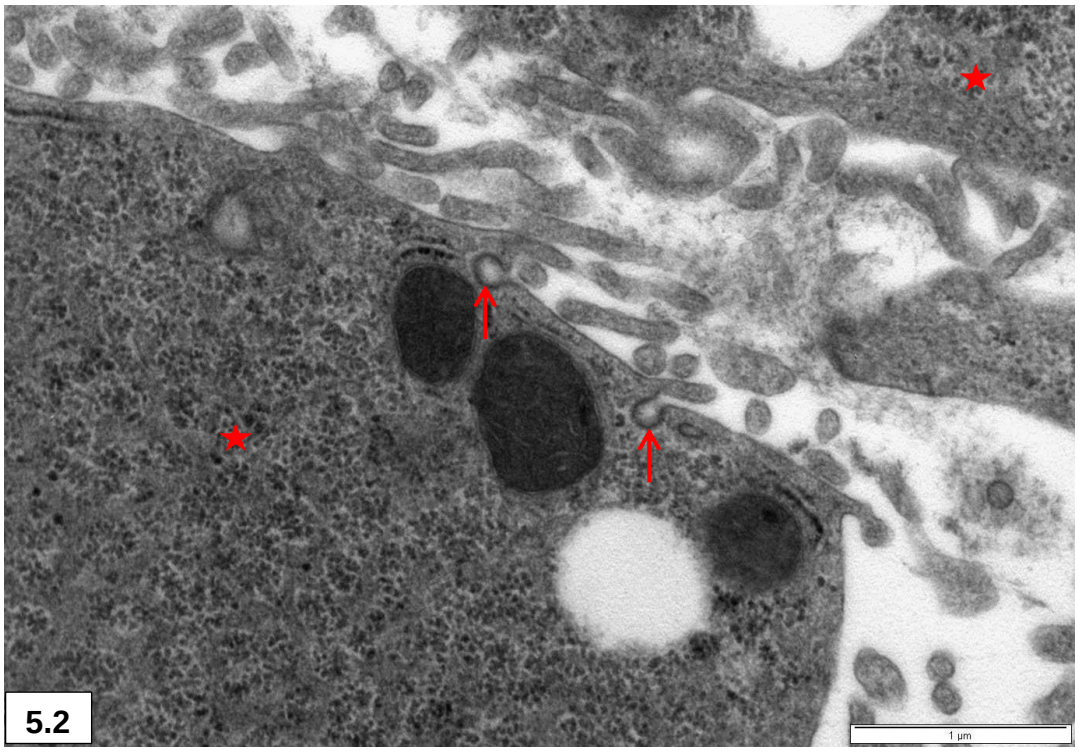

Figure 5.2: Pinocytotic vesicles (arrows) between microvilli of a hepatocyte. Note association of hepatocytes (stars) in two groups of hepatocytes.

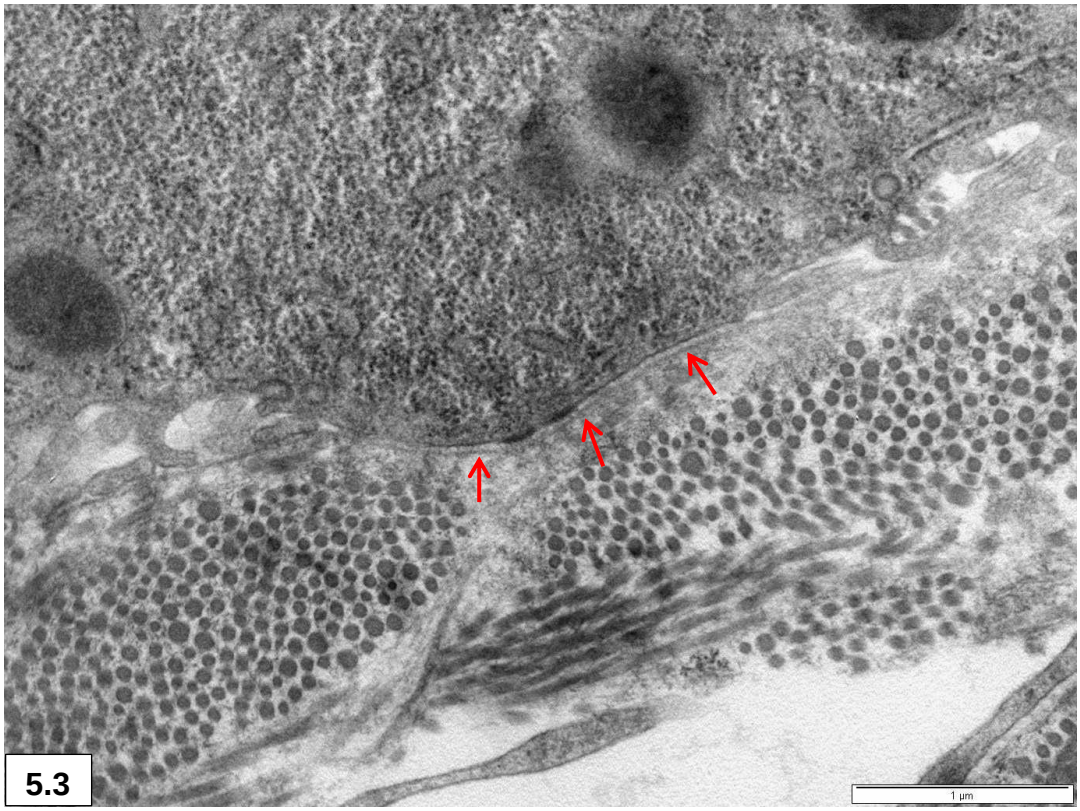

Figure 5.3: Basal lamina (arrows) lining the surface of the hepatocyte directly adjacent to Glisson's capsule.

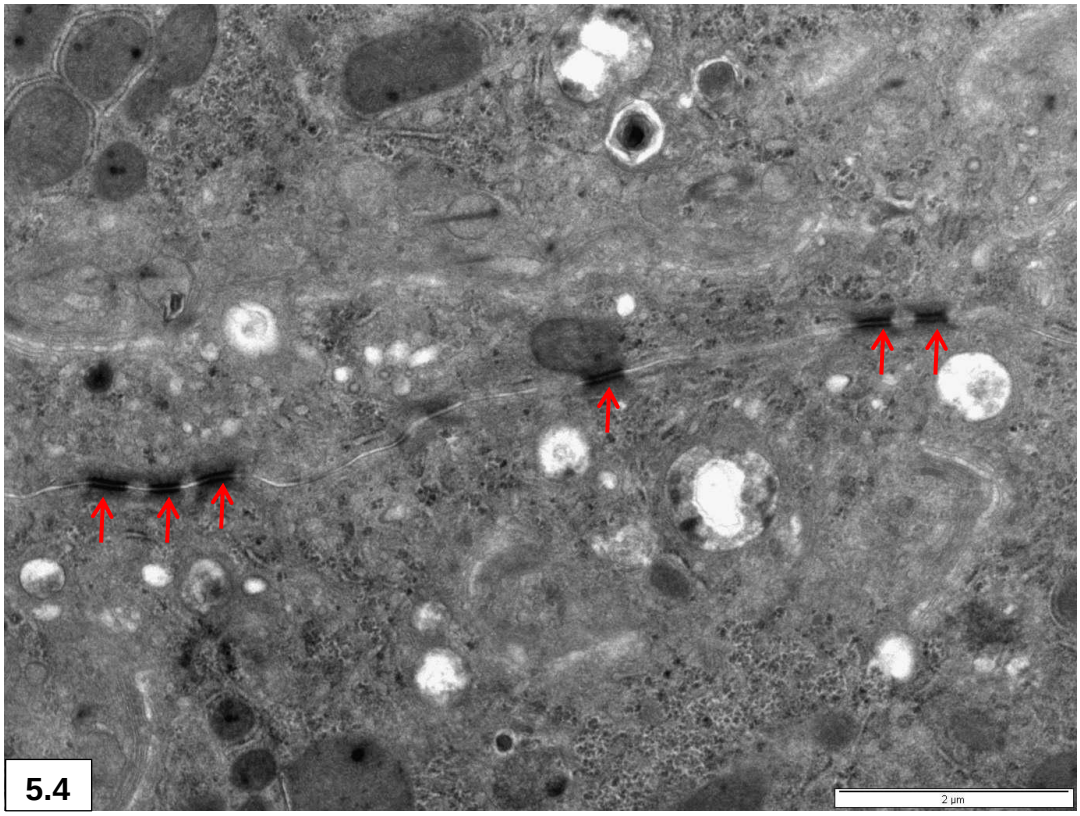

Figure 5.4: The lateral surface of two adjoining hepatocytes demonstrating desmosomes (arrows). Note the close apposition of the apposed cell membranes in this region.

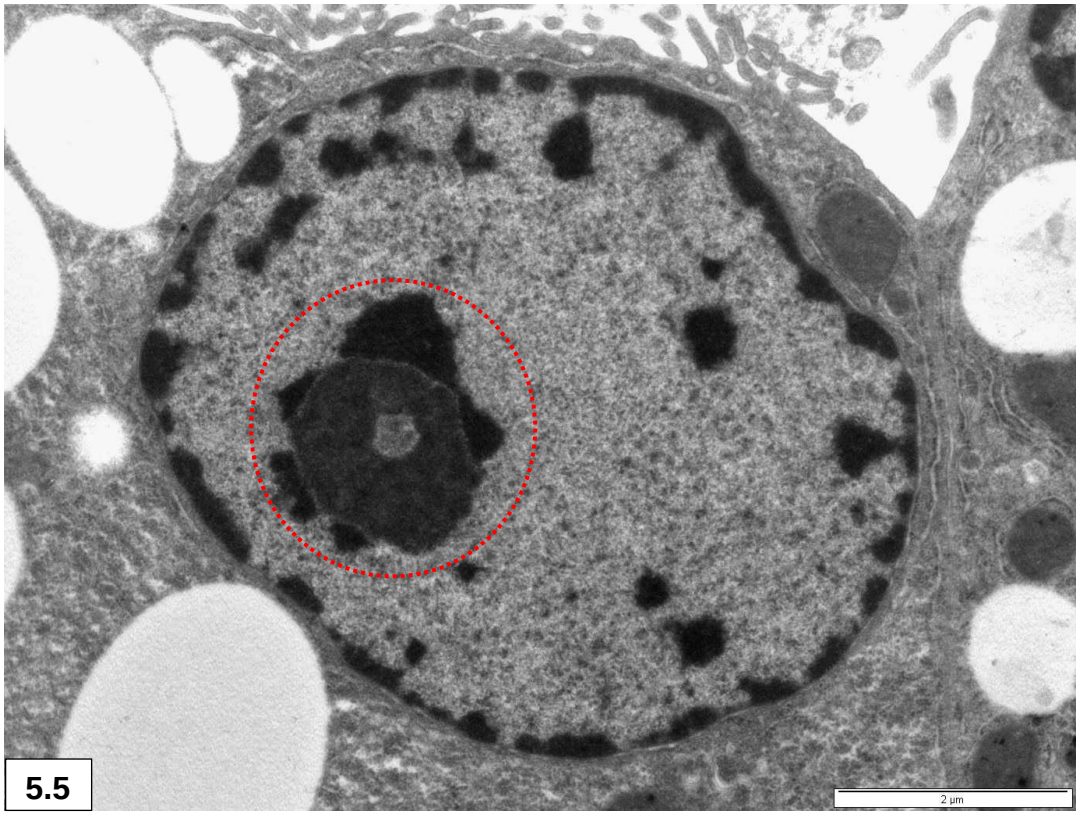

Figure 5.5: Prominent nucleolus (dashed circle) surrounding an open space containing nuclear matrix. Note heterochromatin masses throughout the nucleus, and forming a definite rim along the nuclear membrane.

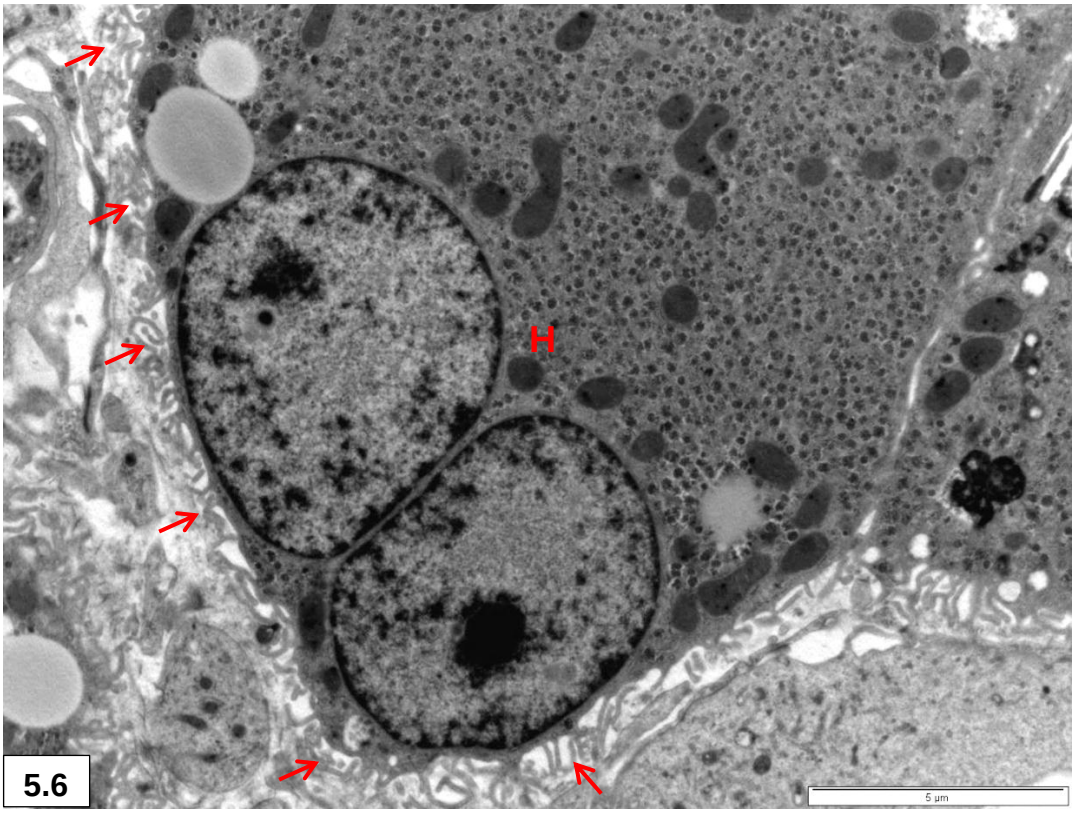

Figure 5.6: Bi-nucleated hepatocyte (**H**). Note the microvilli at the surface of the hepatocyte protruding into the space of Disse (arrows).

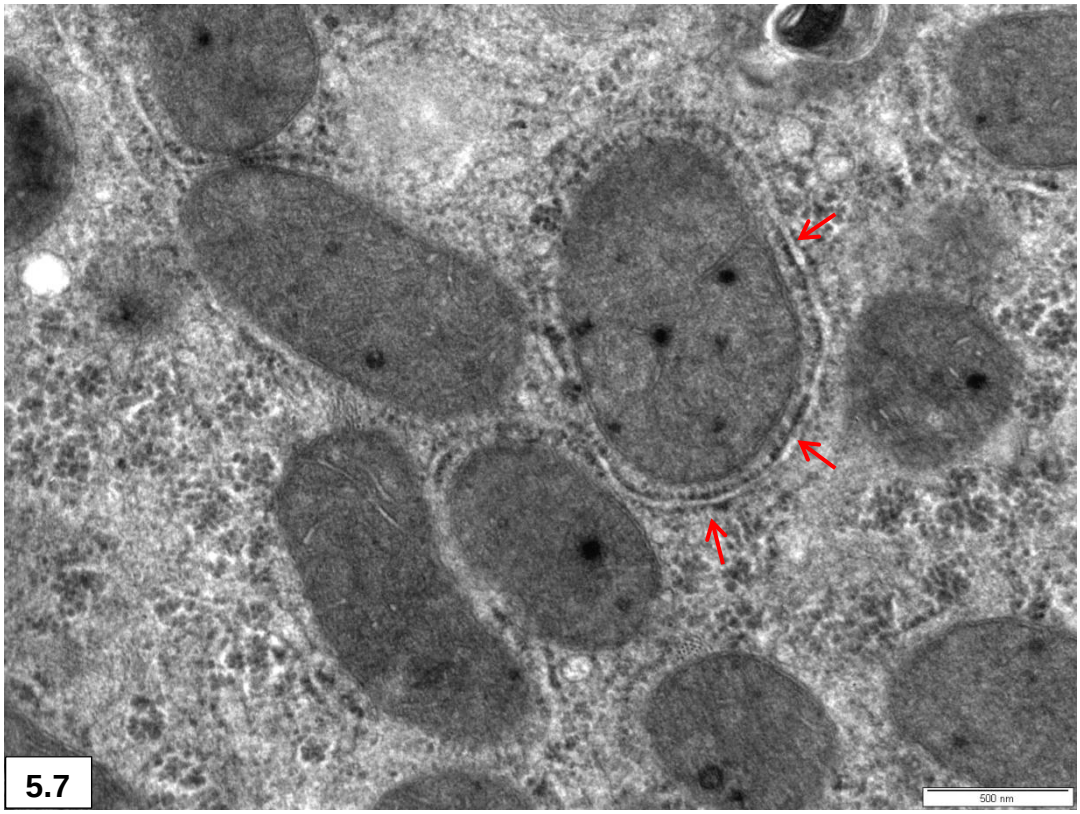

Figure 5.7: GER (arrows) often surrounded mitochondria. Note mitochondrial matrix granules and cristae.

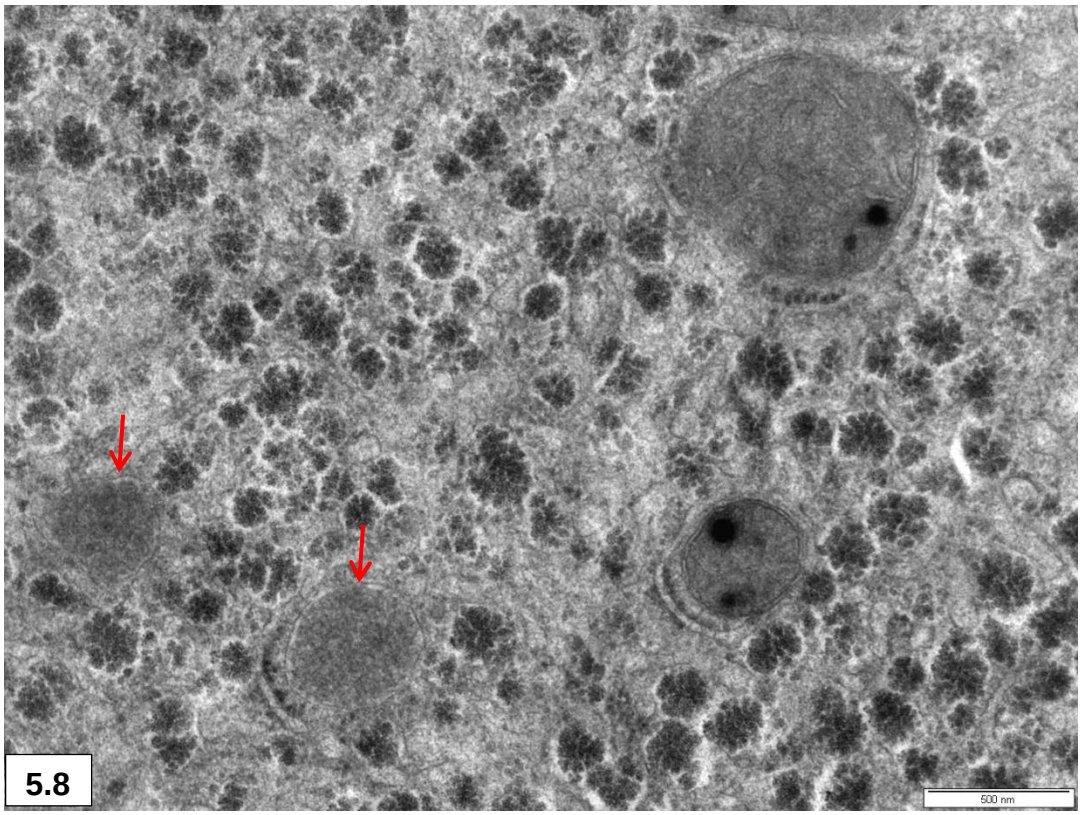

Figure 5.8: Single-membrane-bound peroxisomes (arrows) with amorphous contents of medium electron density. Note glycogen rosettes, mitochondrial matrix granules and cristae.

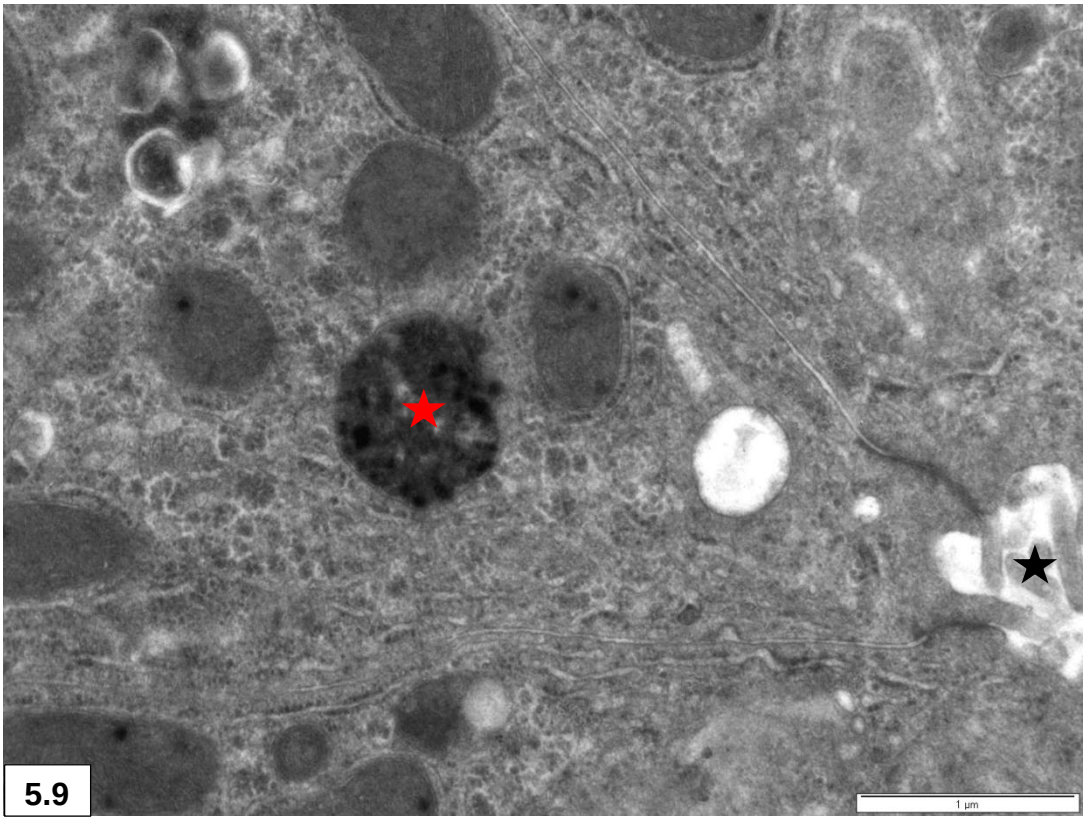

Figure 5.9: A lysosome filled with hemosiderin granules (red star) present at the apical tip of a hepatocyte. Note the bile canaliculus (black star).

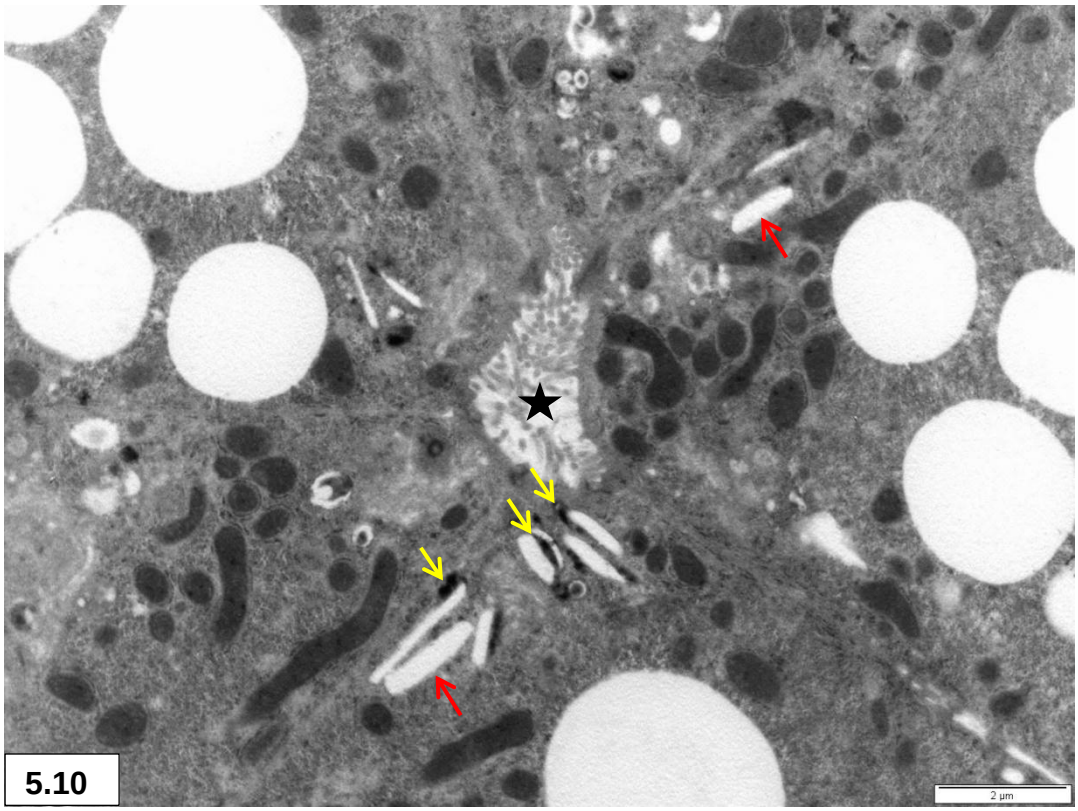

Figure 5.10: Cholesterol slits (red arrows) and slit-like spaces associated with lysosomes (yellow arrows) in the apical region of hepatocytes. Note bile canaliculus (star).

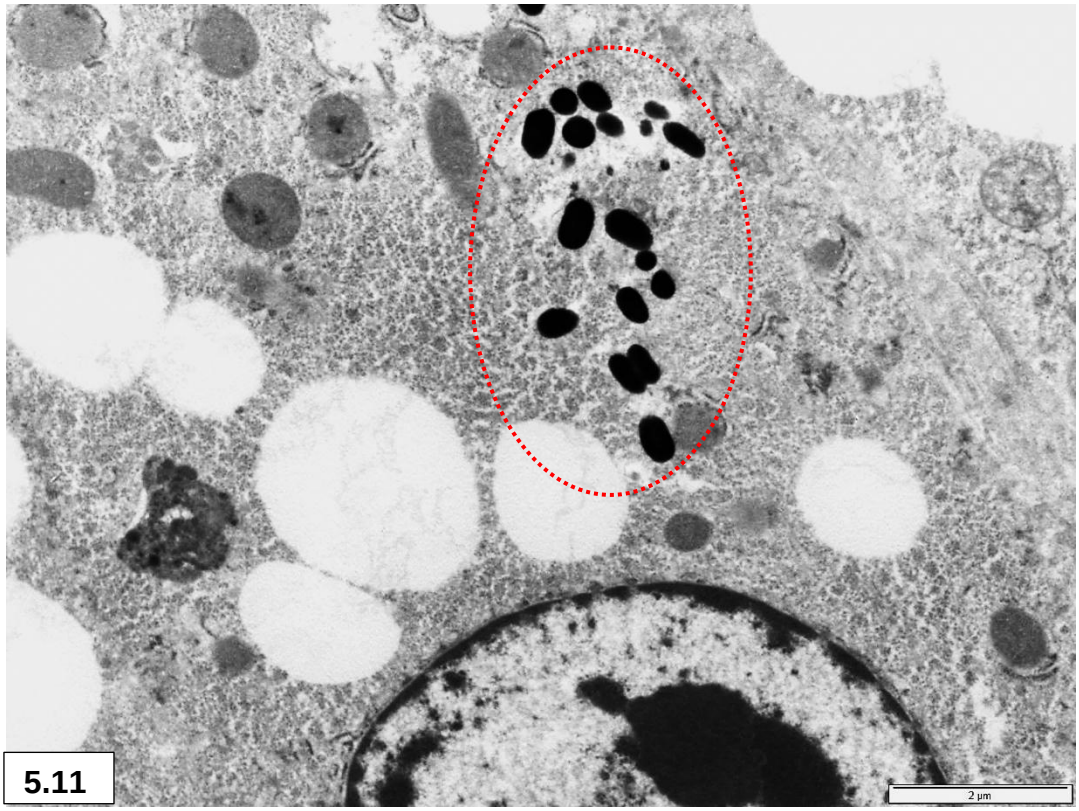

Figure 5.11: Loose lying cytoplasmic melanin granules (encircled) in hepatocyte.

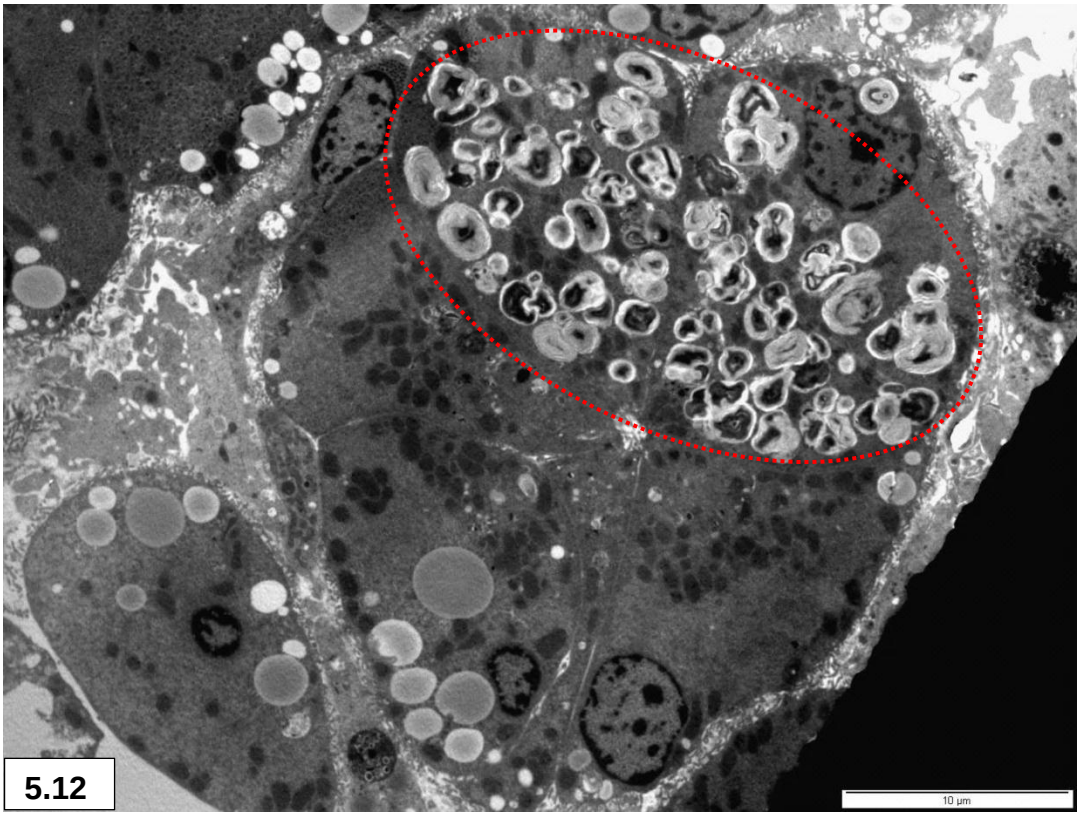

Figure 5.12: Prominent membranous concretions of bile pigment (circle) present in group of hepatocytes.

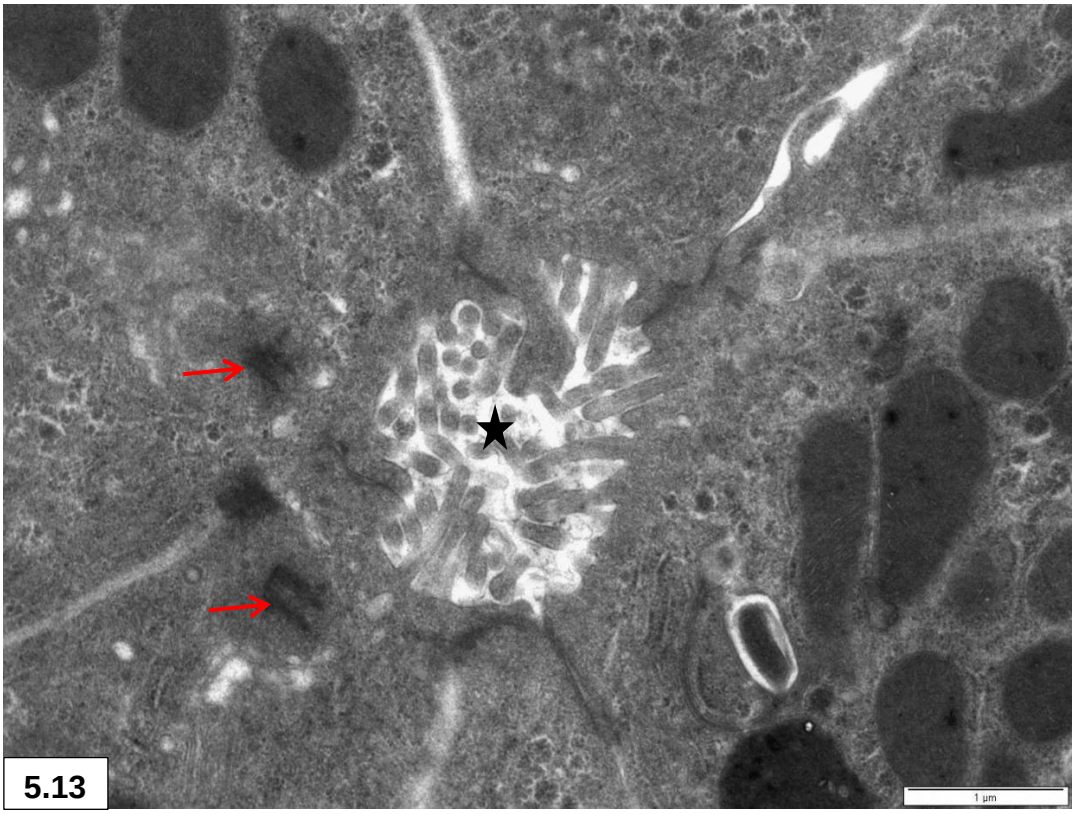

Figure 5.13: Bile canaliculus (star) lined by microvilli. Note centrioles (red arrows).

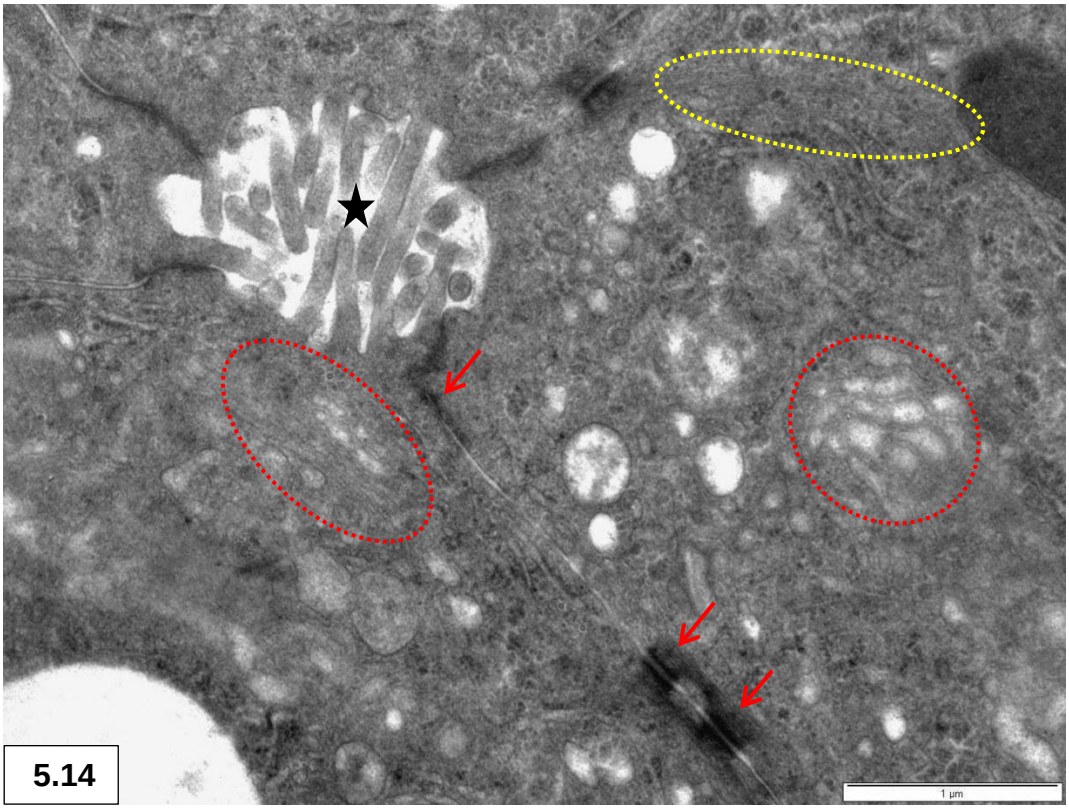

Figure 5.14: Junctional complexes (arrows) between the lateral cell membranes sealing a bile canaliculus (star). Note Golgi (red circles) and microfilaments (yellow circle).

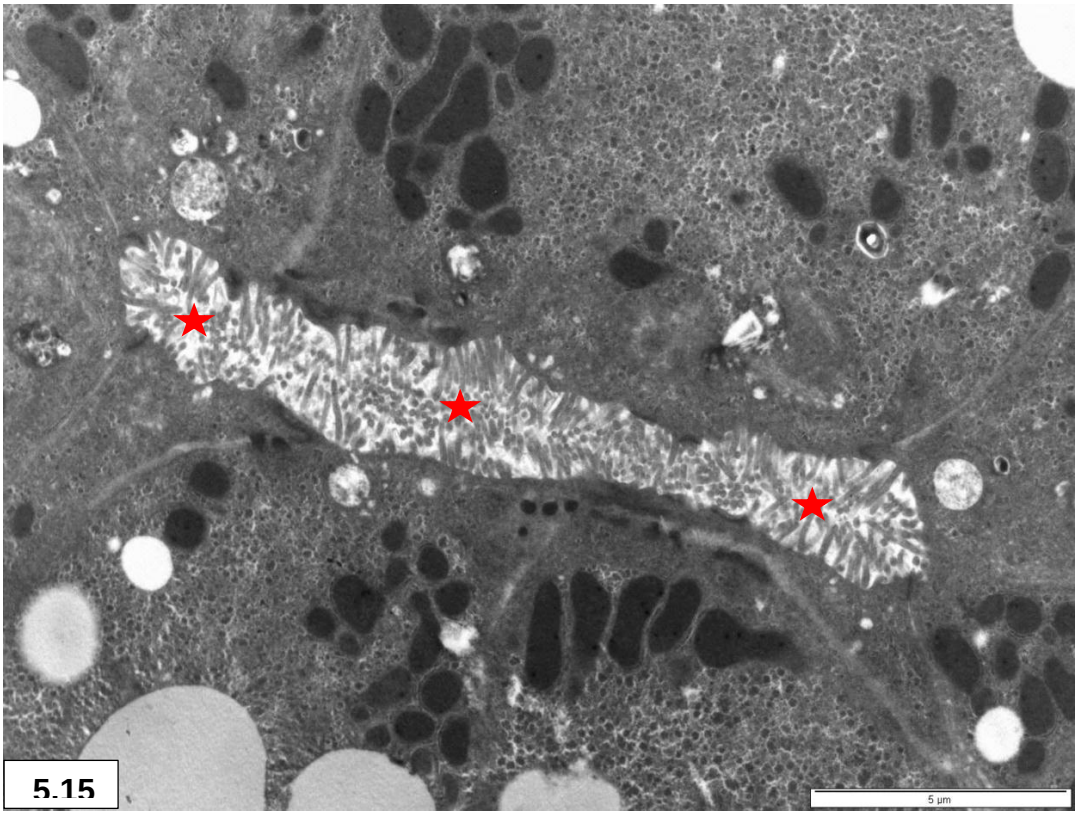

Figure 5.15: A **l**ongitudinal section of a cord of heptocytes with an elongated bile canaliculus (stars).

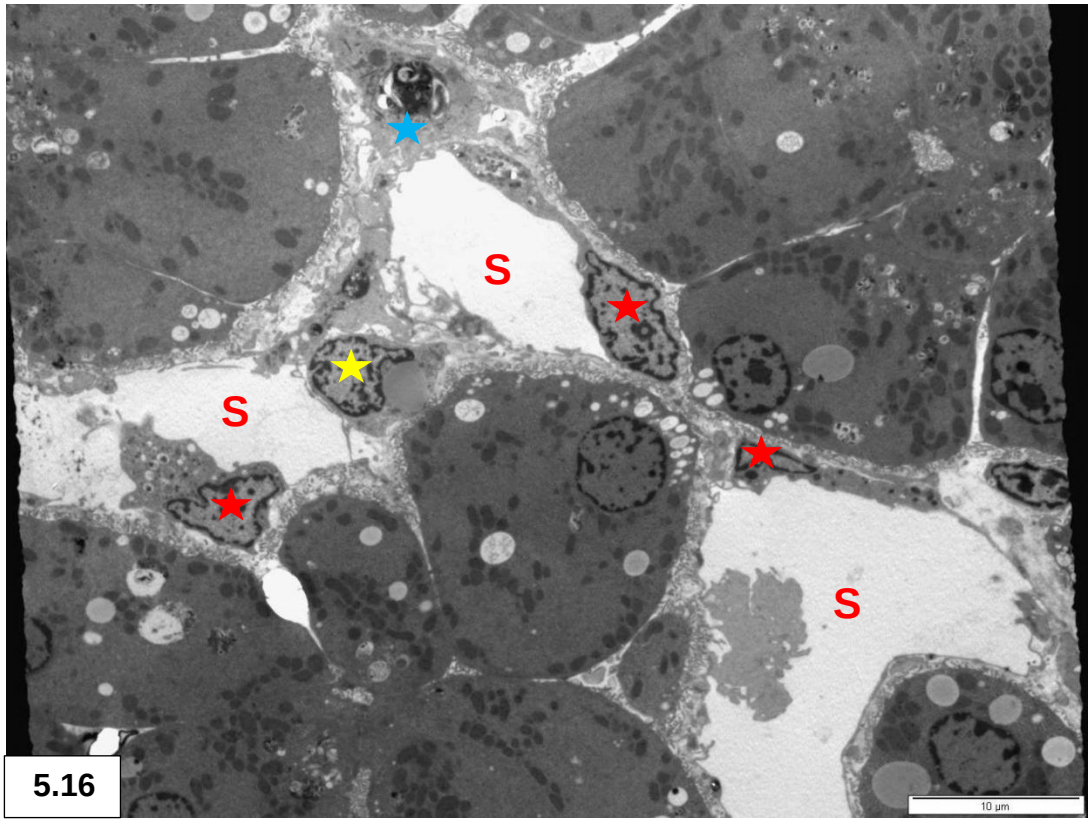

Figure 5.16: Flat and bulky endothelial cells (red stars) lining angular sinusoids (**S**) between adjacent groups of hepatocytes. Stellate cell (yellow star), Kupffer cell (blue star).

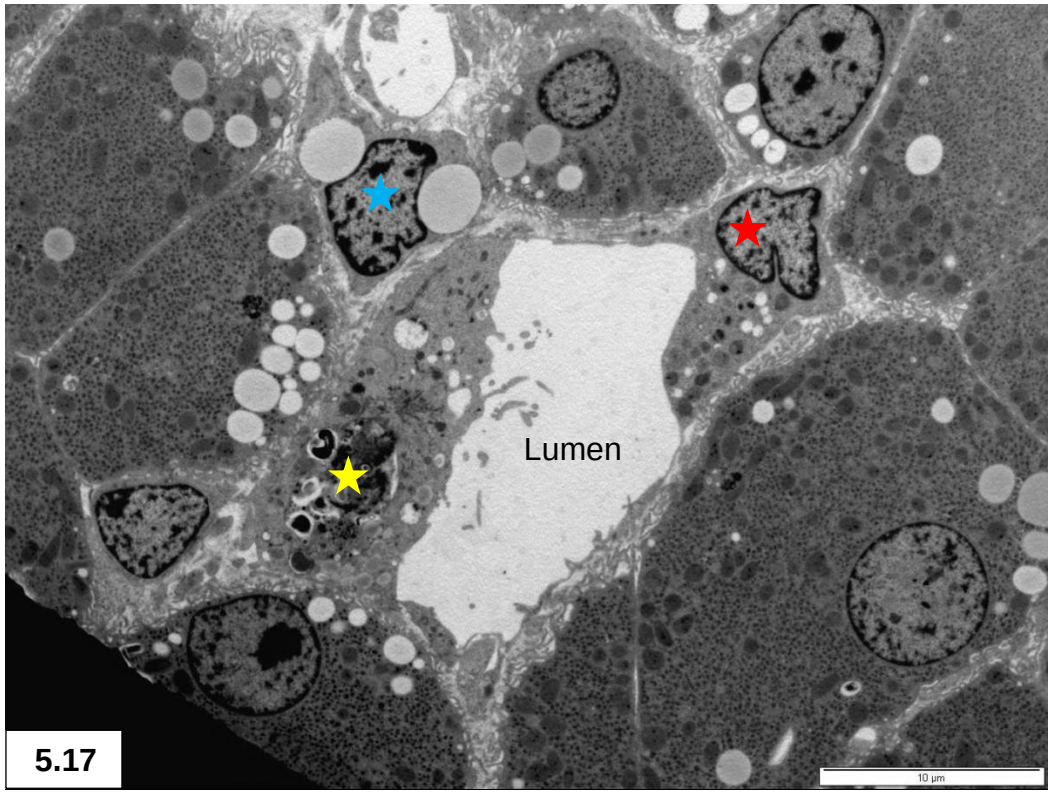

Figure 5.17: Endothelial cell (red star) with long extensions. A Kupffer cell (yellow star) forms part of the sinusoidal lining. Note stellate cell (blue star) containing lipid droplets in the space of Disse.

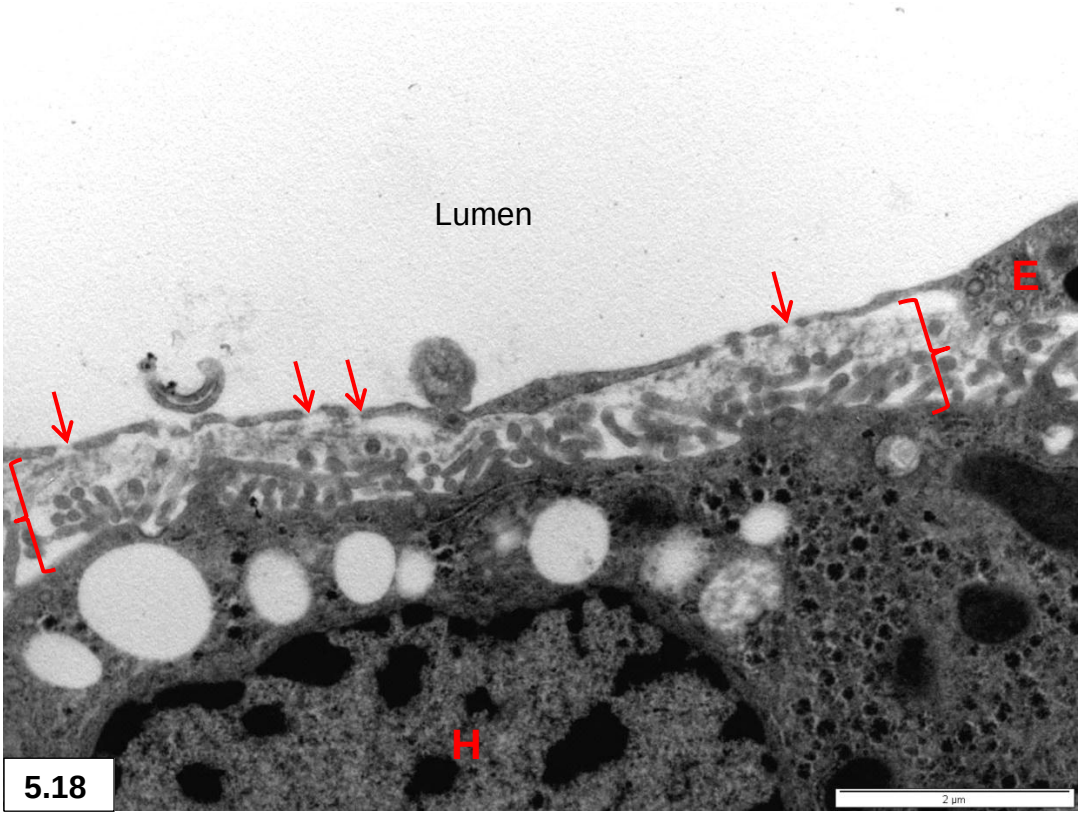

Figure 5.18: Fenestrated cytoplasmic extensions (arrows) of endothelial cell (**E**). Space of Disse (brackets) filled with surface microvilli of hepatocyte (**H**).

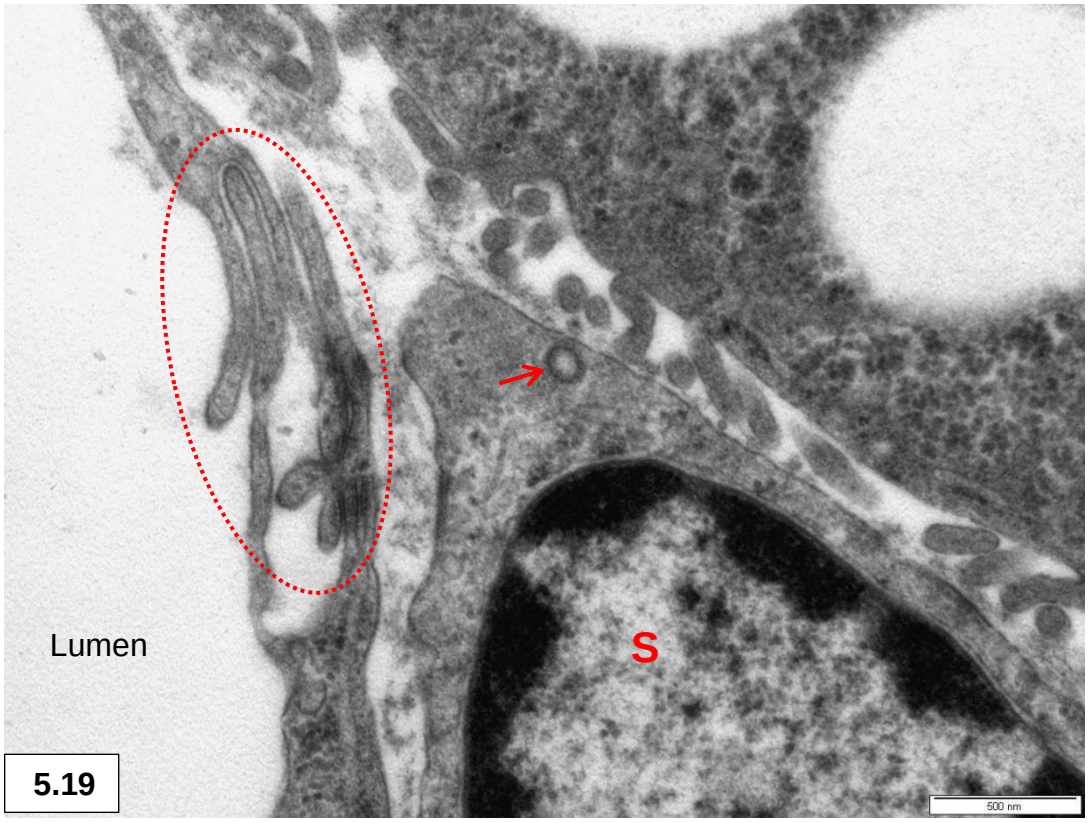

Figure 5.19: Overlapping endothelial cell extensions with tight junctions (dashed circle). Stellate cell (**S**) with coated pit (arrow).

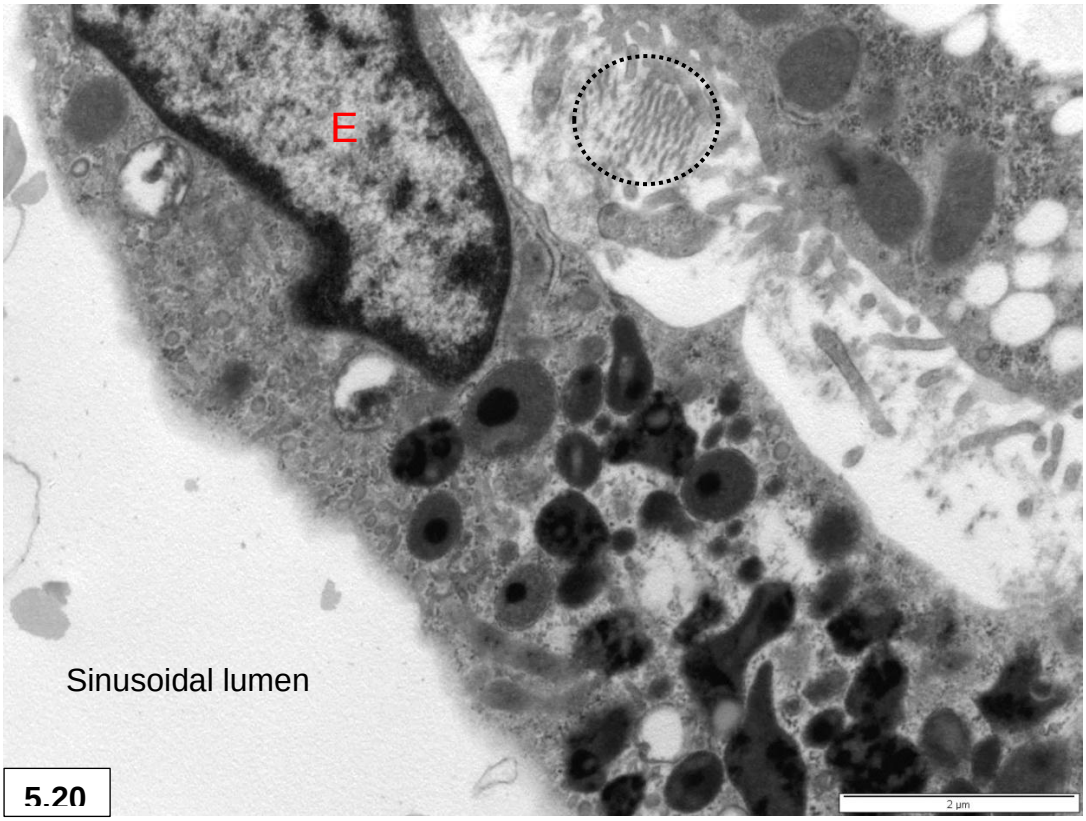

Figure 5.20 & 5.21: Prominent lysosomes with electron-dense contents in endothelial cells (**E**) lining sinusoids. Note collagen fibrils (black circle) and long-spacing collagen fibrils (red circle) in the space of Disse.

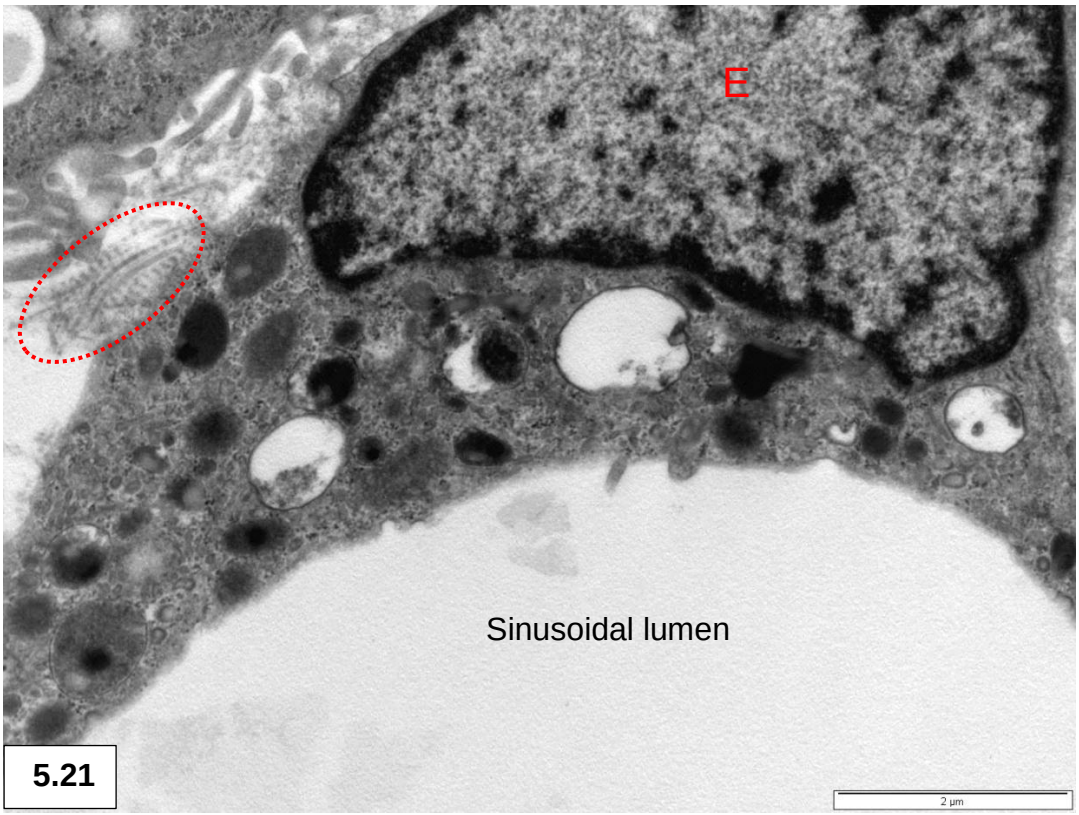

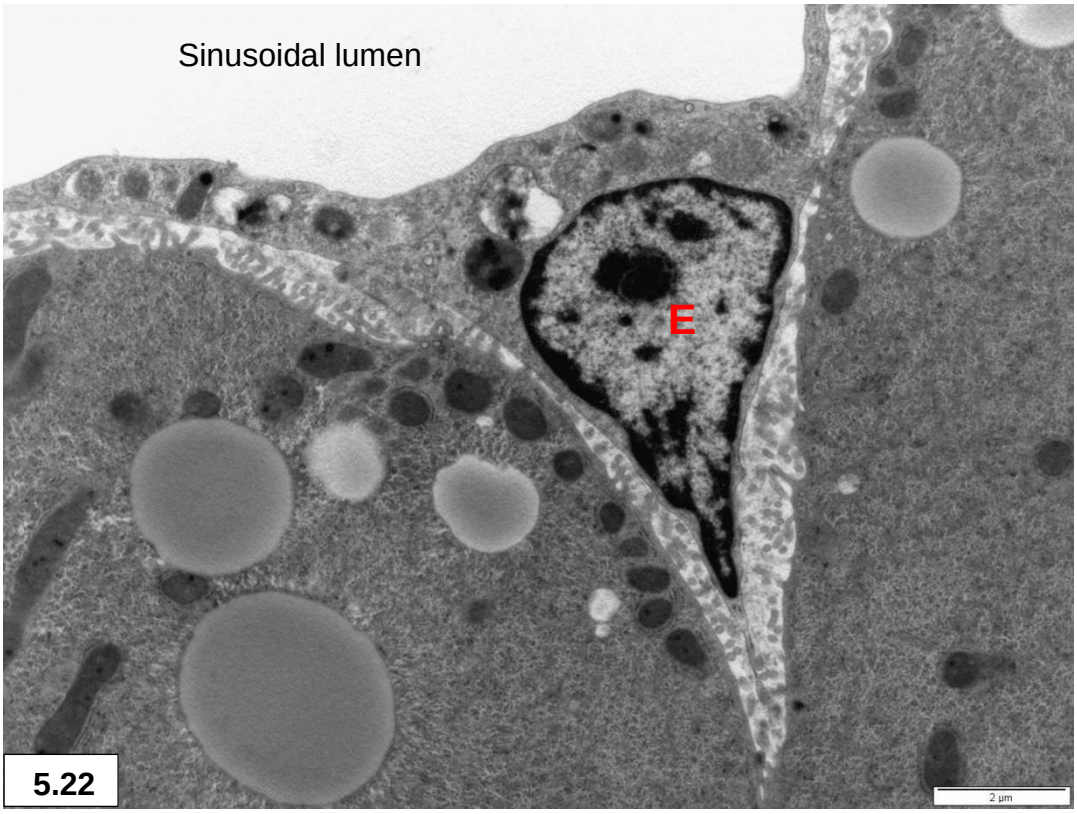

Figure 5.22: Endothelial cell nucleus (**E**) in the recess between neighbouring groups of hepatocytes.

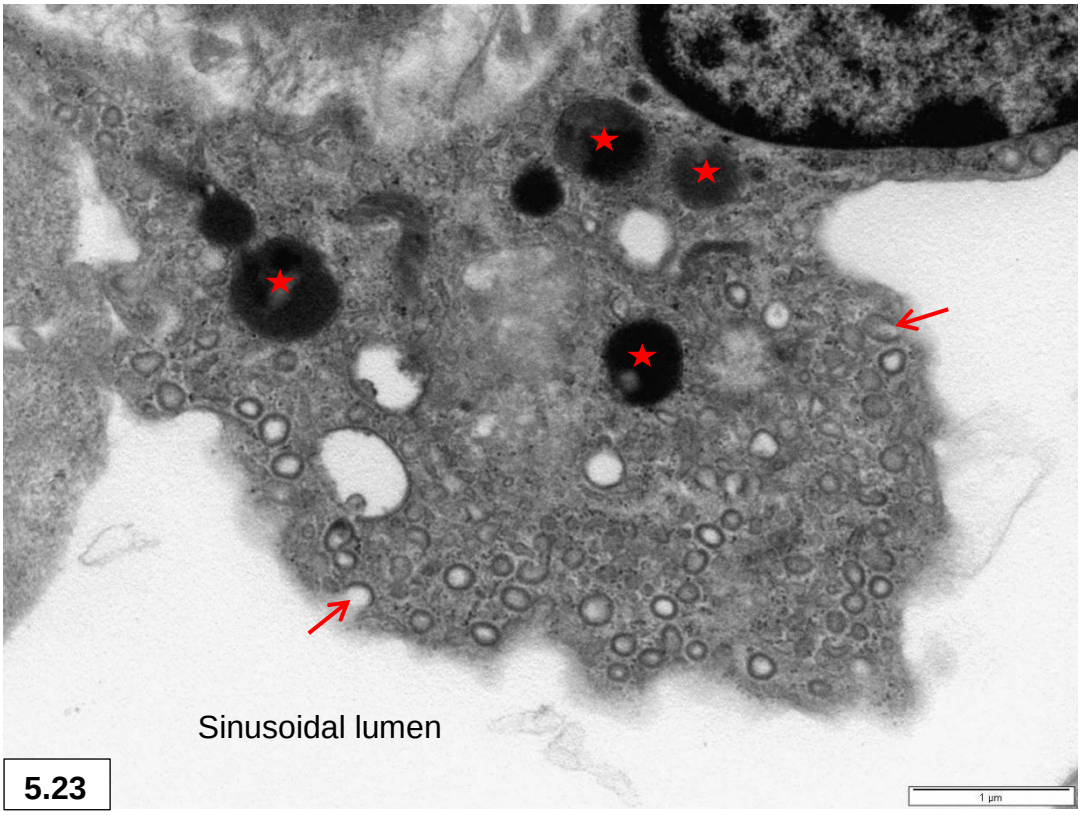

Figure 5.23: Endothelial cell cytoplasm packed with pinocytotic vesicles in different stages of formation. Invagination of the cell membrane (arrows) to form pinocytotic vesicles. Note electron-dense lysosomes (stars).

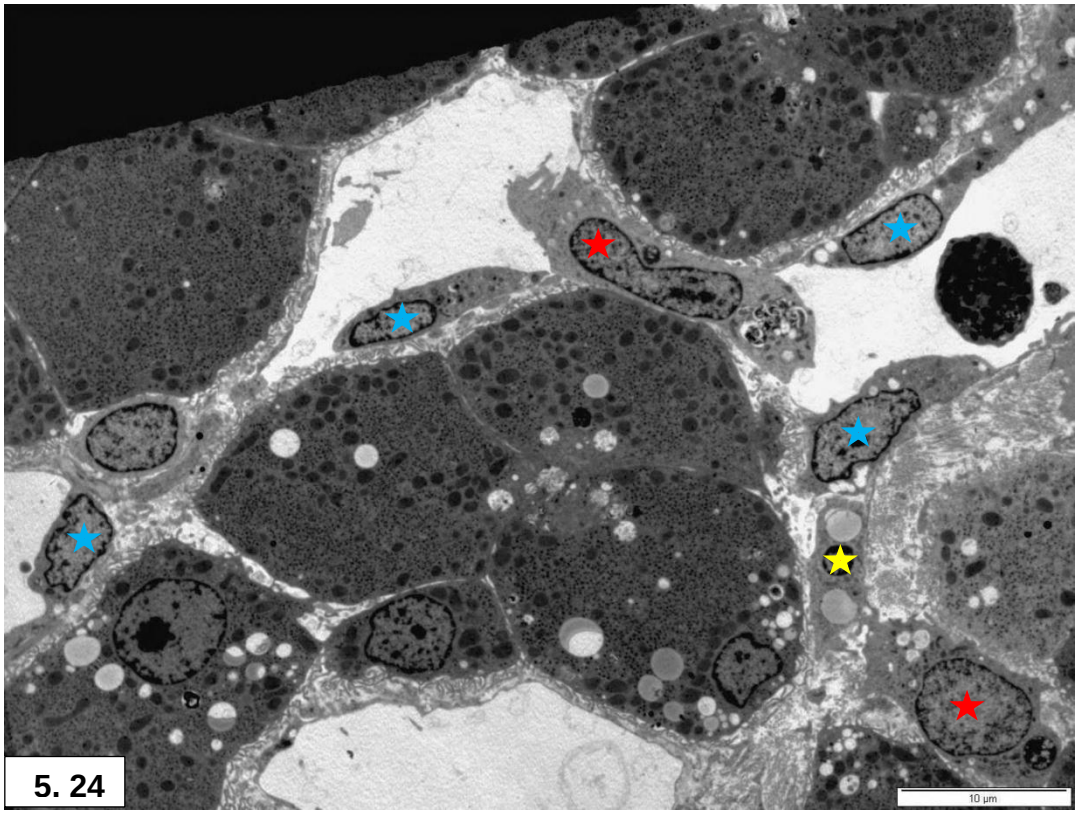

Figure 5.24: Large pleomorphic pigmented Kupffer cell (red star) protruding into the sinusoidal lumen and connecting adjacent sinusoids. Endothelial cell (blue stars), stellate cell (yellow star).

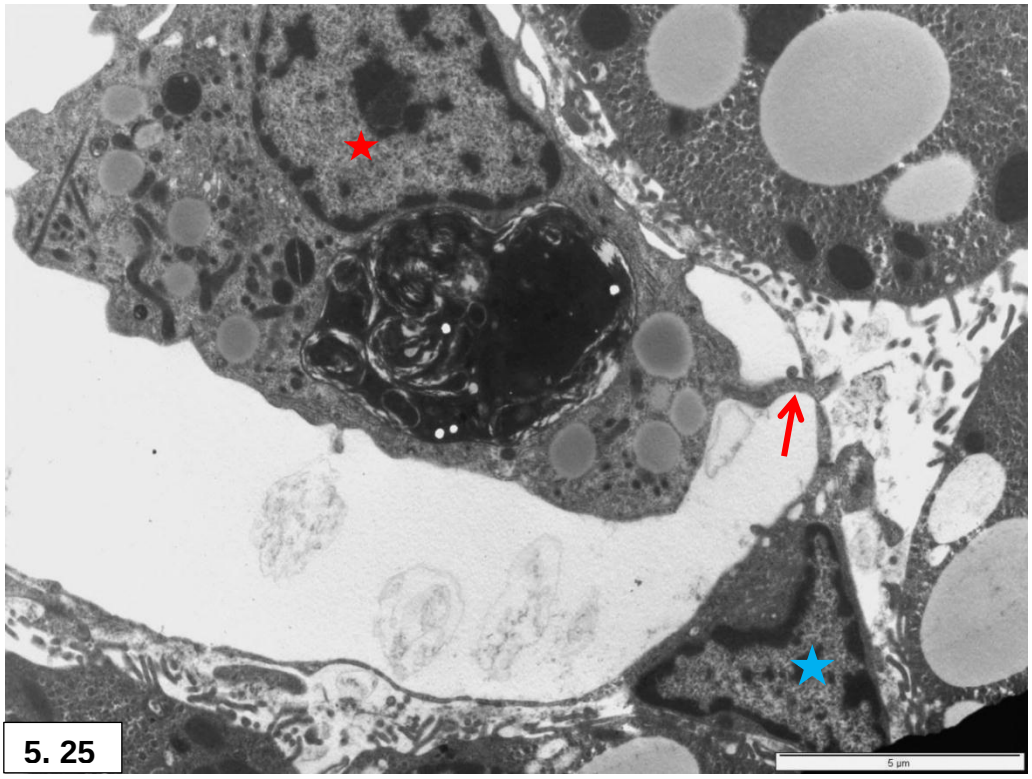

Figure 5.25: Filopodium (arrow) of Kupffer cell (red star) penetrating through endothelium fenestrae. Note cytoplasmic lipid droplets and large phagosome in Kupffer cell. Endothelial cell (blue stars).

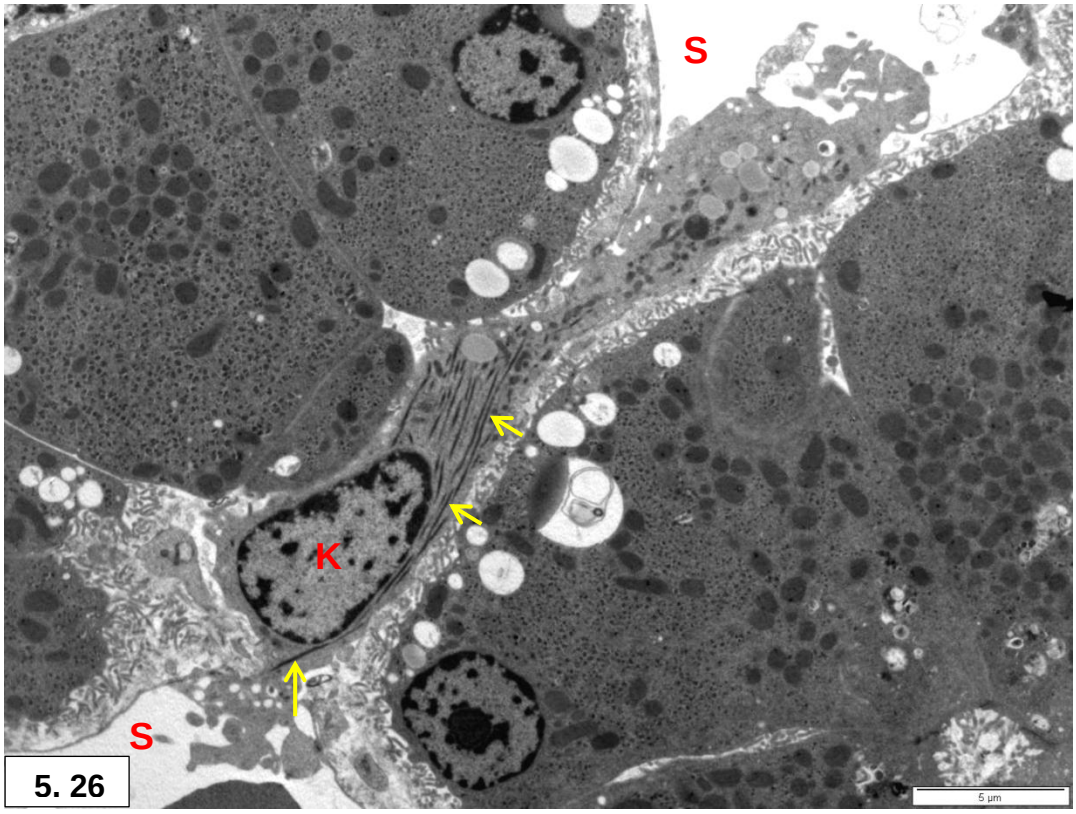

Figure 5.26: Kupffer cell (**K**) insertion between groups of hepatocytes forming a bridge between adjacent sinusoids (**S**). Note longitudinal tubulosome profiles (arrows).

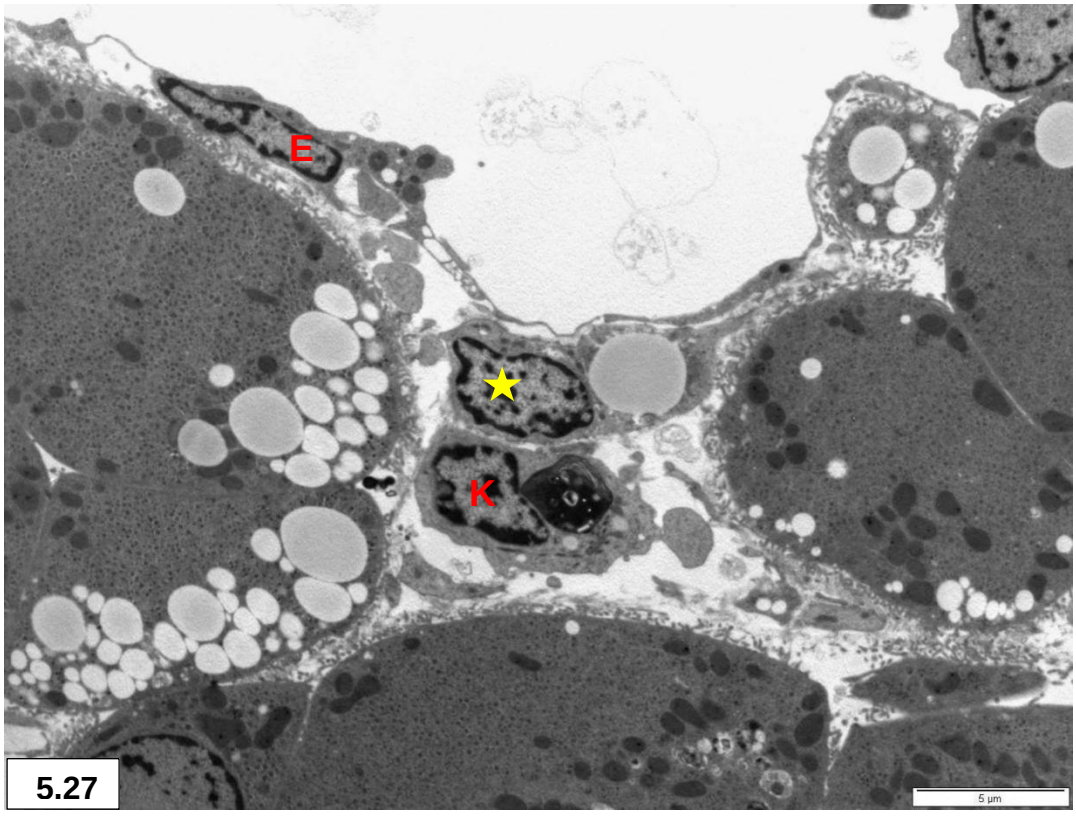

Figure 5.27: Kupffer cell (**K**) located in the space of Disse. Note stellate cell (star) containing a lipid droplet and endothelial cell (**E**) lining a sinusoid.

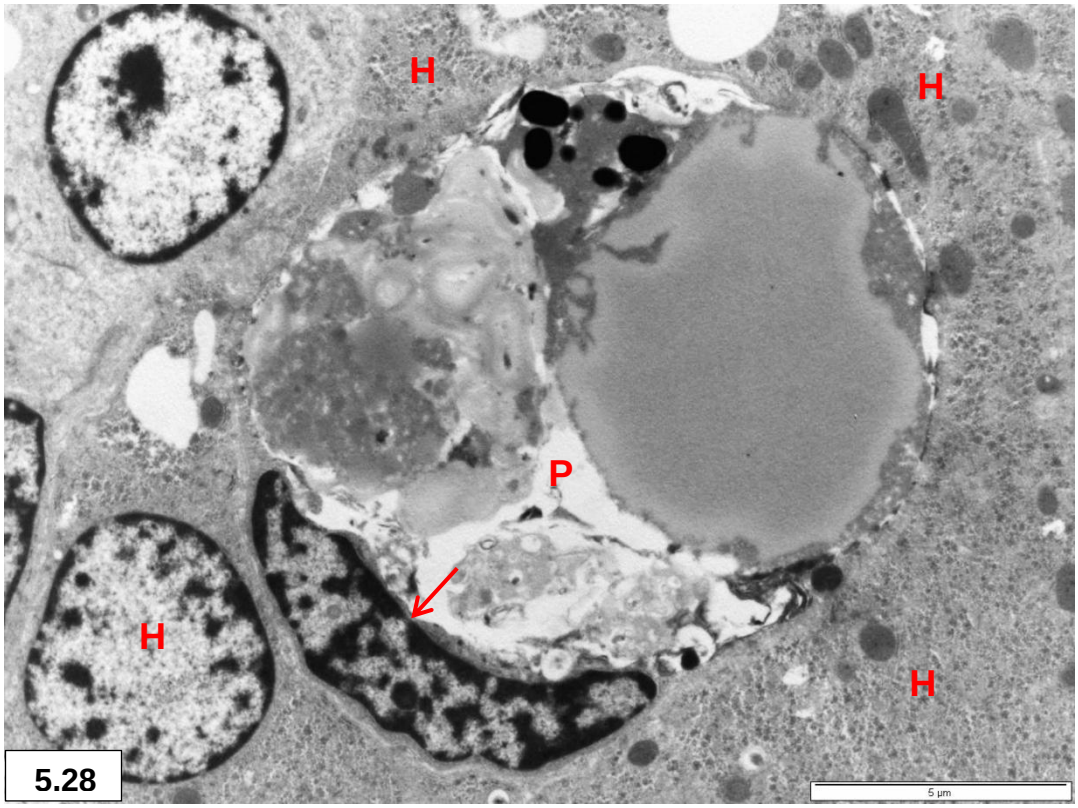

Figure 5.28 & 5.29: Pigmented cells (**P**) forming part of the hepatocyte (**H**) cell cords. Eccentric displacement of nuclei (arrows) by large inclusions containing melanin granules and other constituents. Note stellate cell (star) containing a lipid droplet.

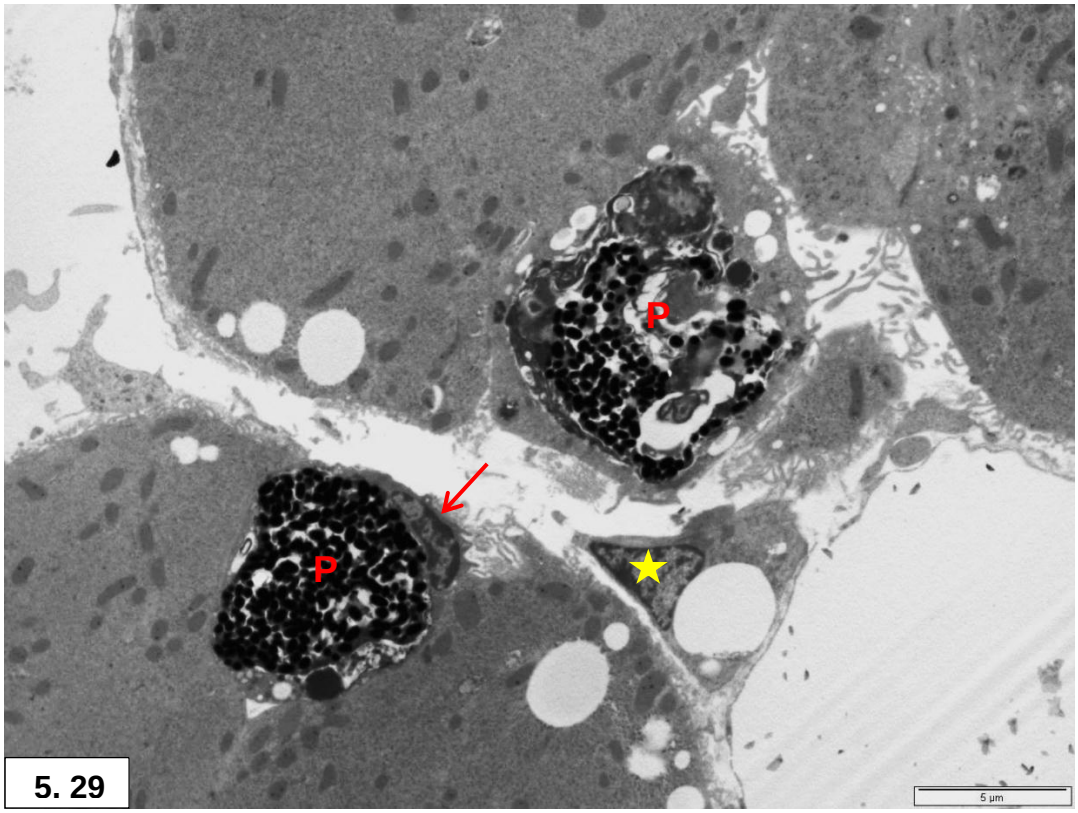

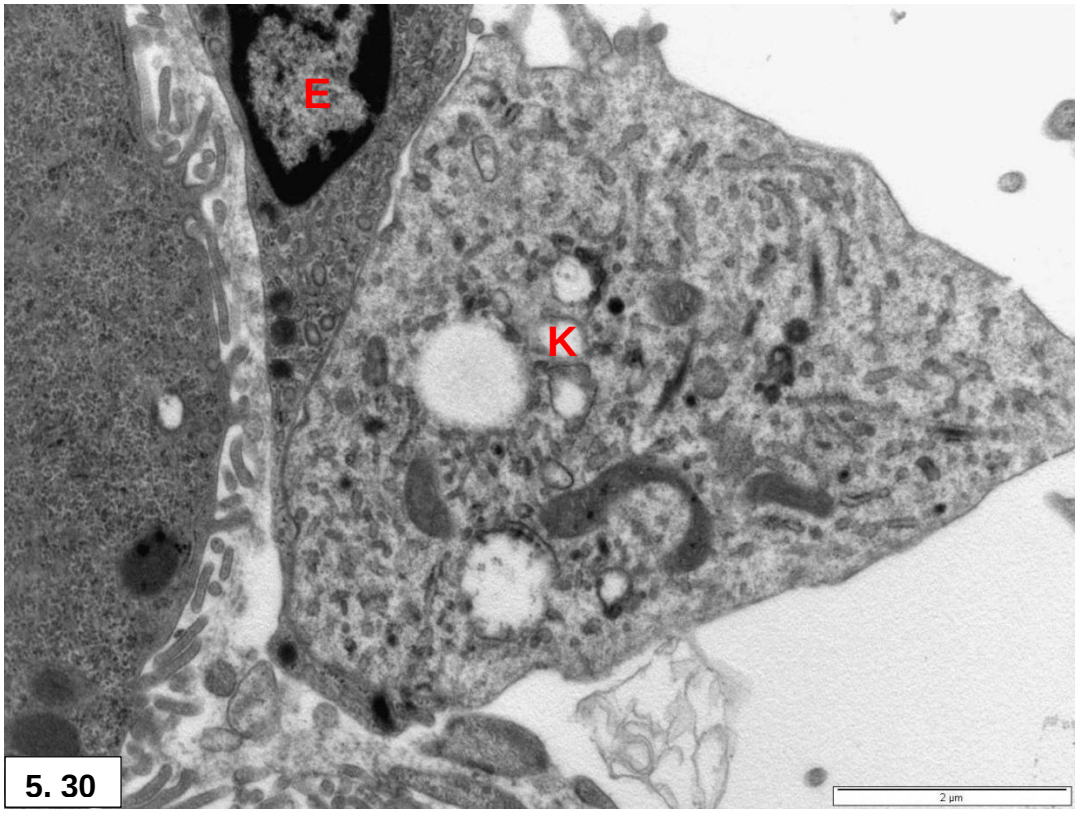

Figure 5.30: Close contact between Kupffer (**K**) and endothelial cell (**E**).

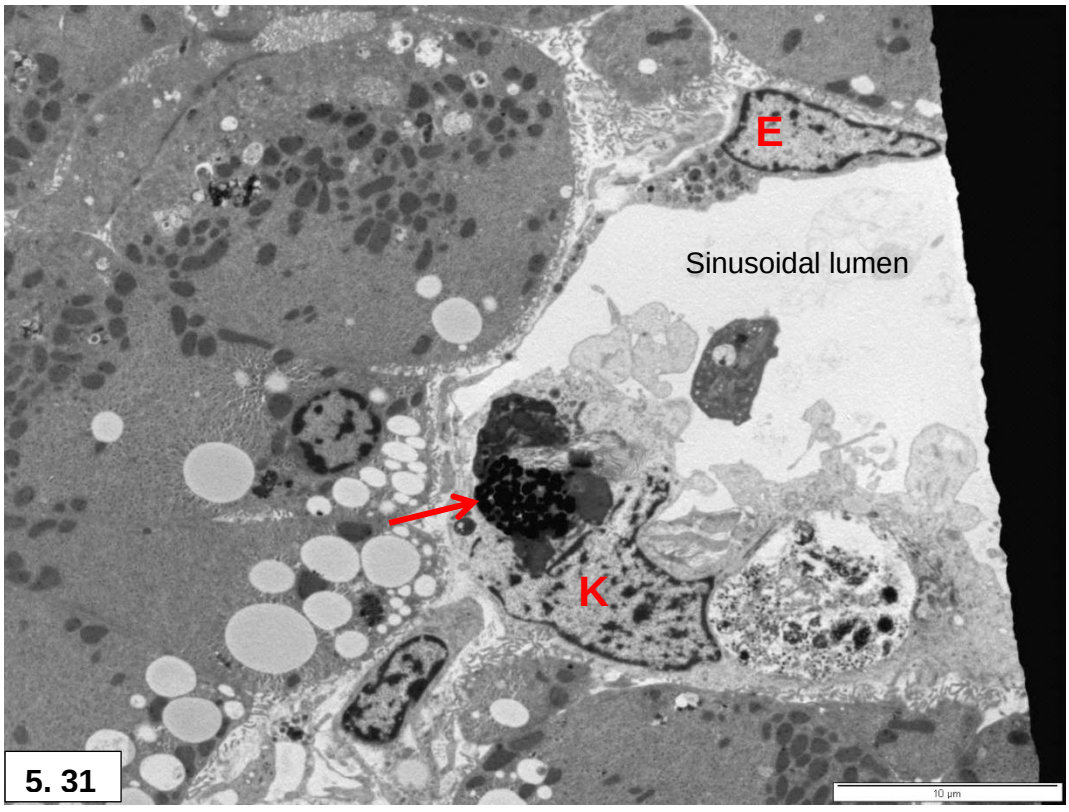

Figure 5.31: Melanin granules (arrow) present in luminal Kupffer cell (**K**) forming part of the sinusoidal lining. Endothelial cell (**E**).

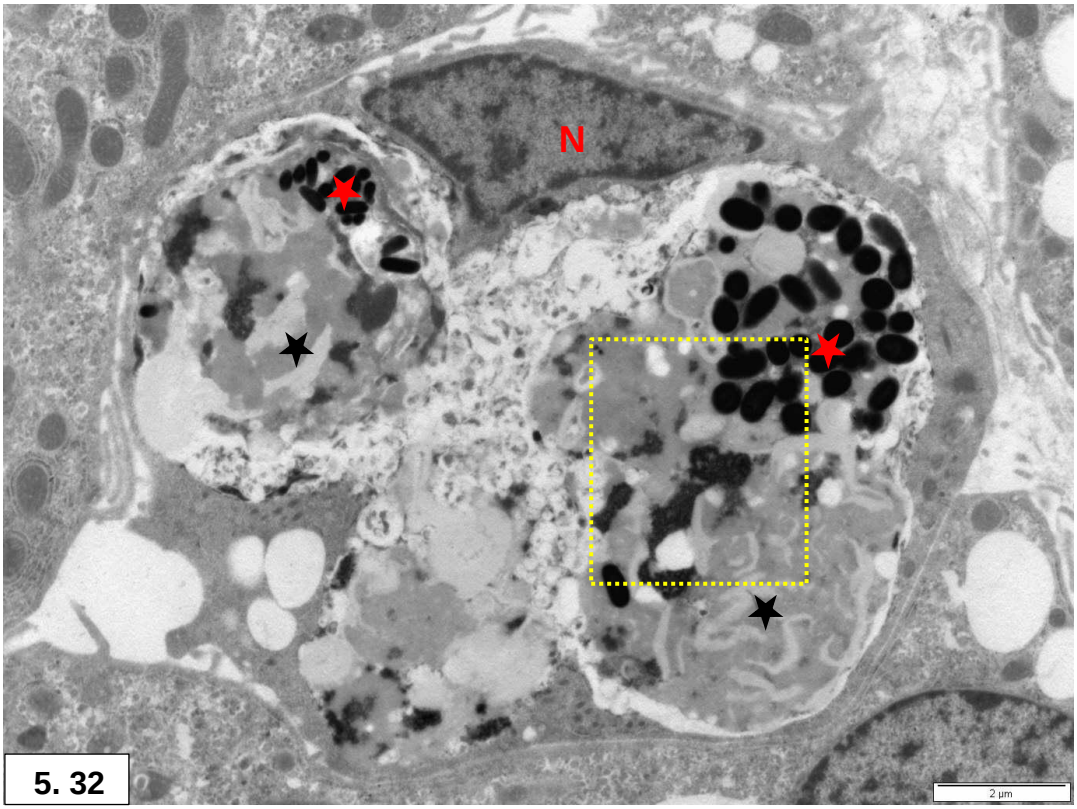

Figure 5.32: Pigmented cell containing melanin granules (red stars) mixed with electron-lucent fragments (ceroid) (black stars). Note eccentric displacement of nucleus (**N**).

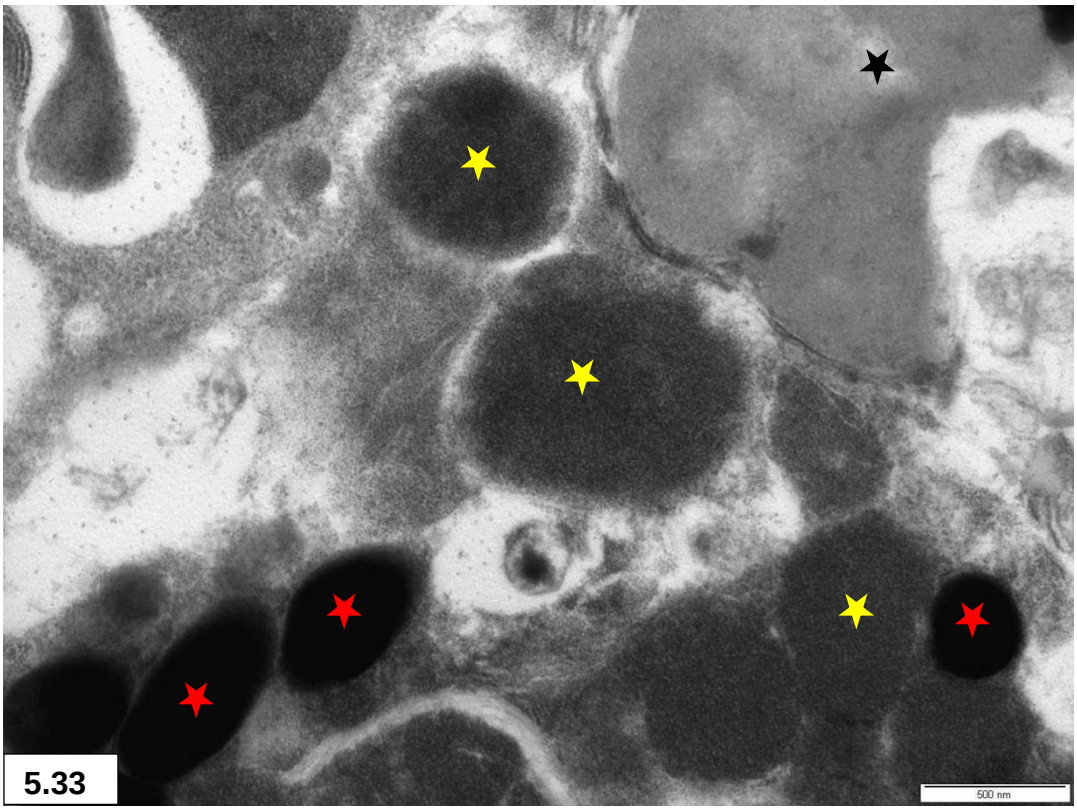

Figure 5.33: Higher magnification of a similar area to that blocked in Fig. 5.32. Note melanin granules (red stars), fine granular hemosiderin component (yellow stars) and ceroid (black stars).

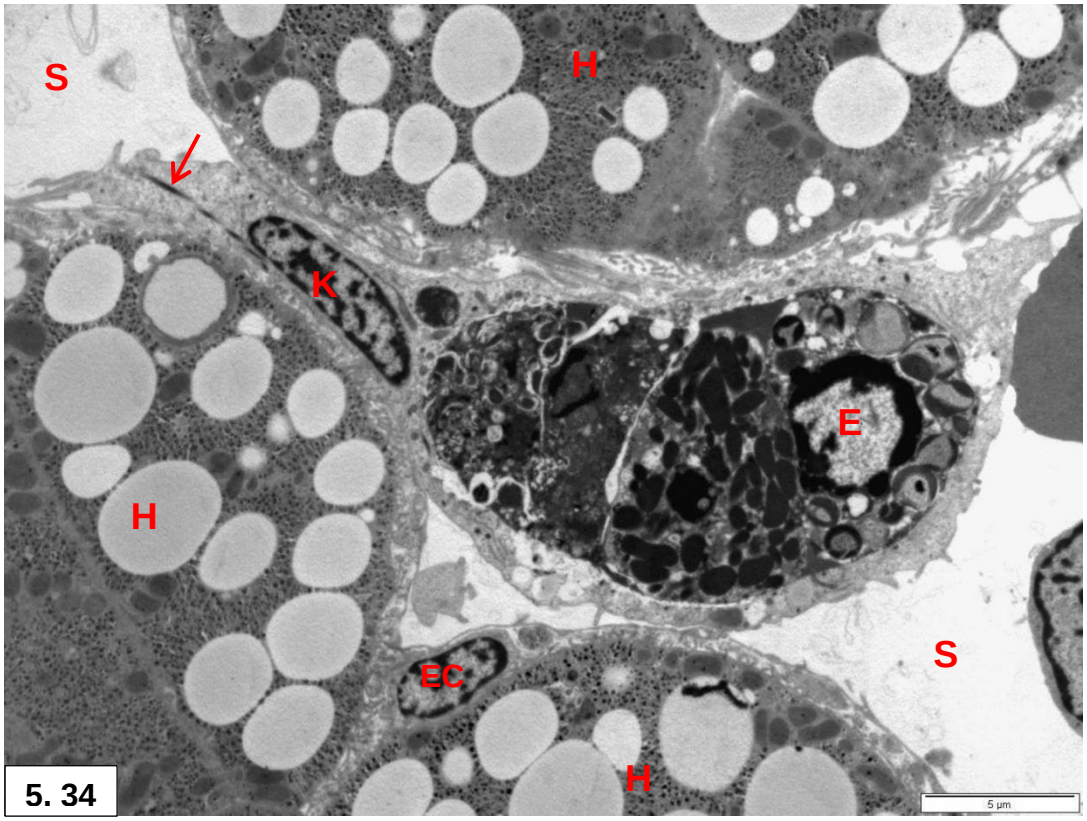

Figure 5.34: Engulfment of eosinophil (**E**) by Kupffer cell (**K**). Note Kupffer cell insertion between adjacent sinusoids (**S**) and cytoplasmic tubulosomes (arrow). Hepatocytes (**H**), endothelial cell (**EC**).

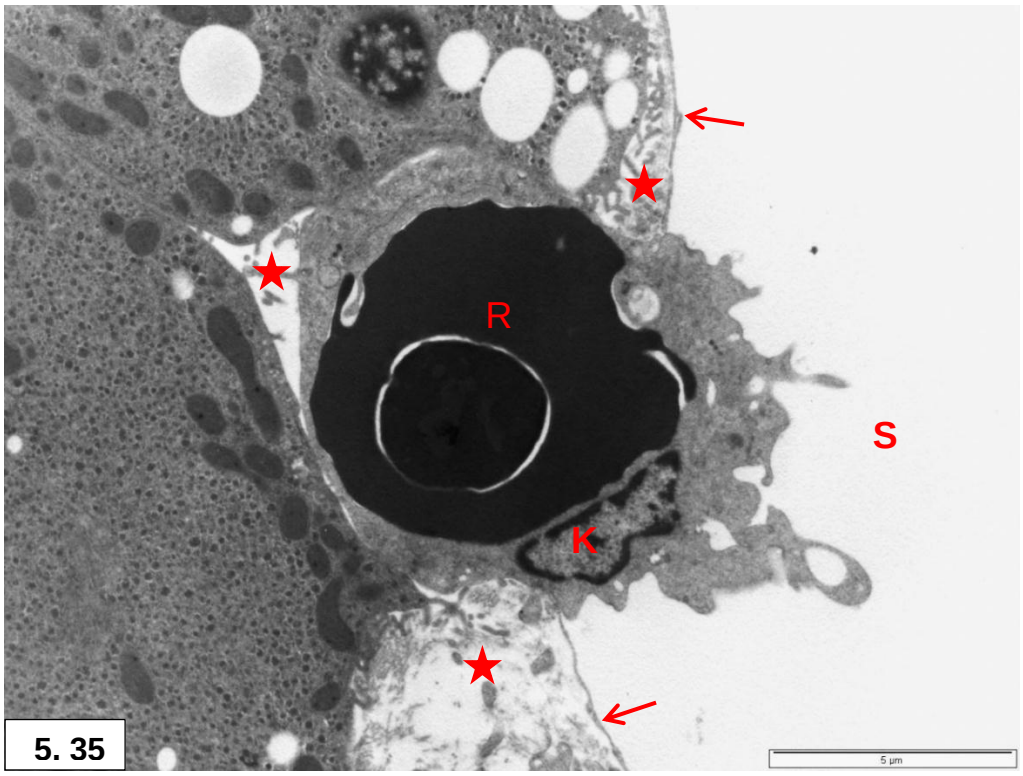

Figure 5.35: Engulfment of red blood cell (**R**) by Kupffer cell (**K**) that extends from the space of Disse (stars) through the endothelium (arrows) into the lumen of a sinusoid (**S**).

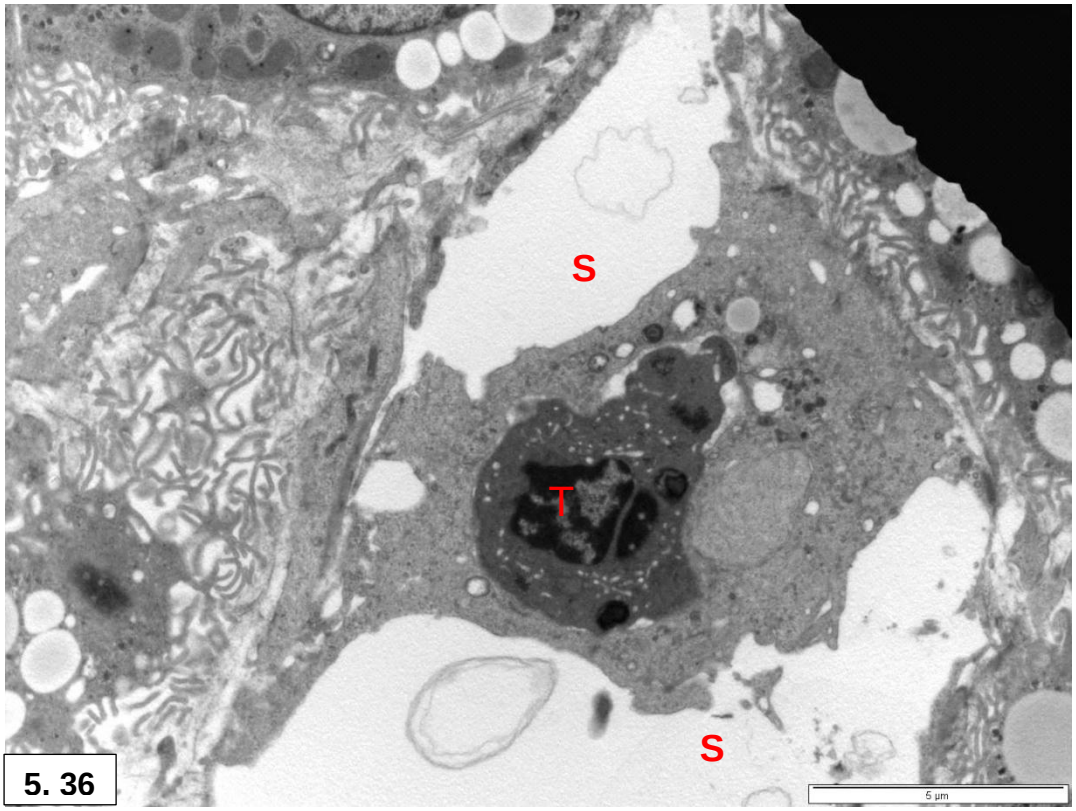

Figure 5.36: Kupffer cell bridging a sinusoidal lumen (**S**) and engulfing a thrombocyte (**T**).

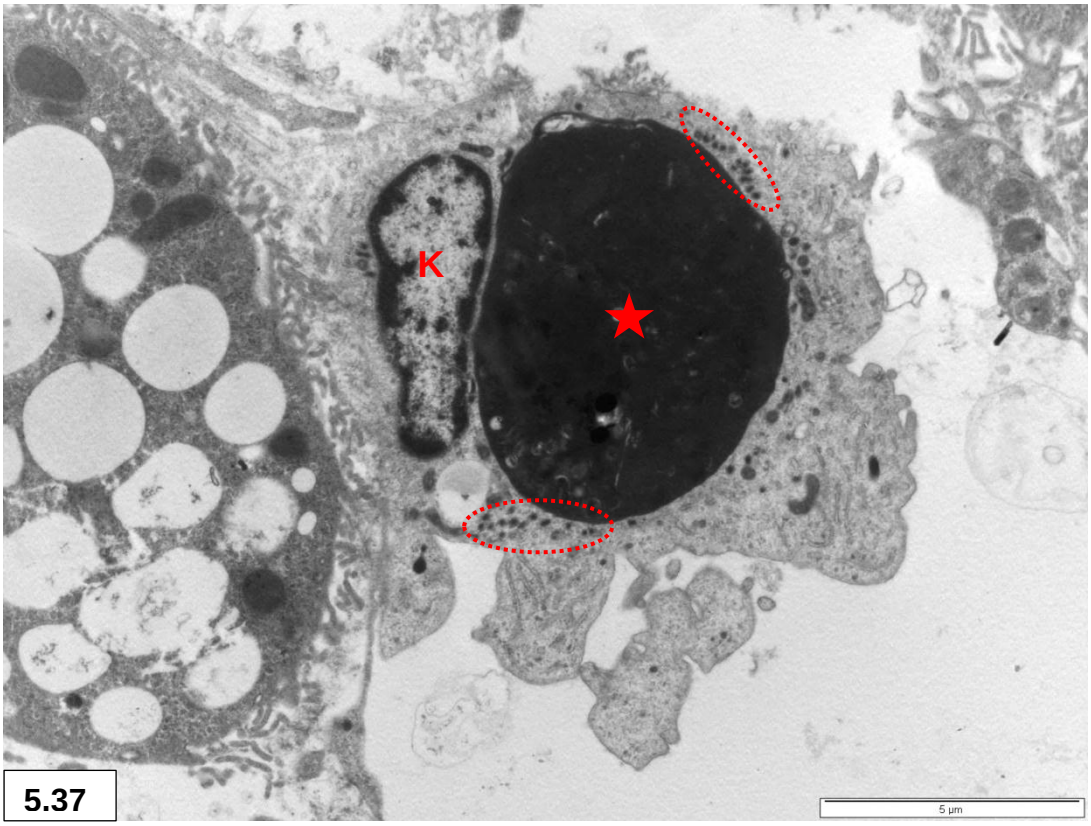

Figure 5.37: Tubulosomes (dashed circles) in Kupffer cell (**K**) separated into smaller groups around a phagosome (star).

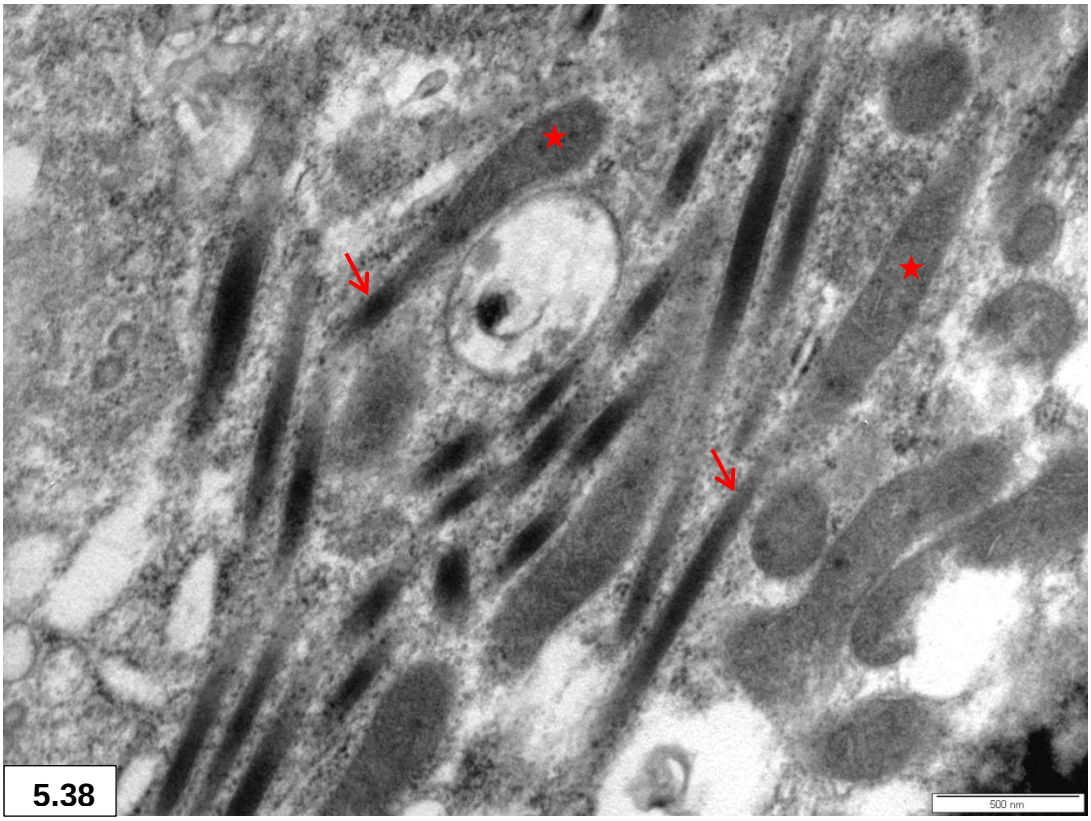

Figure 5.38: Close contact between elongated tubulosomes (arrows) and mitochondria (stars) in Kupffer cell.

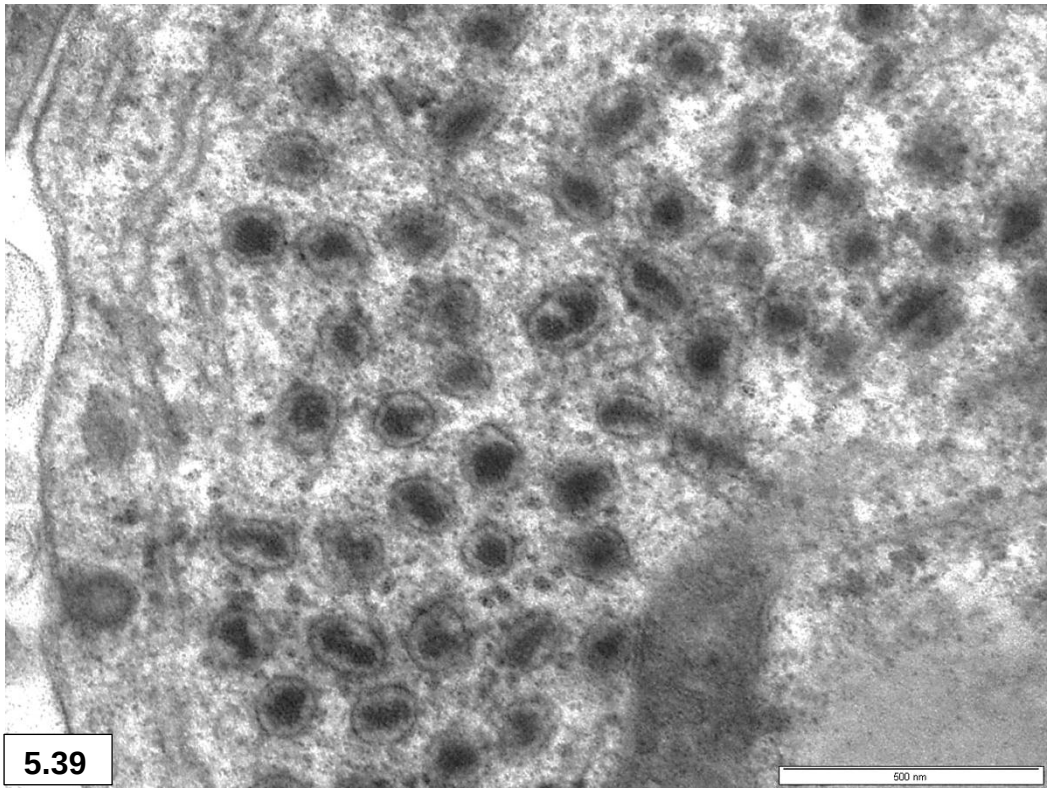

Figure 5.39: Variable cross-sectional interior profiles of tubulosomes: circular and angular contours are apparent. Note single outer membrane.

Figure 5.40: Tubulosome (arrow) illustrating divided interior profiles. Melanin granules (stars).

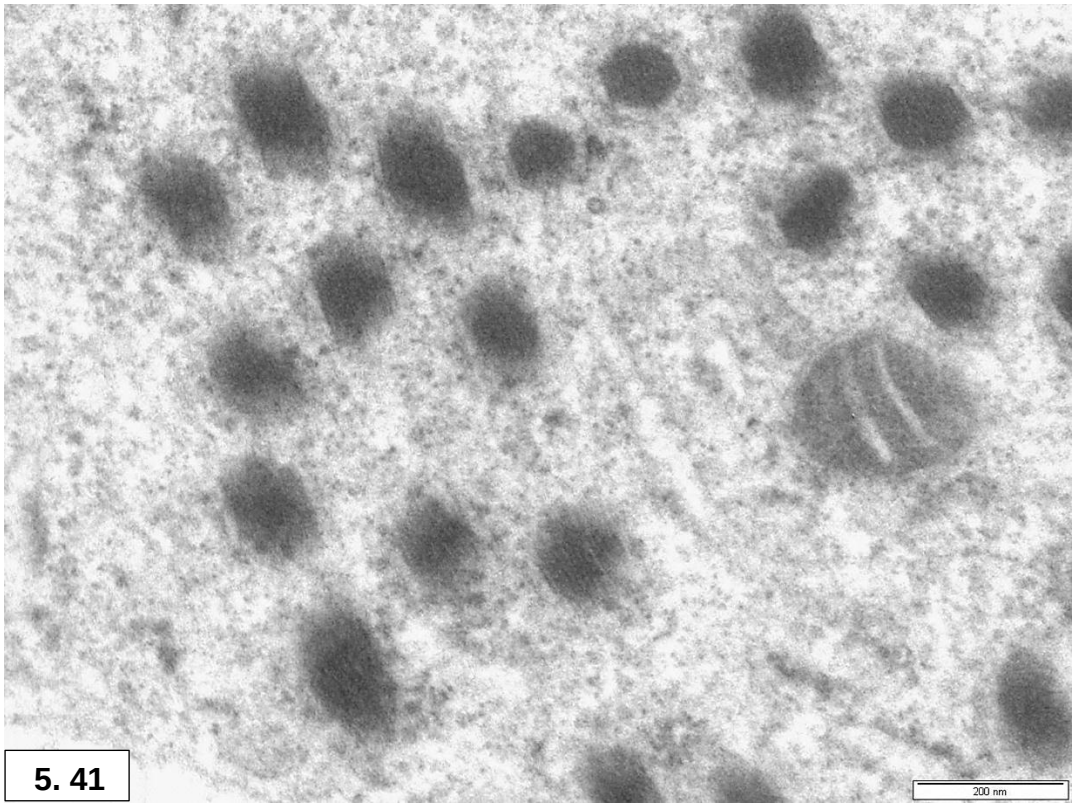

Figure 5.41: Electron-dense filamentous material in tubulosomes.

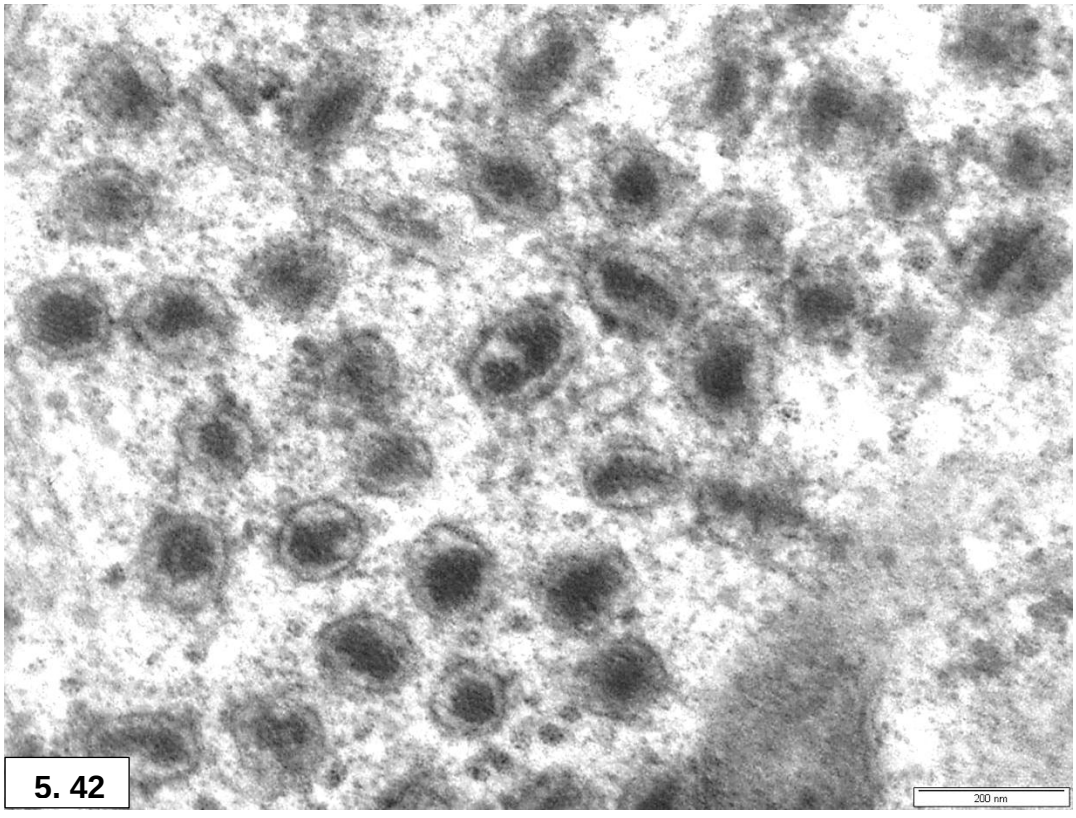

Figure 5.42: Electron-dense crystalline material in tubulosomes.

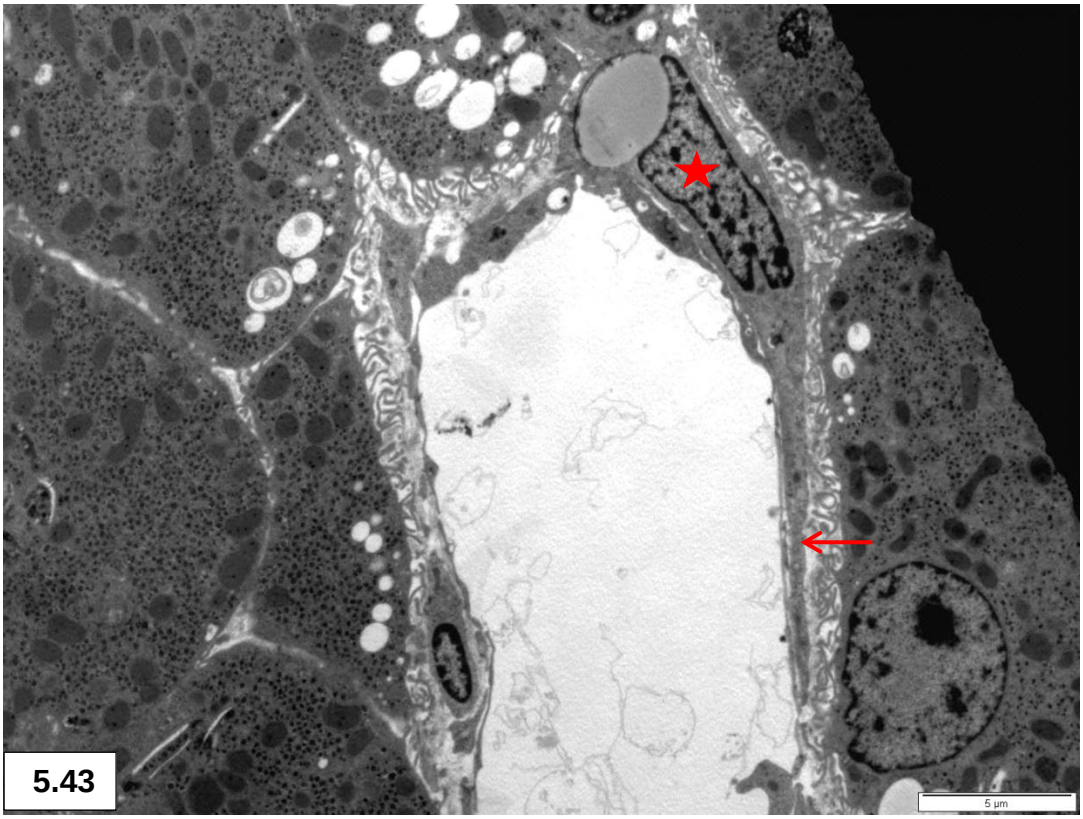

Figure 5.43 & 5.44: Stellate cells (stars) in the space of Disse. Note long cytoplasmic extension (arrow) in close contact with endothelial cell and prominent lipid droplet in the cytoplasm.

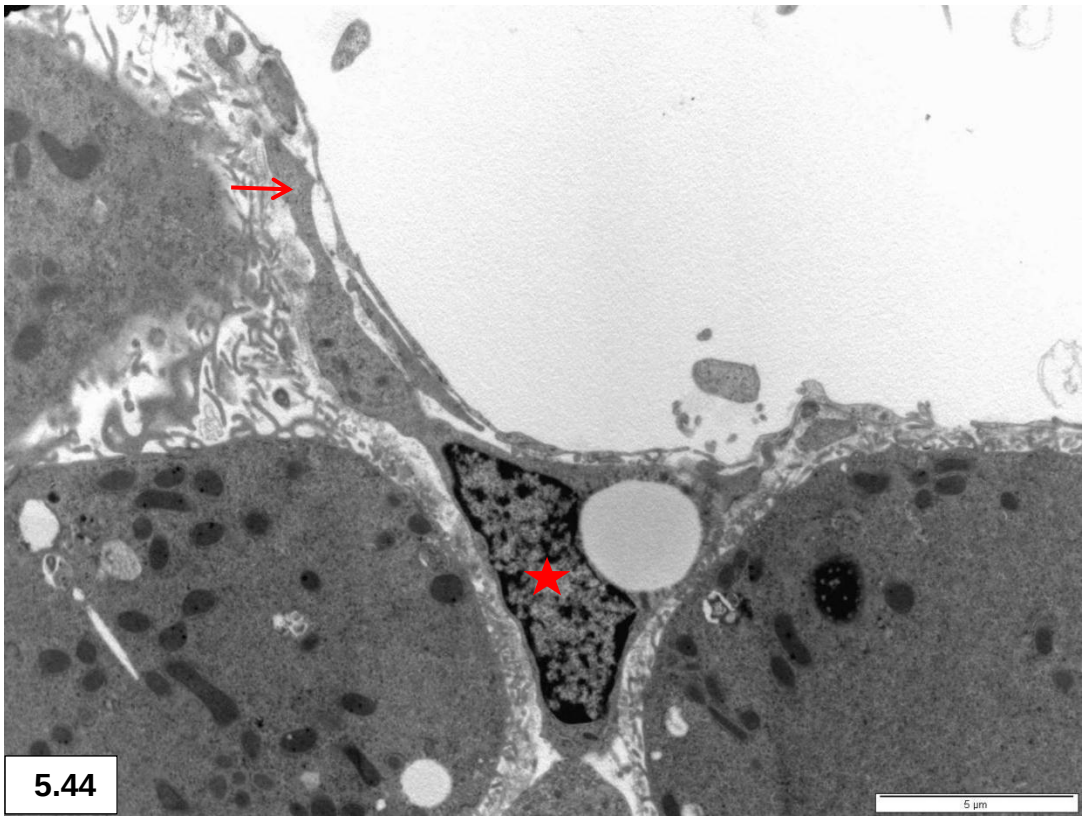

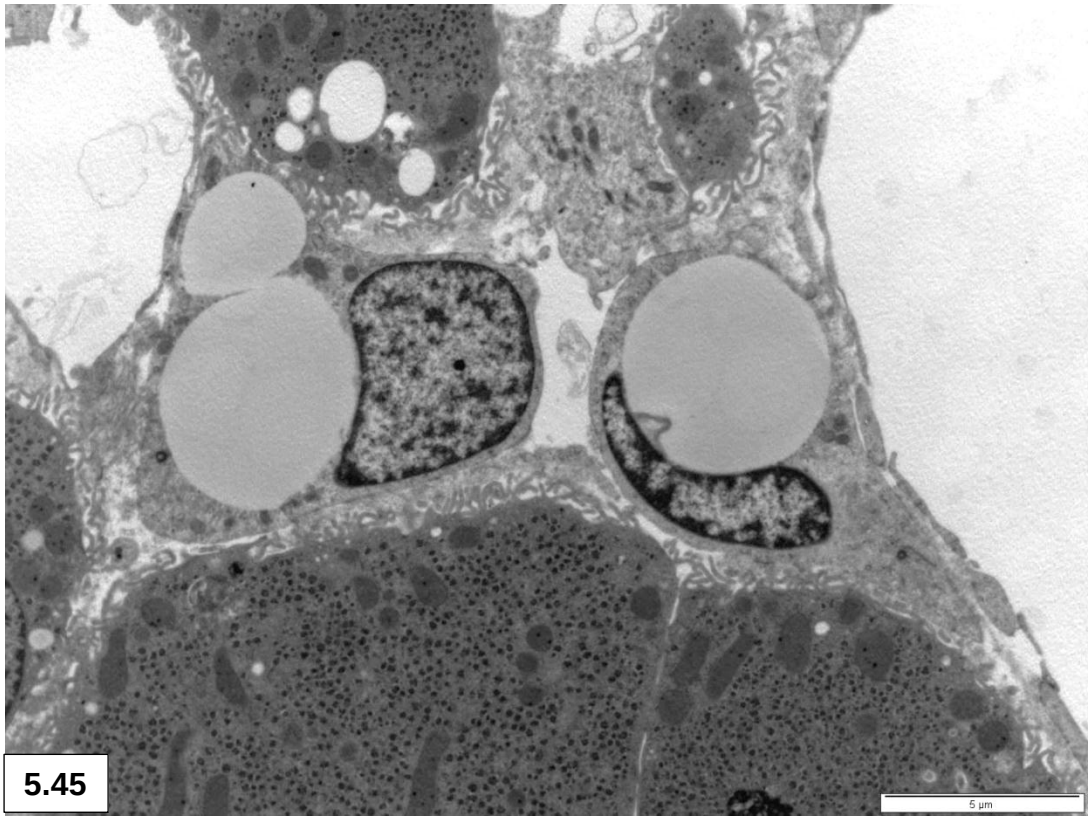

Figure 5.45 & 5.46: Prominent, non-membrane bound lipid droplets in stellate cells indenting the nucleus giving it an angular shape. Note close contact with endothelial cell (**E**).

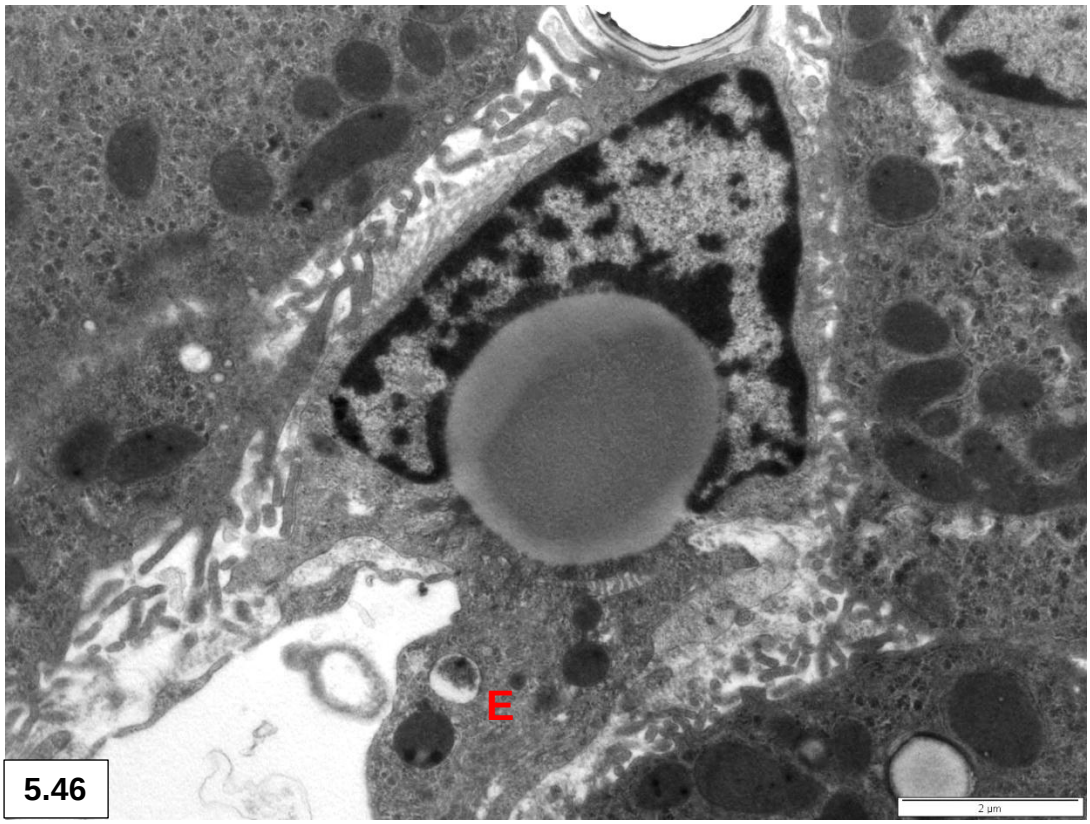

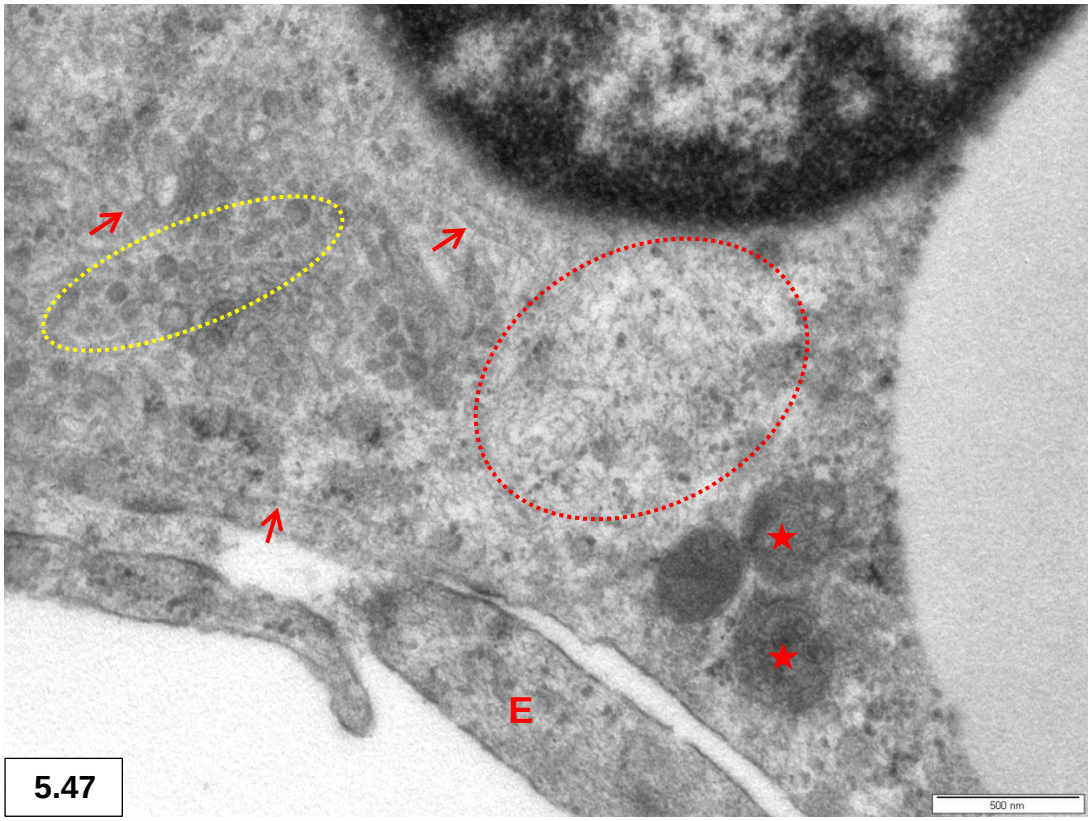

5.47

Figure 5.47 & 5.48: Cytoplasmic filaments (red dashed circle), microtubules (red arrows) and multivesicular bodies (stars) in stellate cells. Cytoplasmic structure with the periodicity of long-spacing collagen (yellow arrow). Note coated (black arrow) and pinocytotic vesicles (yellow dashed circle), and centriole (blue arrow). Endothelial extensions (**E**).

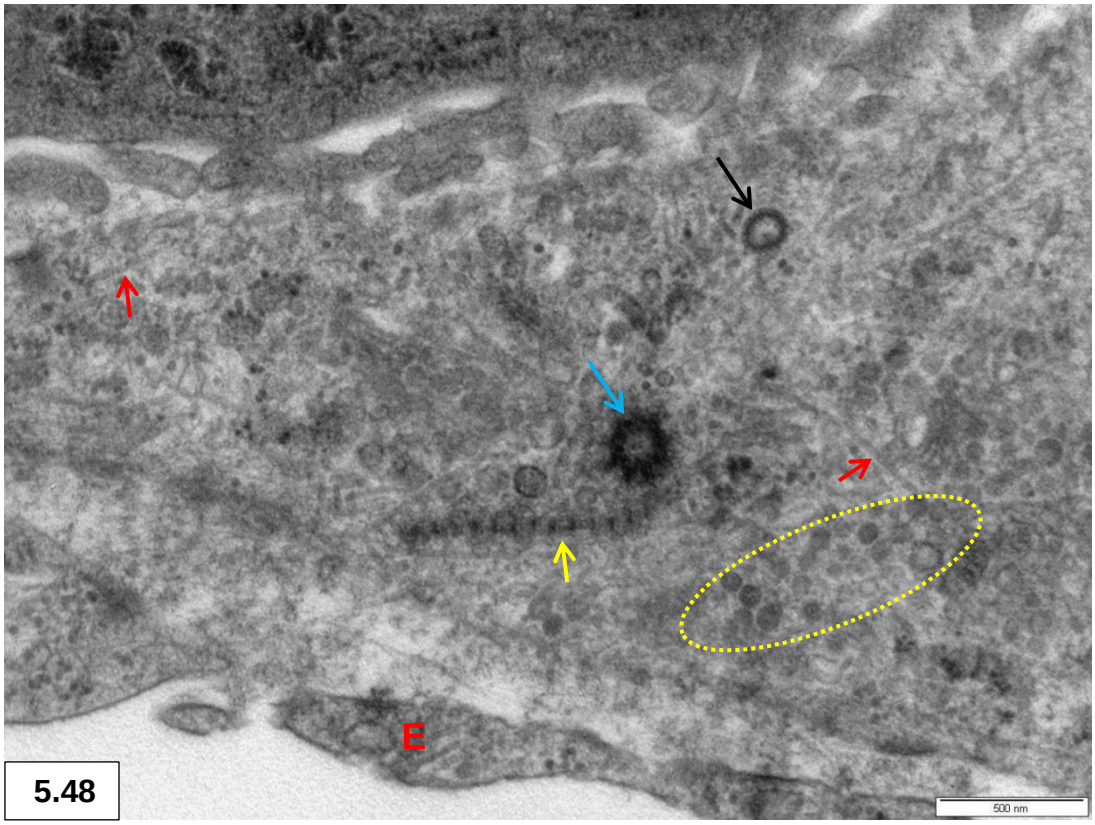

5.48

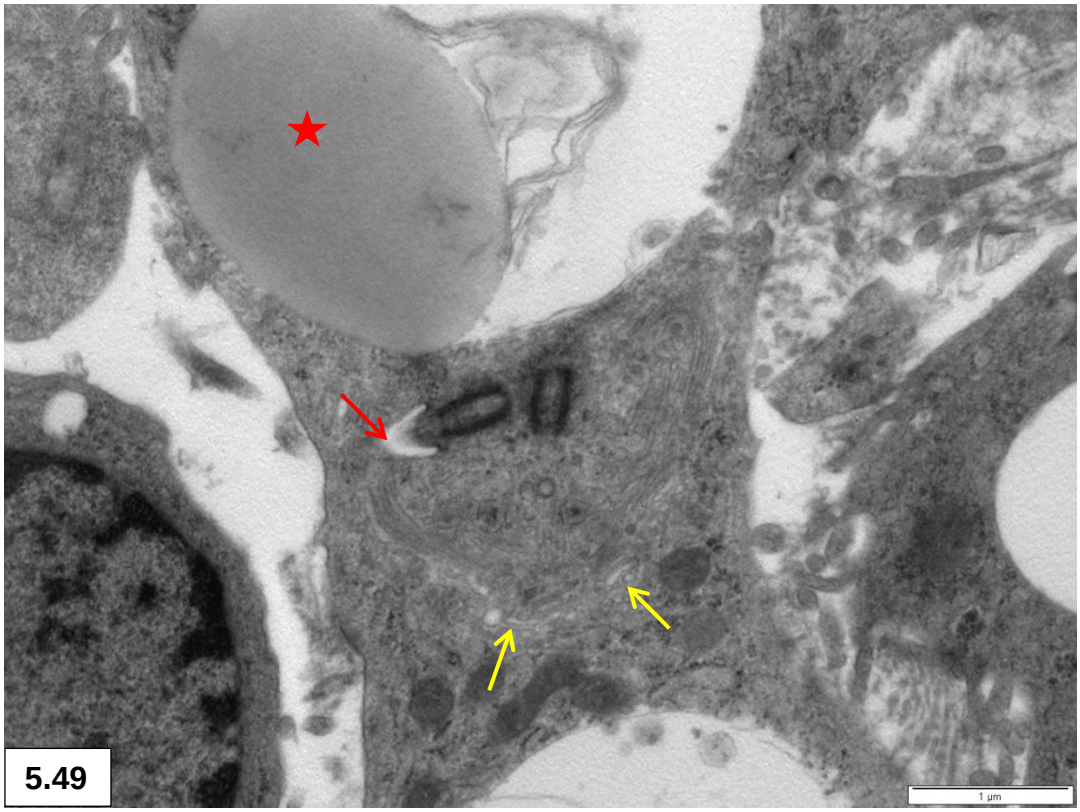

Figure 5.49: Centriole pair forming a ciliary basal body in a stellate cell. Note the intracytoplasmic ciliary canal (red arrow), Golgi (yellow arrows) and lipid droplet (star).

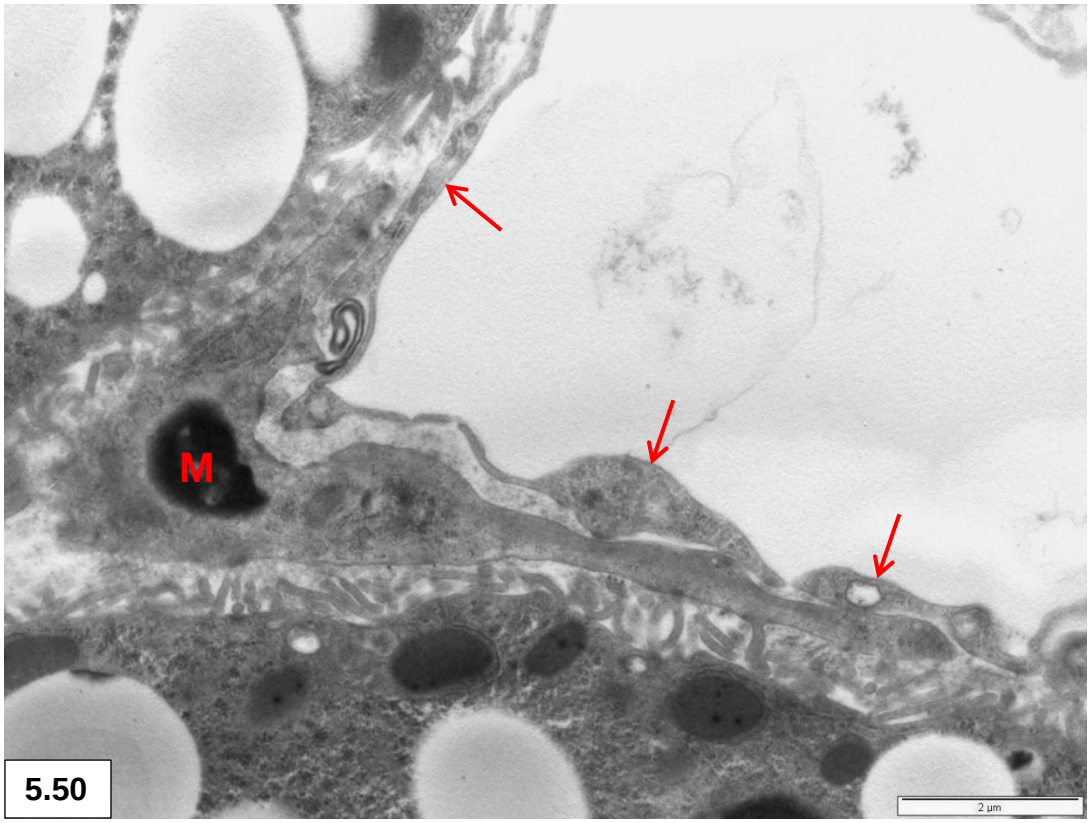

Figure 5.50: Myofibroblastic cell (**M**) with subendothelial extensions in the space of Disse. Endothelial cell (arrows).

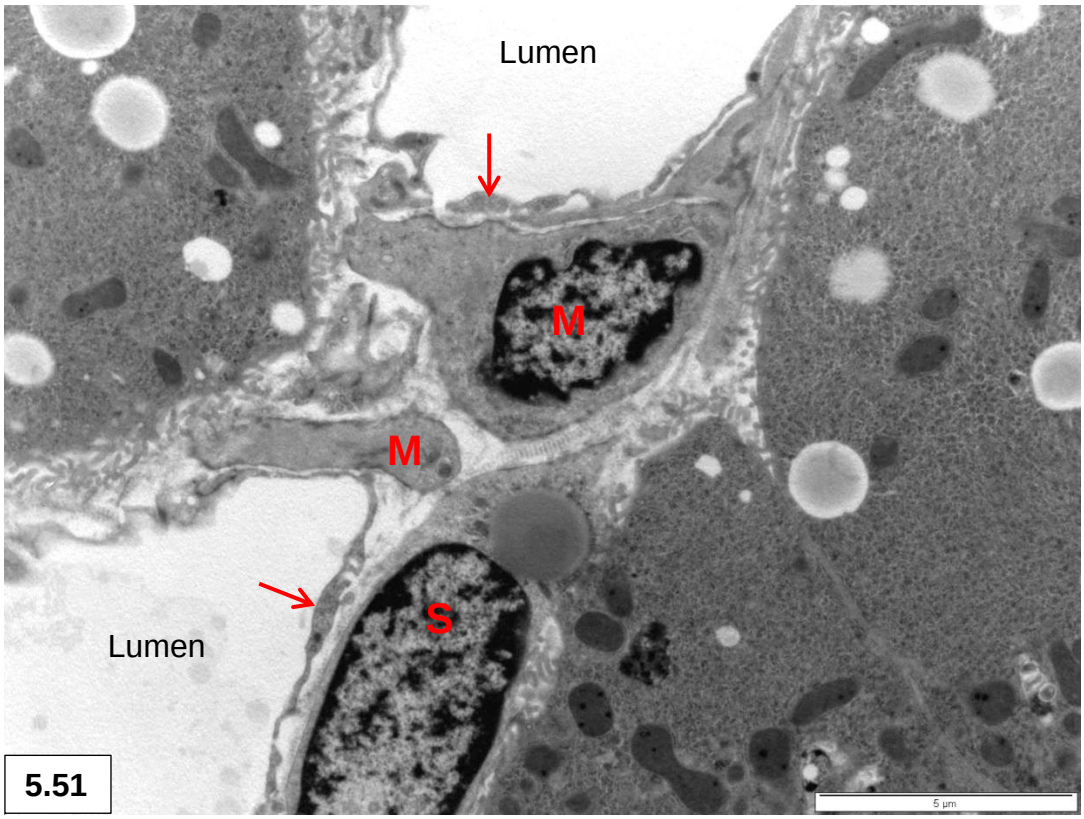

Figure 5.51 : Myofibroblastic cells (**M**) and stellate cell (**S**) containing a lipid droplet occupying the same area in the space of Disse. Endothelial cells (arrows).

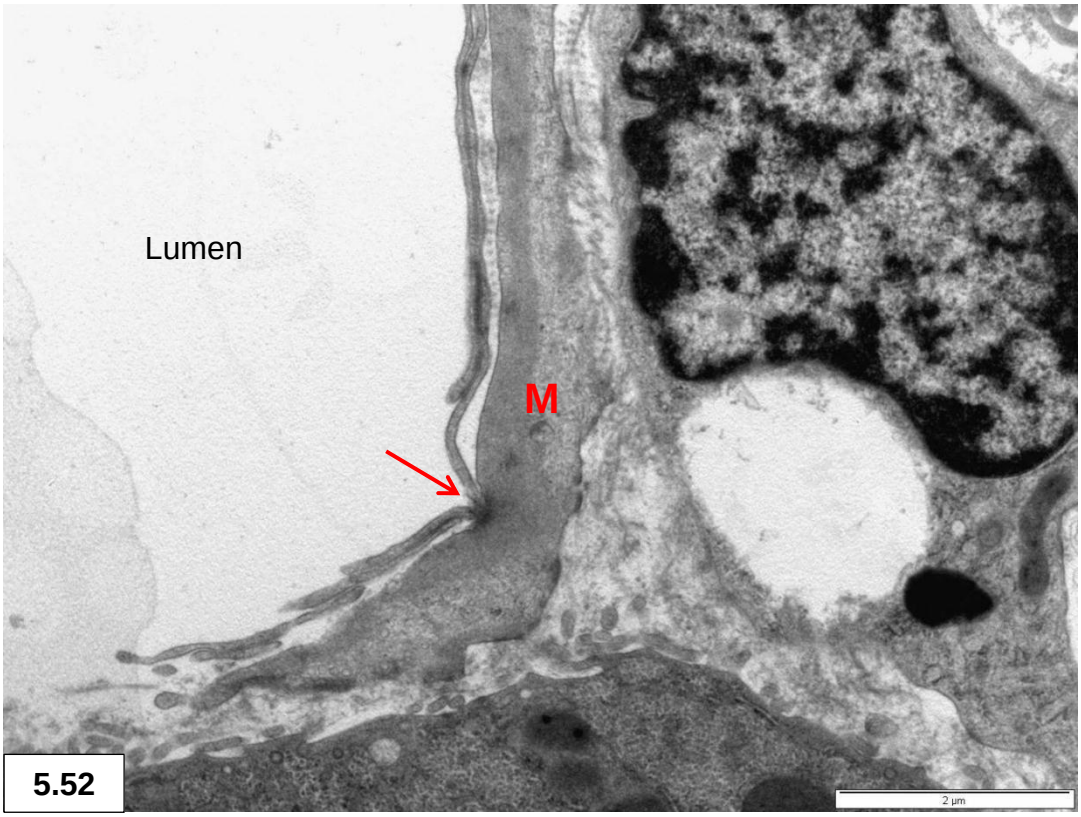

Figure 5.52: Myofibroblastic cell extension (**M**) touching an endothelial cell (arrow).

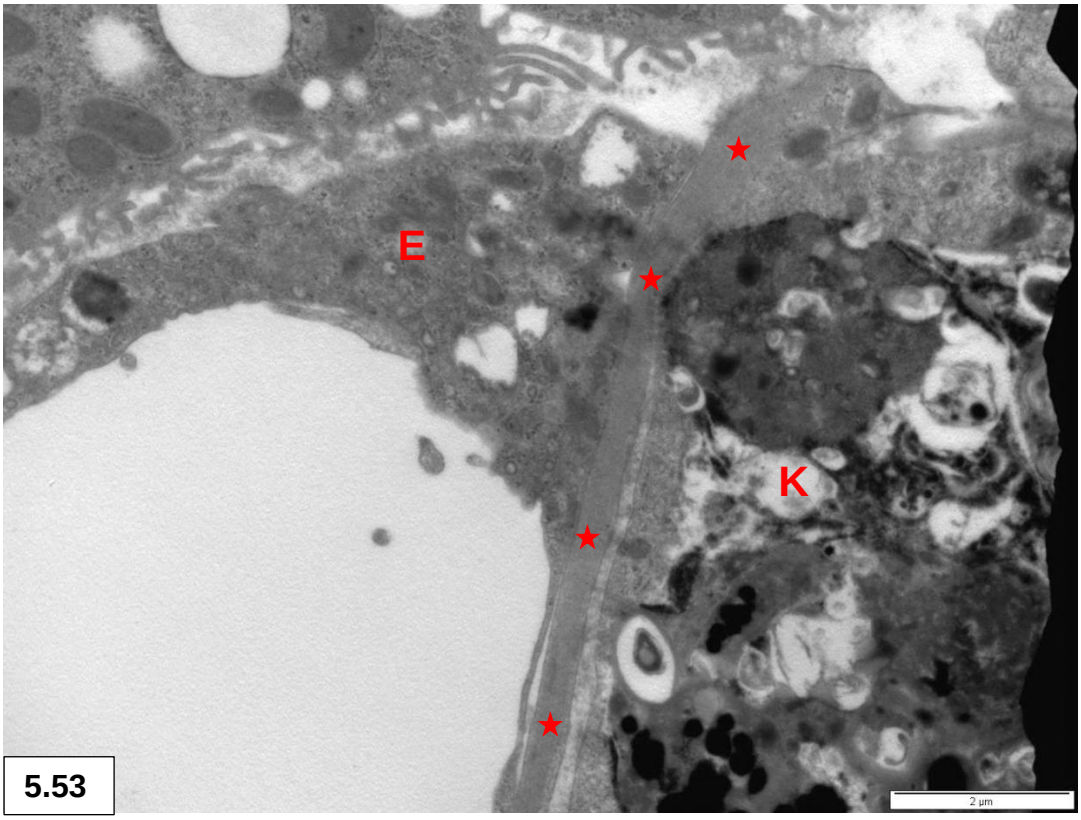

Figure 5.53: Cytoplasmic extension (stars) of a myofibroblastic cell in close contact with an endothelial (E) and a Kupffer cell (K).

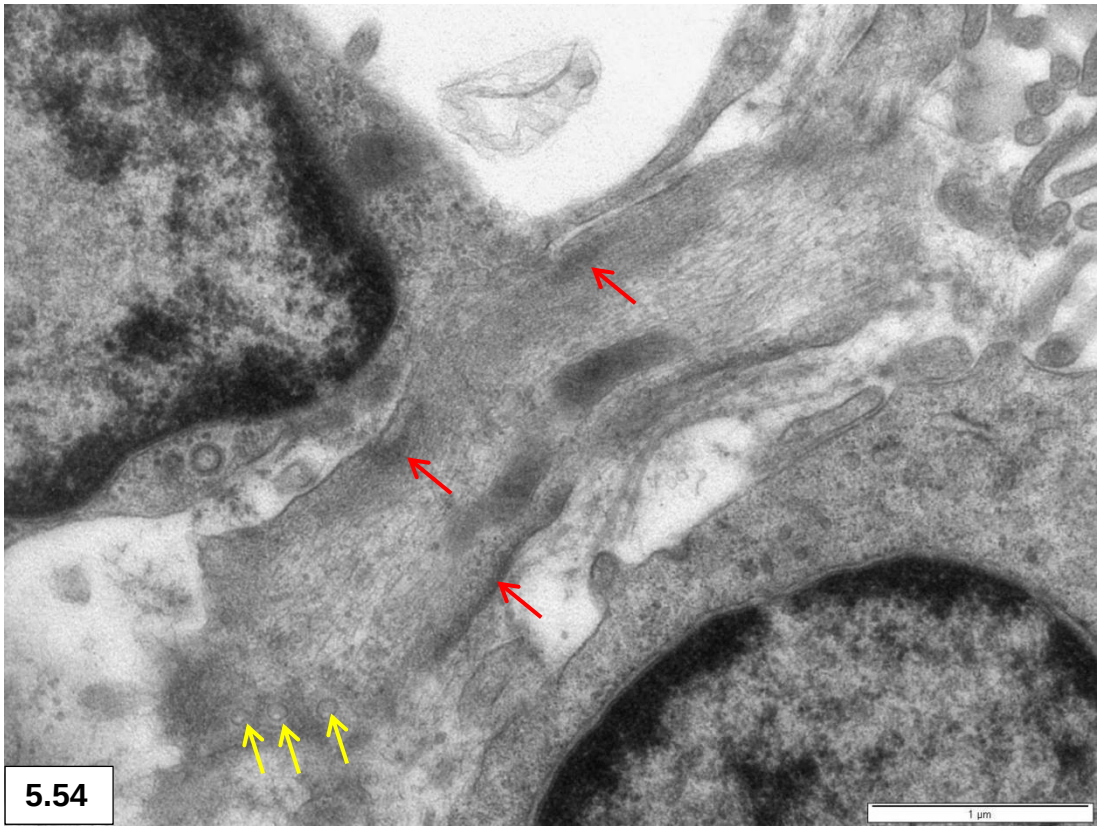

Figure 5.54 & 5.55: Filaments forming subplasmalemmal densities (red arrows) in a myofibroblastic cell. Pinocytotic vesicles (yellow arrows).

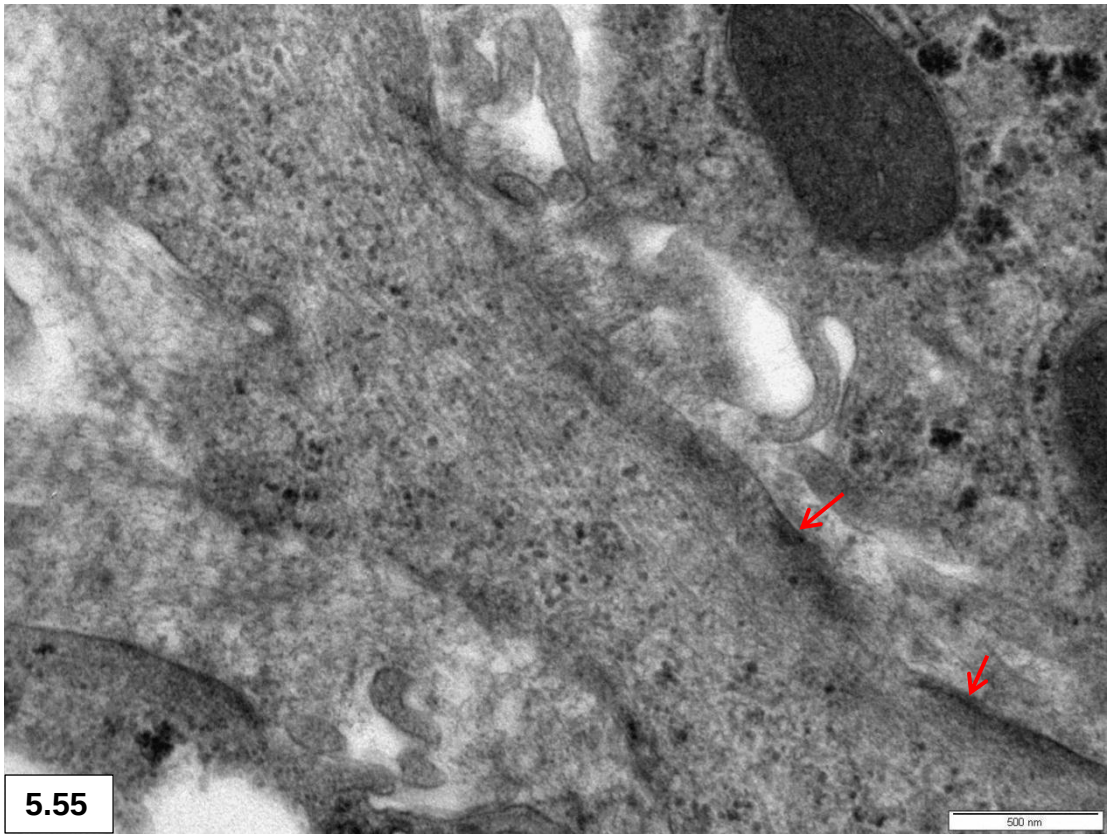

Figure 5.55: Myofibroblastic cell cytoplasm containing numerous longitudinally disposed microtubules. Note subplasmalemmal densities (red arrows).

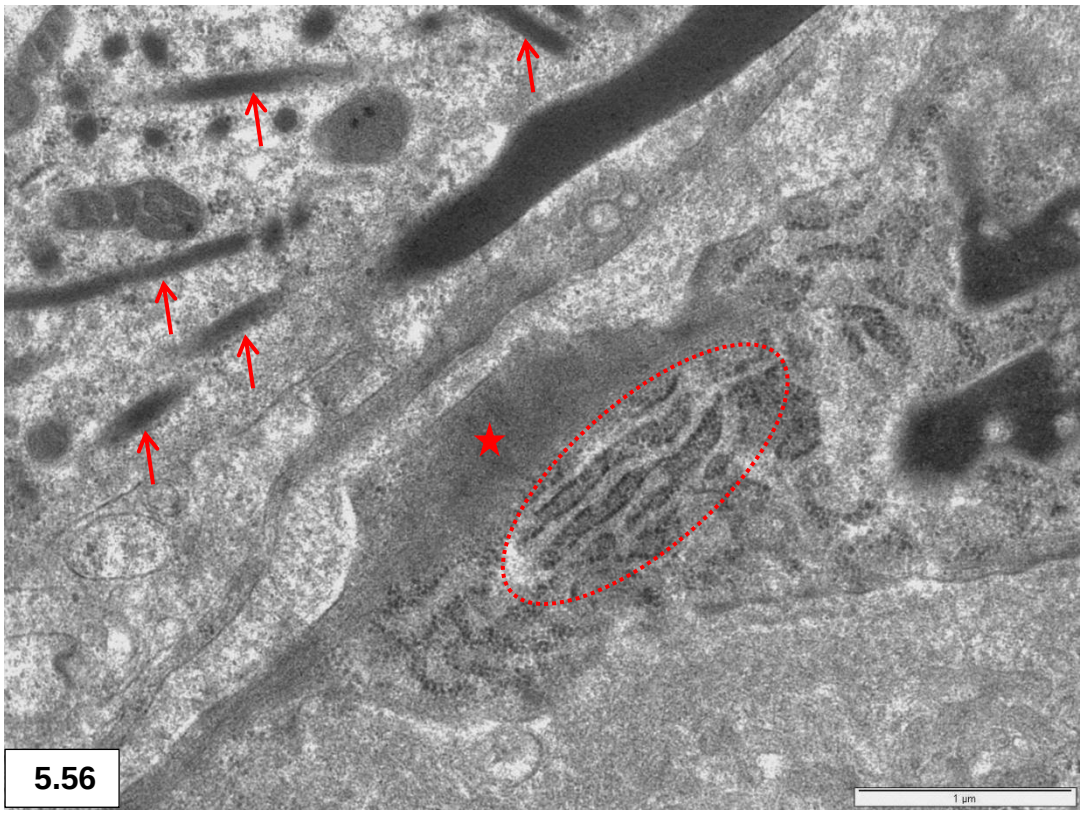

Figure 5.56: Dilated GER (dashed circle) and fine filaments (star) in a myofibroblastic cell. Note tubulosomes (arrows) in a neighbouring Kupffer cell.

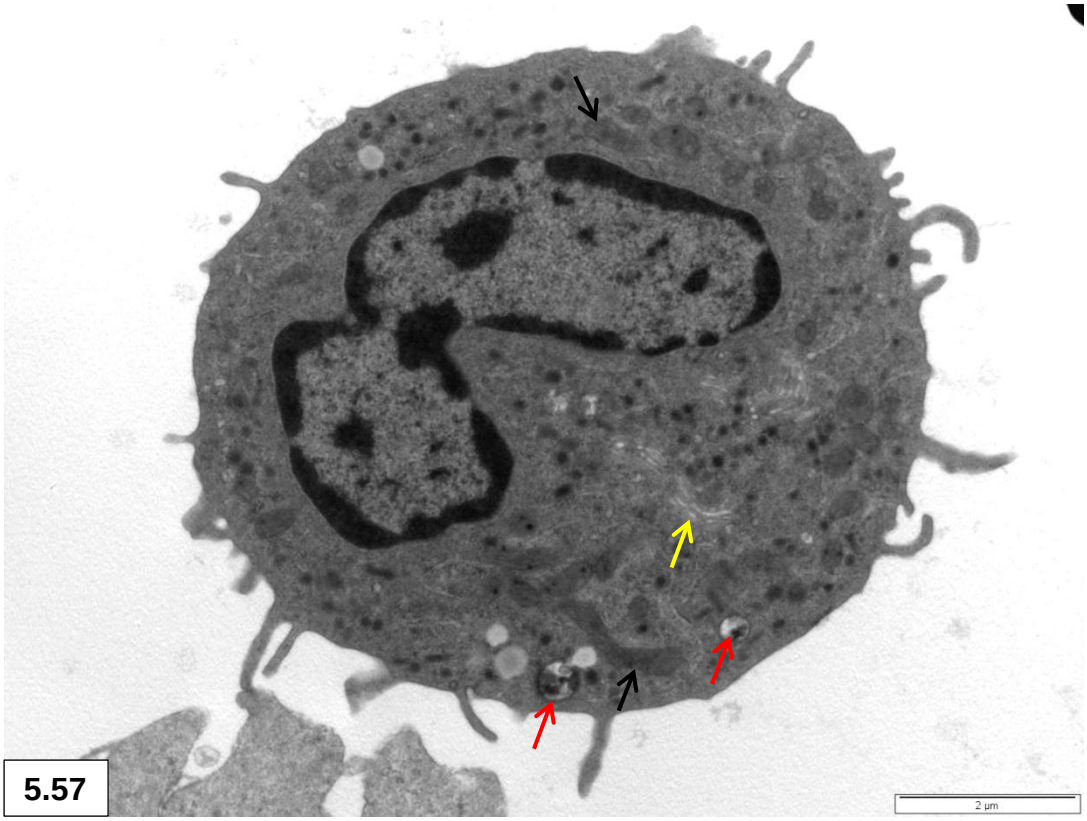

Figure 5.57 & 5.58: Pit cells with pseudopodia and indented eccentric nucleus present in a sinusoid. Note the many small membrane-bound electron dense granules and larger membrane-bound clear vesicles with electron-dense contents (red arrows). Golgi (yellow arrows), mitochondria (black arrows).

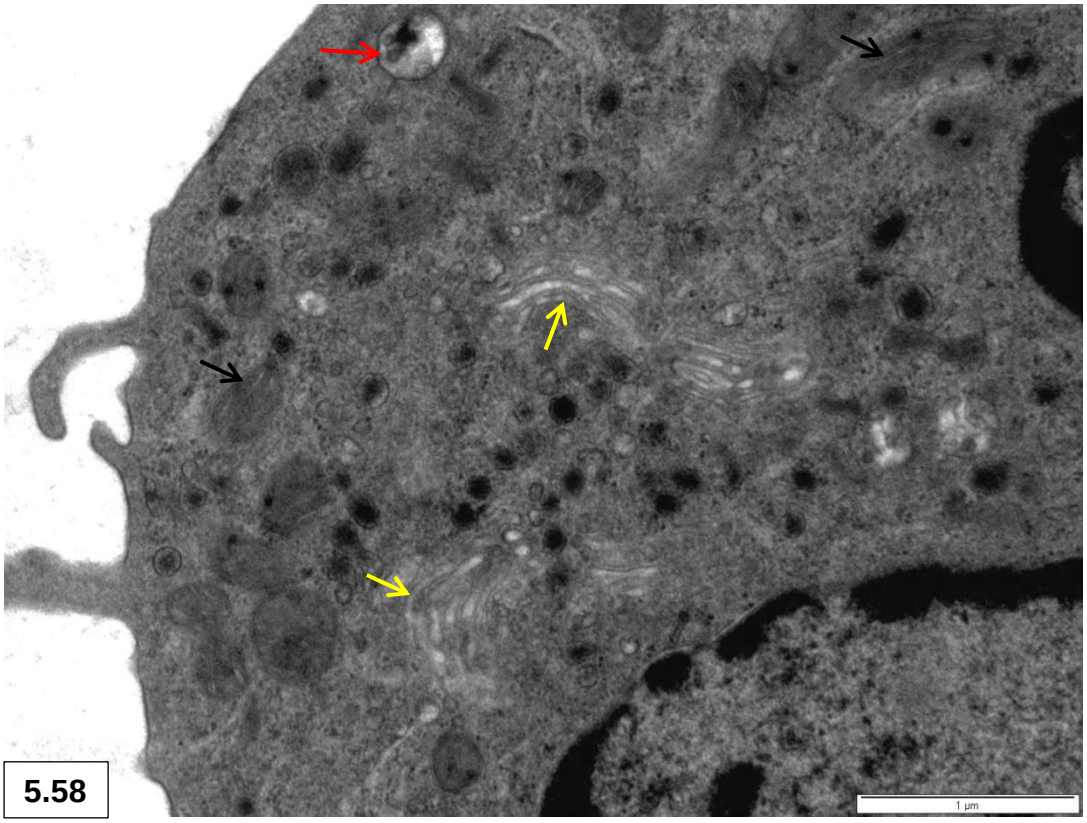

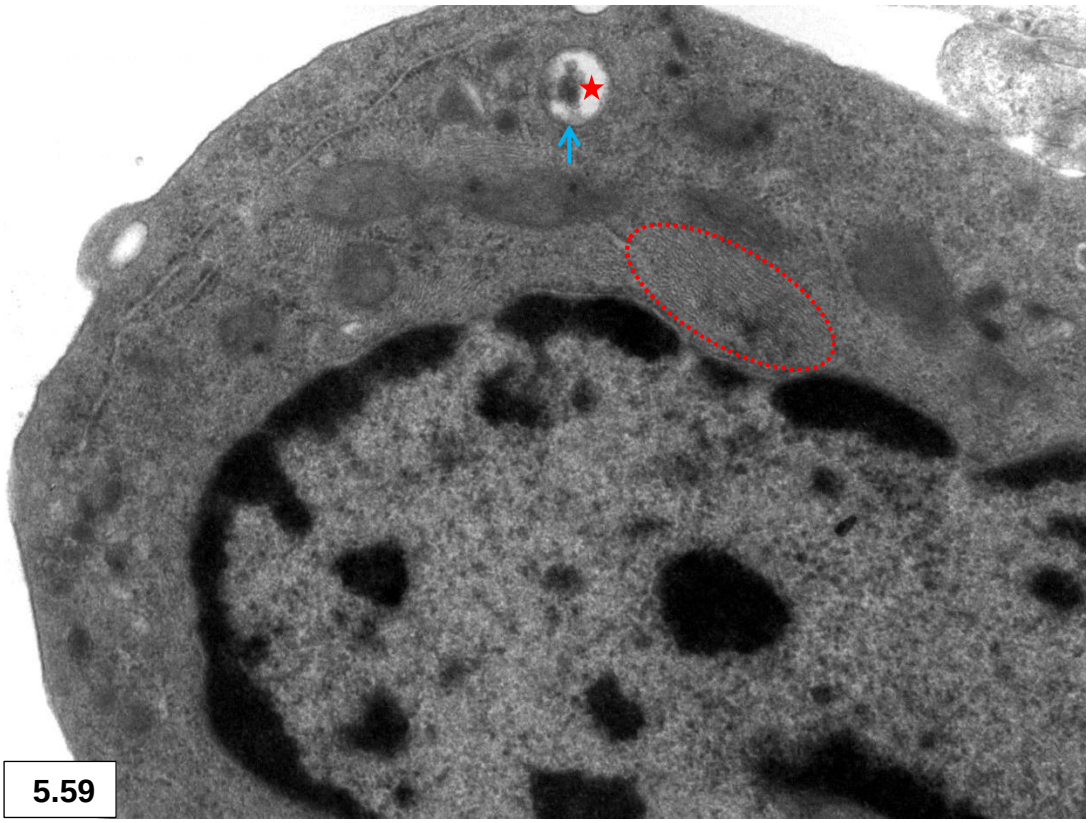

5.59

Figure 5.59 & 5.60 : Intermediate filaments (dashed circle) in pit cells. Note large membrane-bound clear vesicles (blue arrows), some with electron-dense contents (red star). Multivesicular bodies (red arrows), endocytotic vesicles (yellow arrows), lipid droplet (yellow star) and Golgi (black arrow).

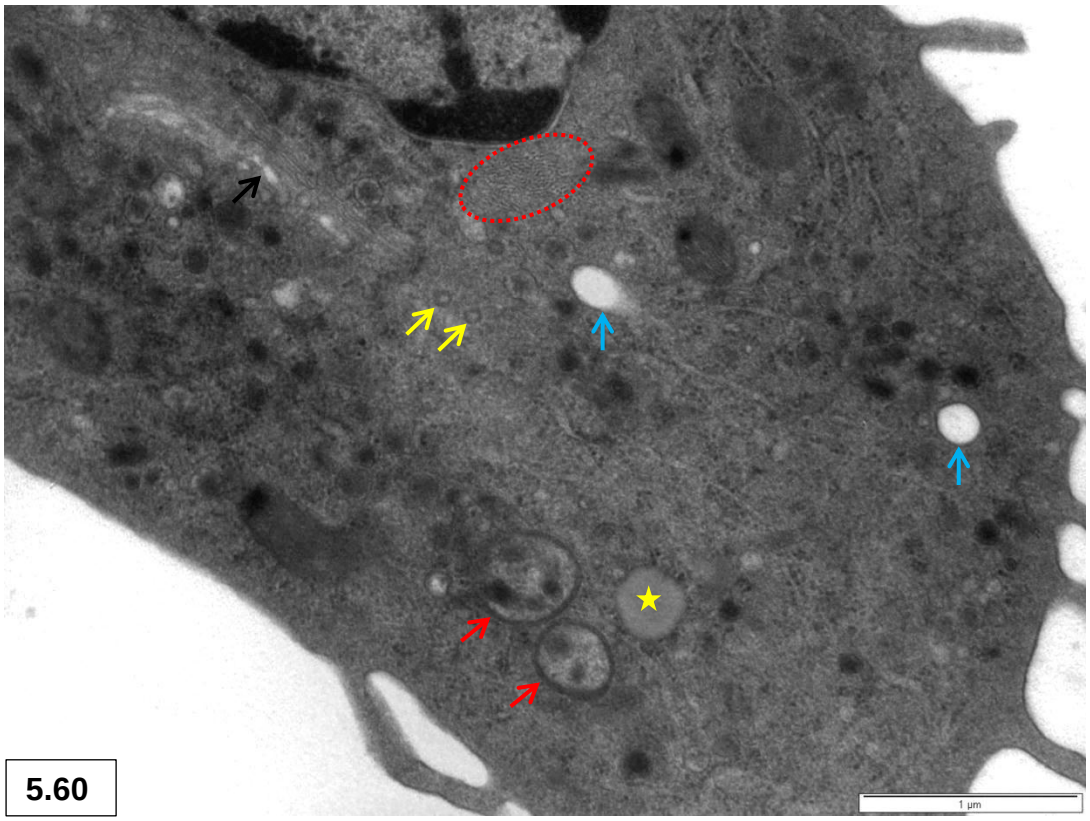

5.60

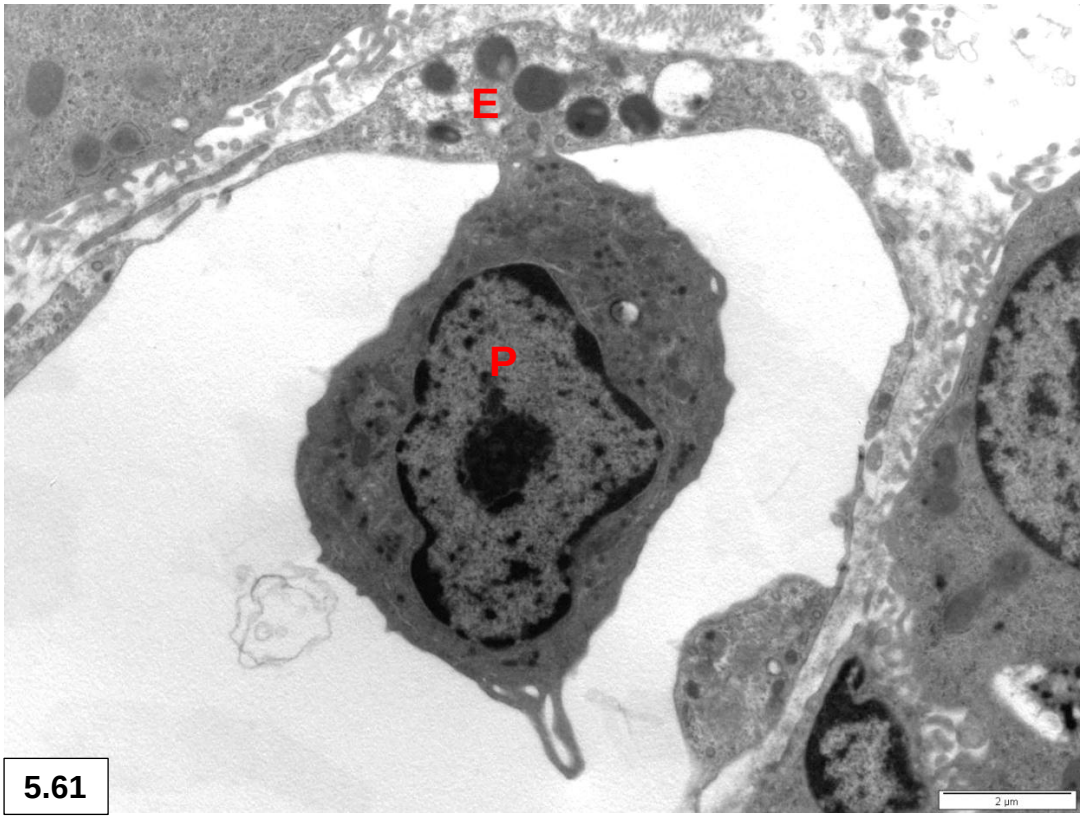

5.61

Figure 5.61 & 5.62: Contact of pit cells (**P**), containing small membrane-bound granules, with an endothelial cell (**E**) and the lamellapodia of a Kupffer cell (**K**).

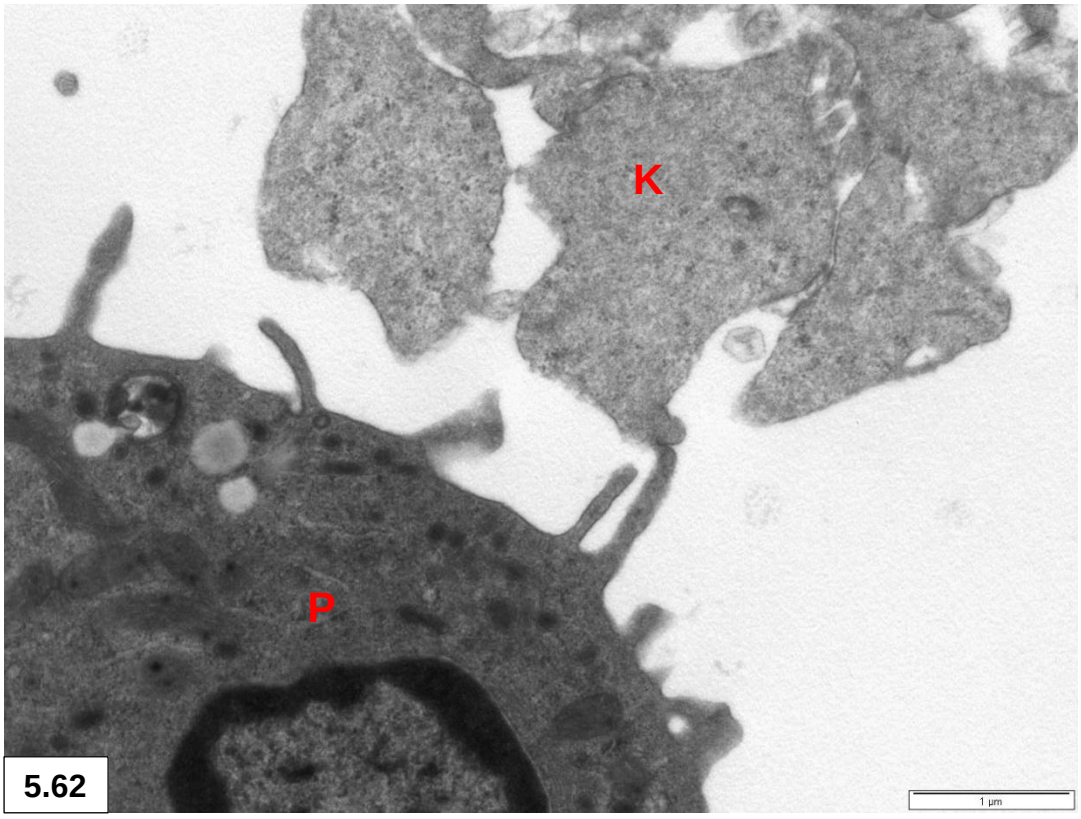

5.62

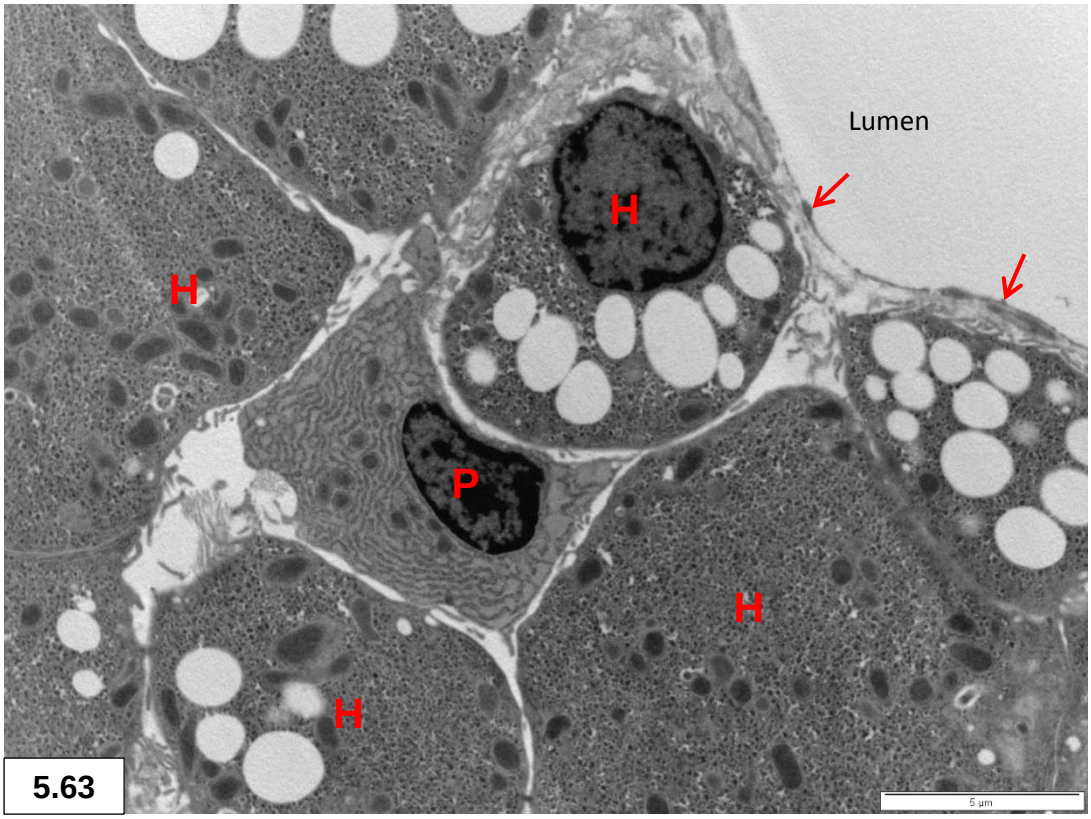

Figure 5.63: Plasma cell (**P**) present among hepatocytes (**H**). Endothelial cell (arrows).

Figure 5.64: Two thrombocytes (**T**) present in a sinusoidal lumen. Note Kupffer cell (**K**) containing tubulosomes and lipid droplets. Endothelial cell (**E**), hepatocytes (**H**), myofibroblastic cell extension (star).

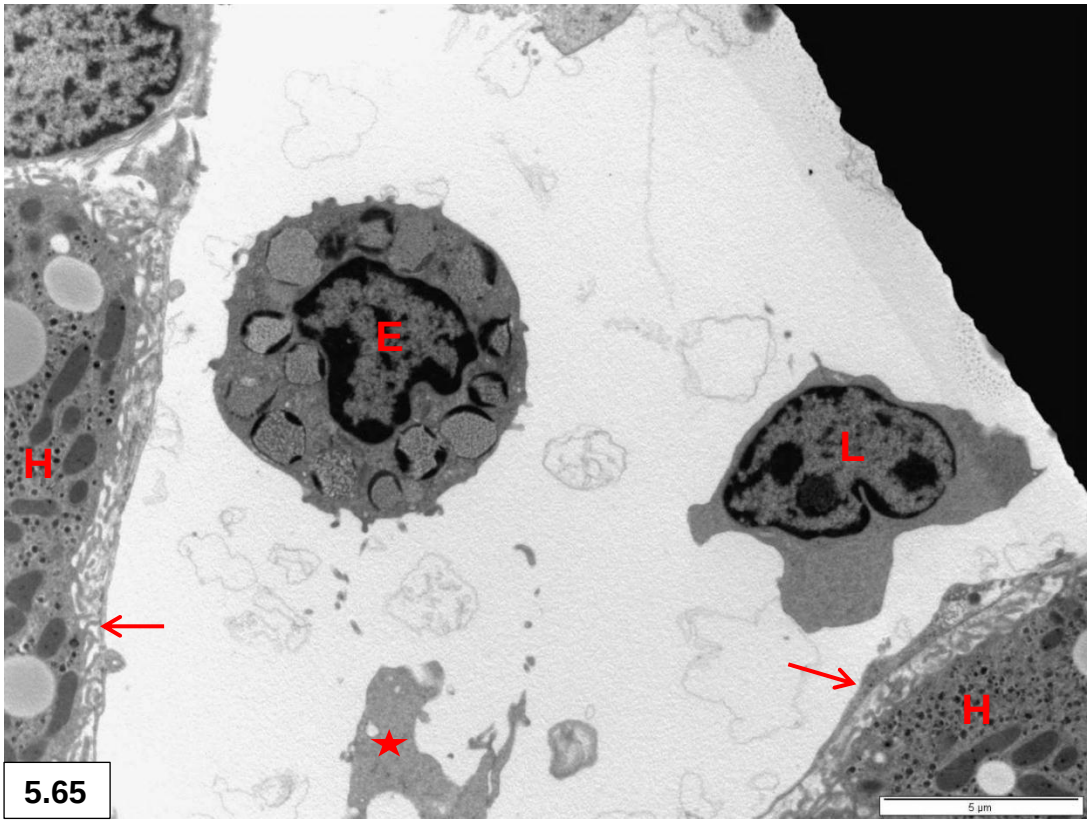

Figure 5.65: Eosinophil (**E**) & lymphocyte (**L**) present in a sinusoidal lumen. Note hepatocytes (**H**), endothelial cell extensions (arrows) and Kupffer cell lamellipodium (star).

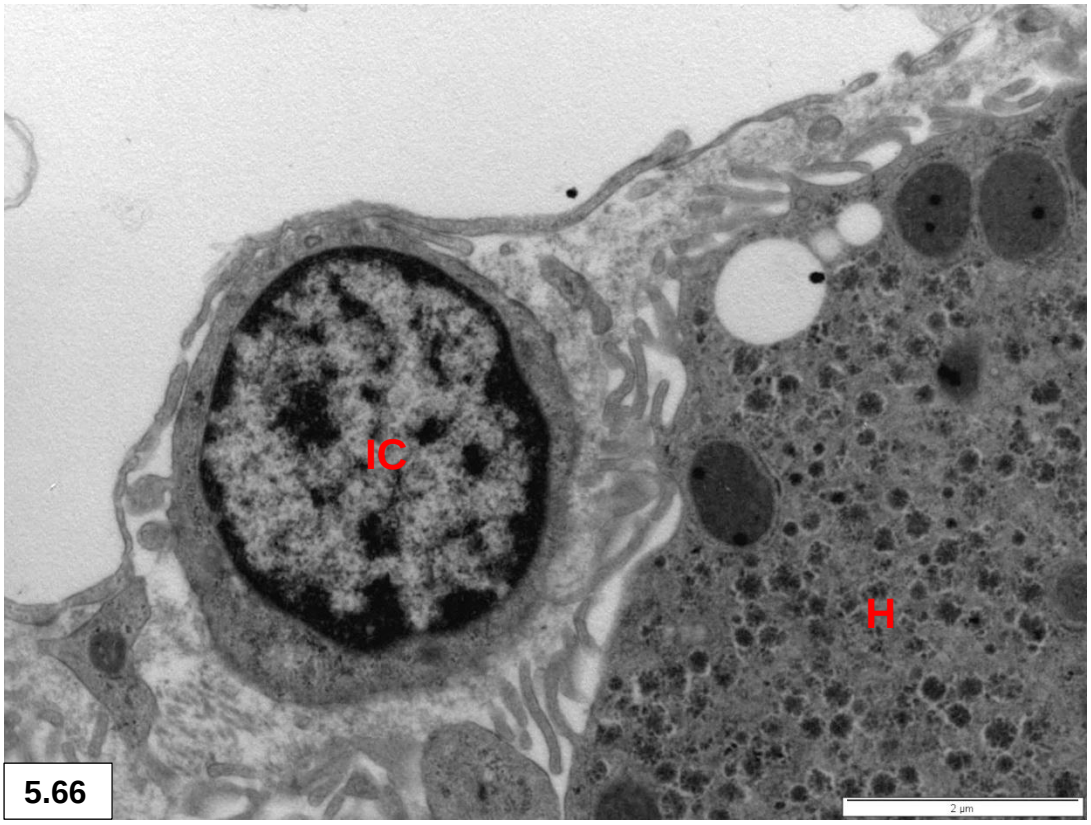

Figure 5.66 & 5.67: Intercalated cells (**IC**) with sparse organelles present in the space of Disse and in a group of hepatocytes.

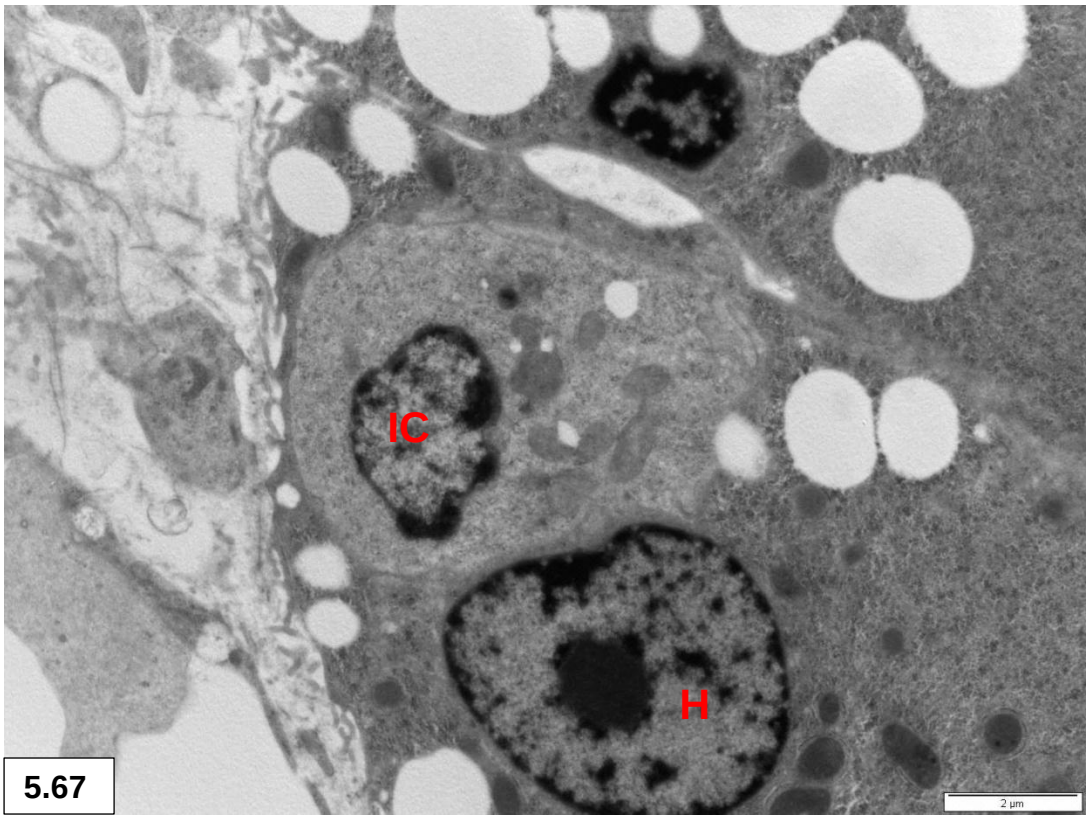

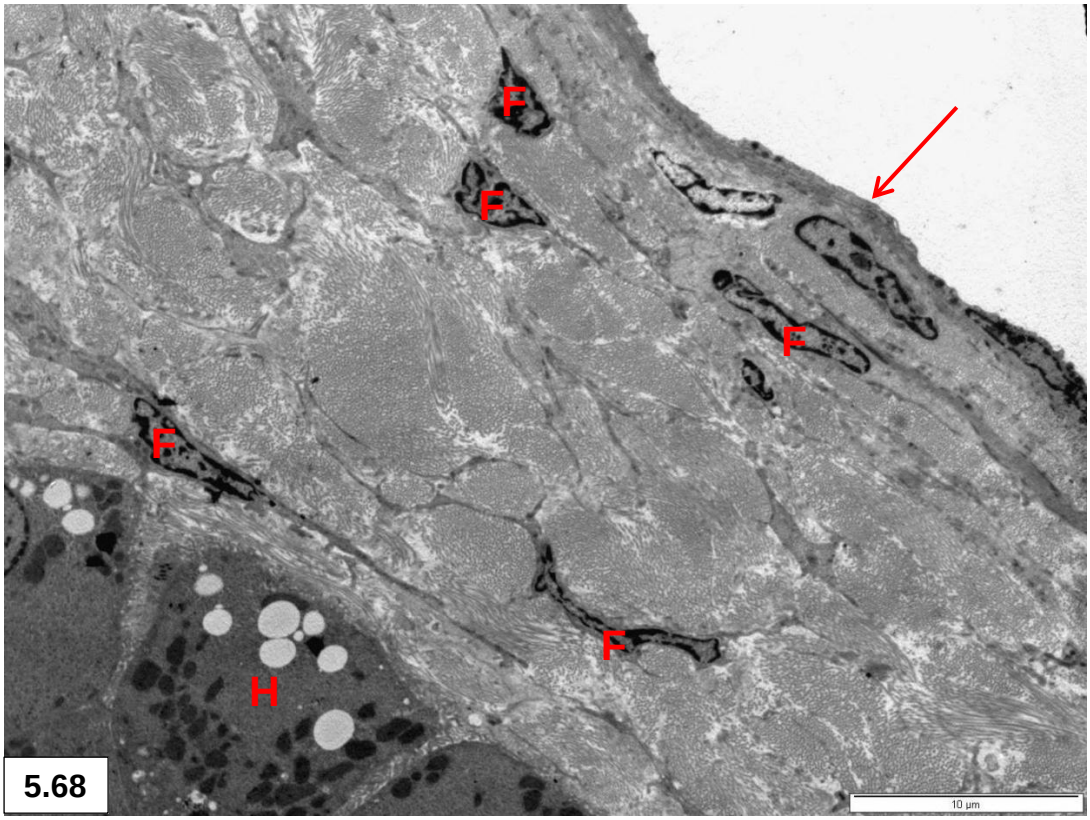

Figure 5.68: Glisson's capsule consisting of mesothelial cells (arrow) and a collagen layer containing fibroblasts (**F**). Hepatocytes (**H**).

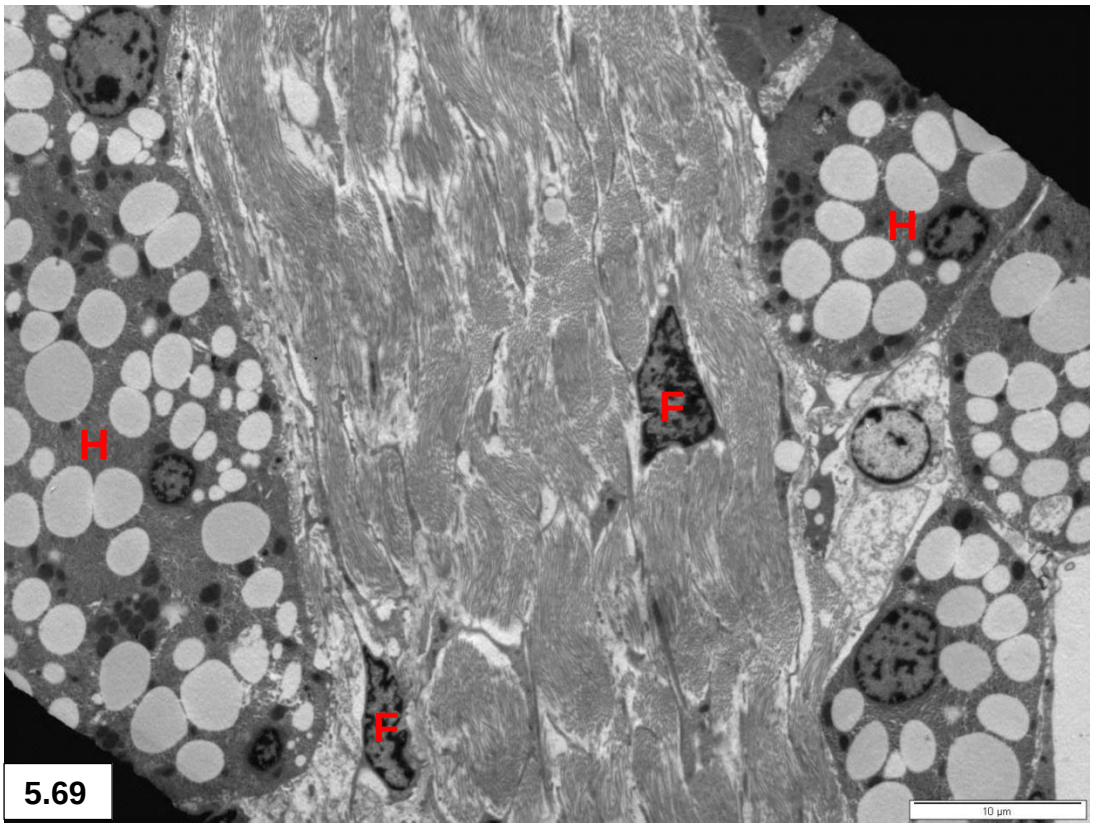

Figure 5.69: Fibrous trabecula between groups of hepatocytes.

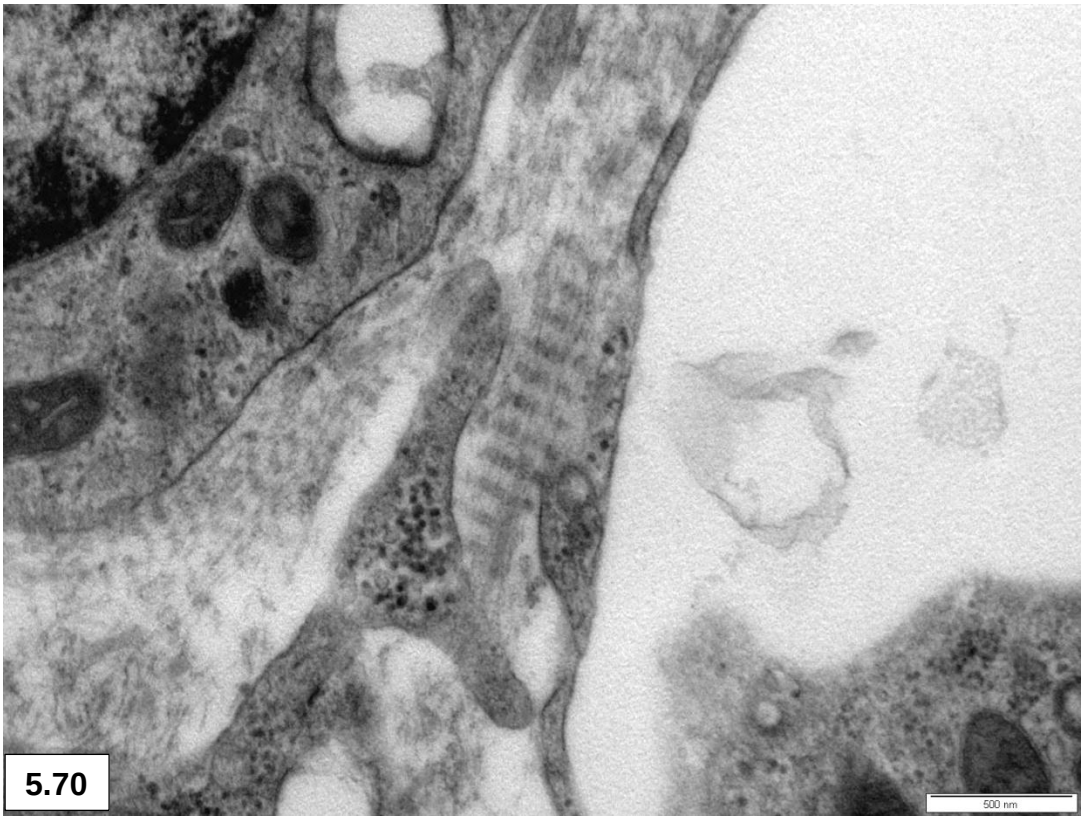

Figure 5.70 & 5.71: Long-spacing collagen fibrils in the space of Disse.

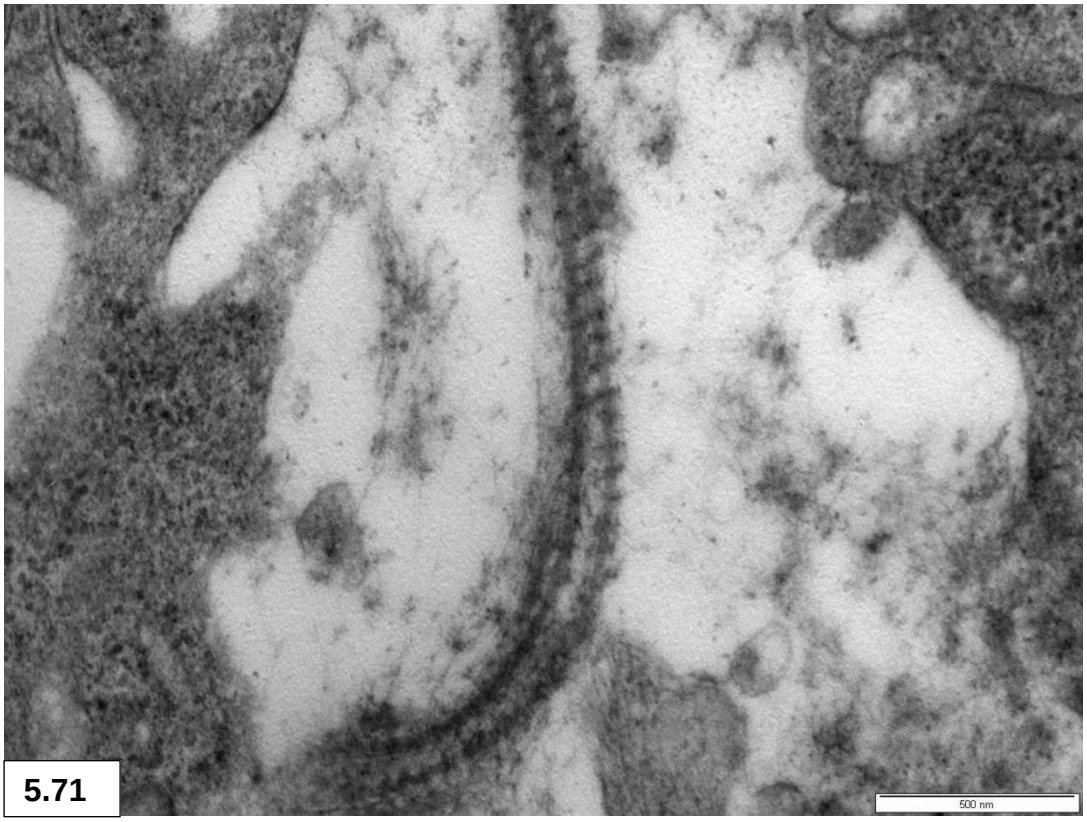

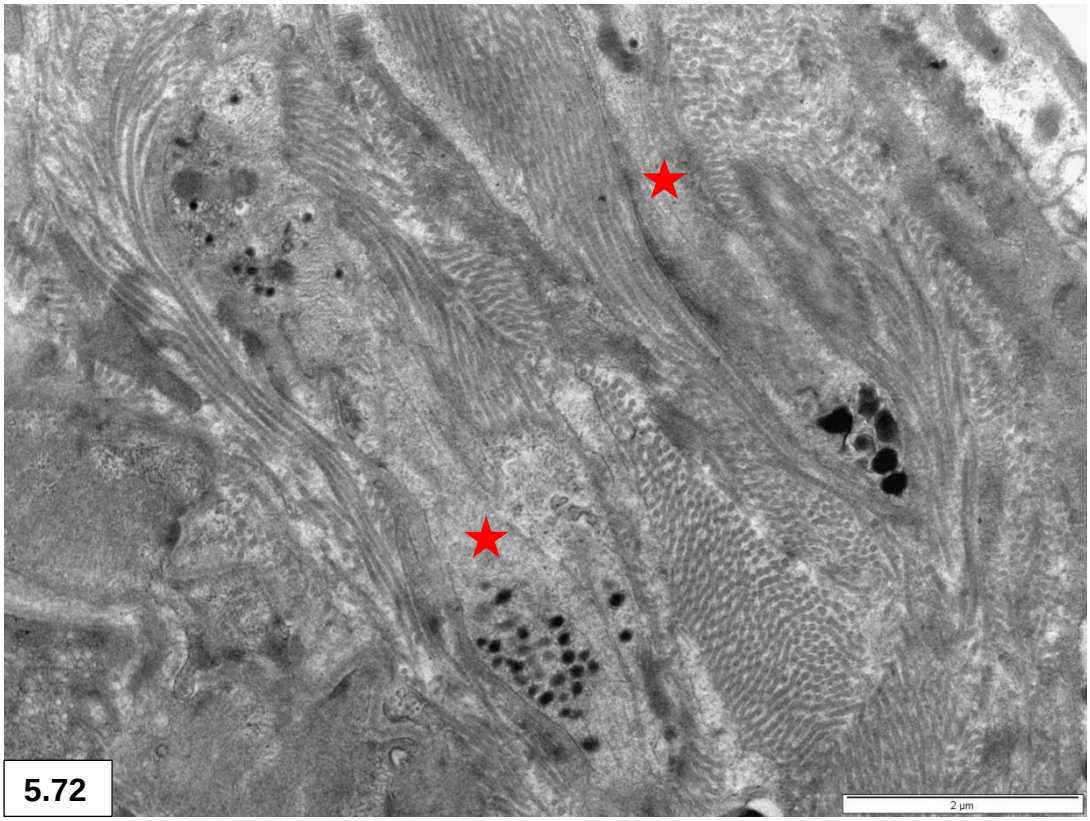

Figure 5.72 & 5.73: Intrahepatic non-myelinated nerves (stars). Note neurosecretory granules, microtubules, mitochondria, intermediate filaments and lysosomes.

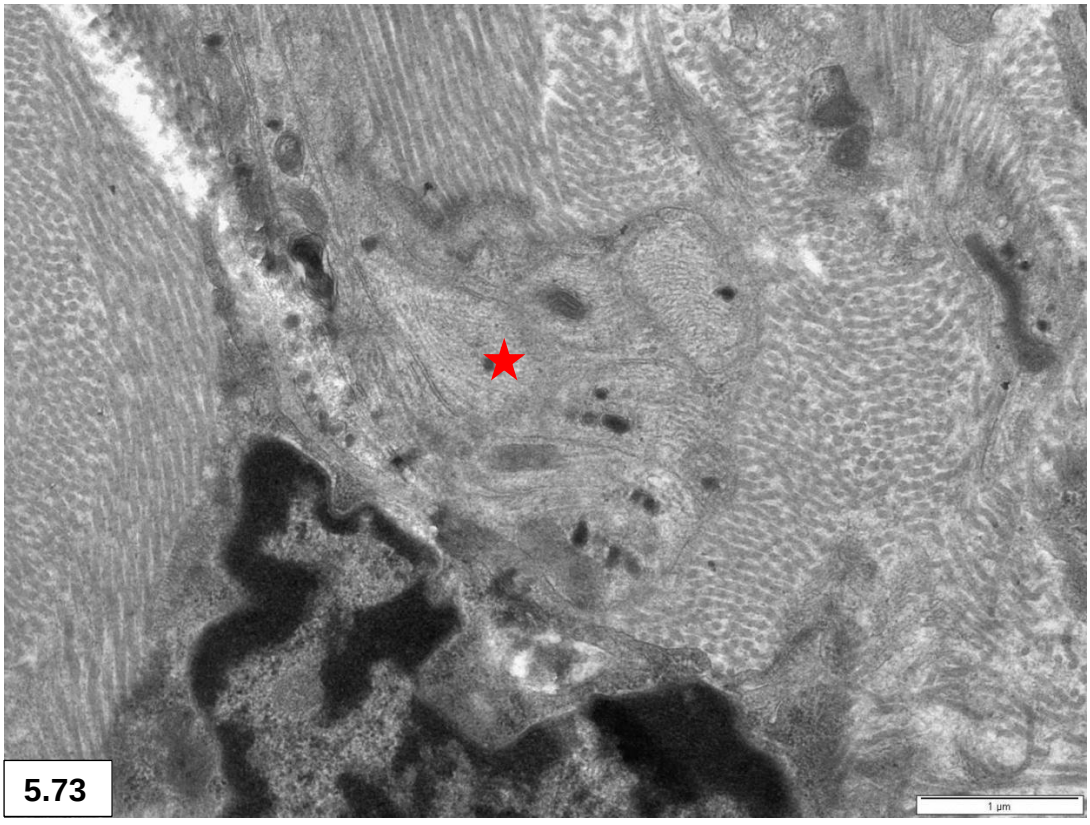

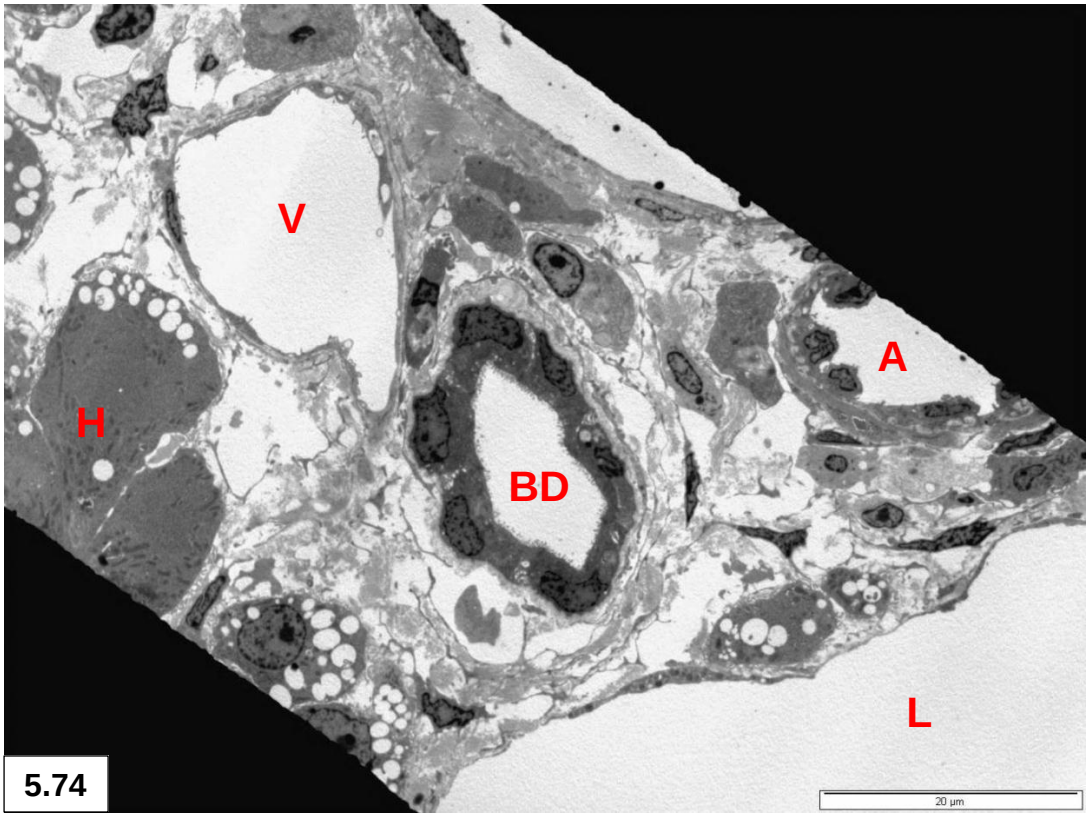

Figure 5.74 & 5.75: Portal tracts consisting of a portal vein (**V**), hepatic artery (**A**) and bile duct (**BD**). Lymphatic vessel (**L**), hepatocytes (**H**). Note collagen fibrils, fibroblasts, lymphocytes and plasma cells in the surrounding stroma.

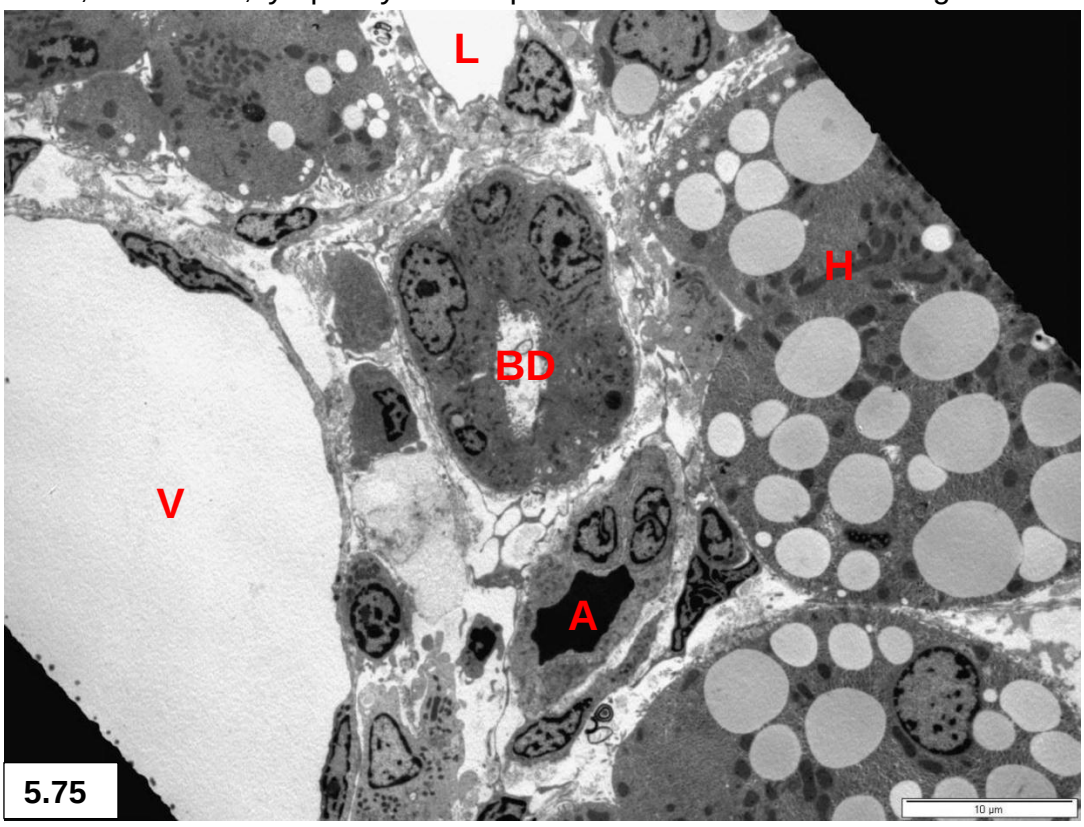

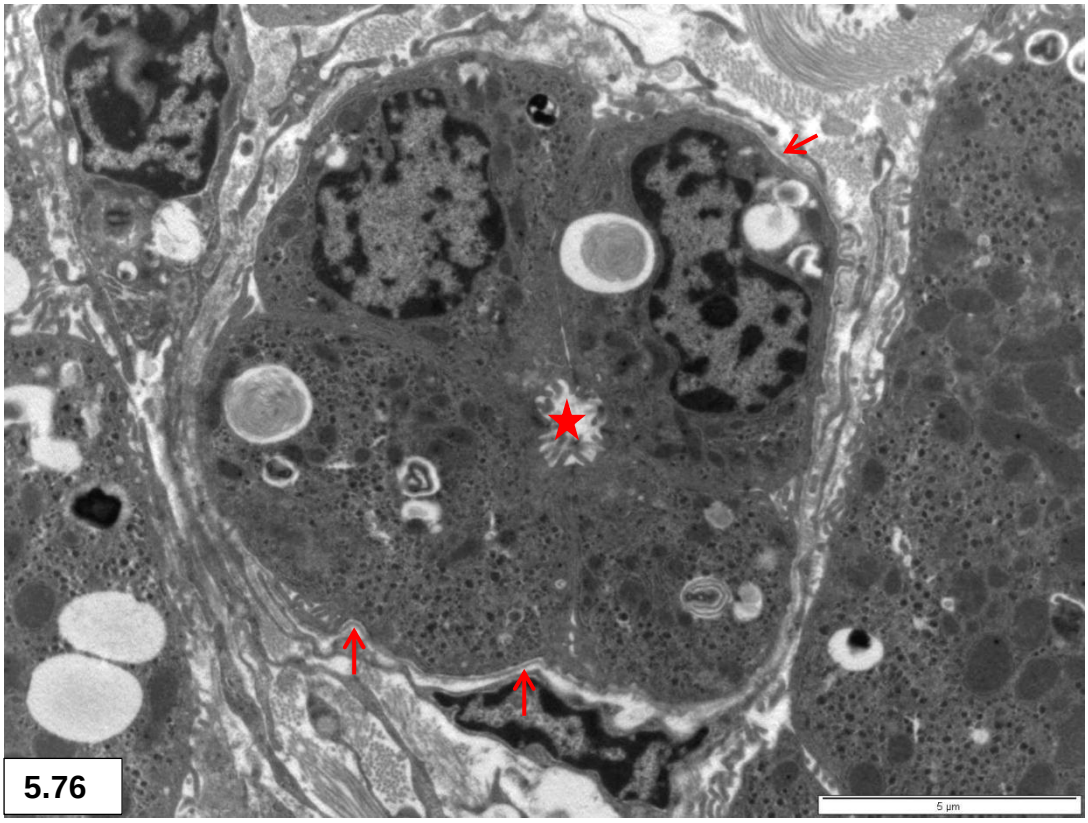

Figure 5.76: Bile duct surrounded by a basal lamina (arrows). Ductal lumen (star).

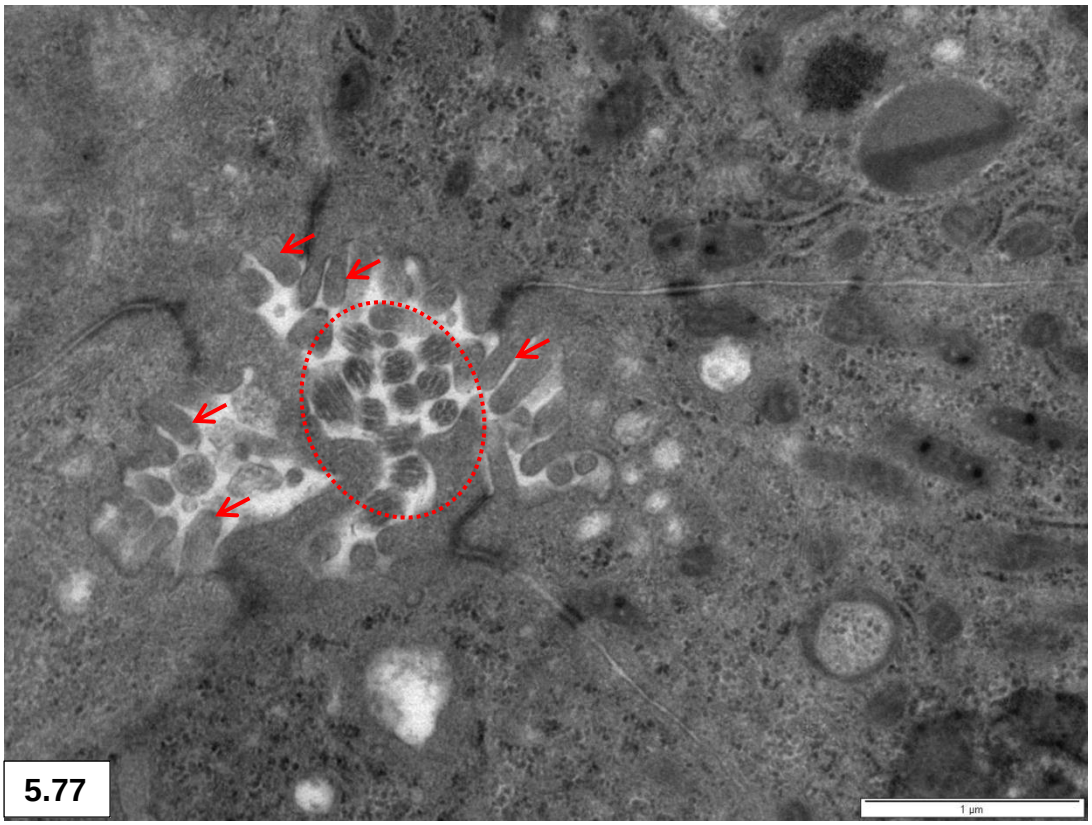

Figure 5.77: Higher magnification of the apical cell surfaces with junctional complexes of a bile duct. Note microvilli (arrows) and cilia (dashed circle) containing microtubules in the ductal lumen.

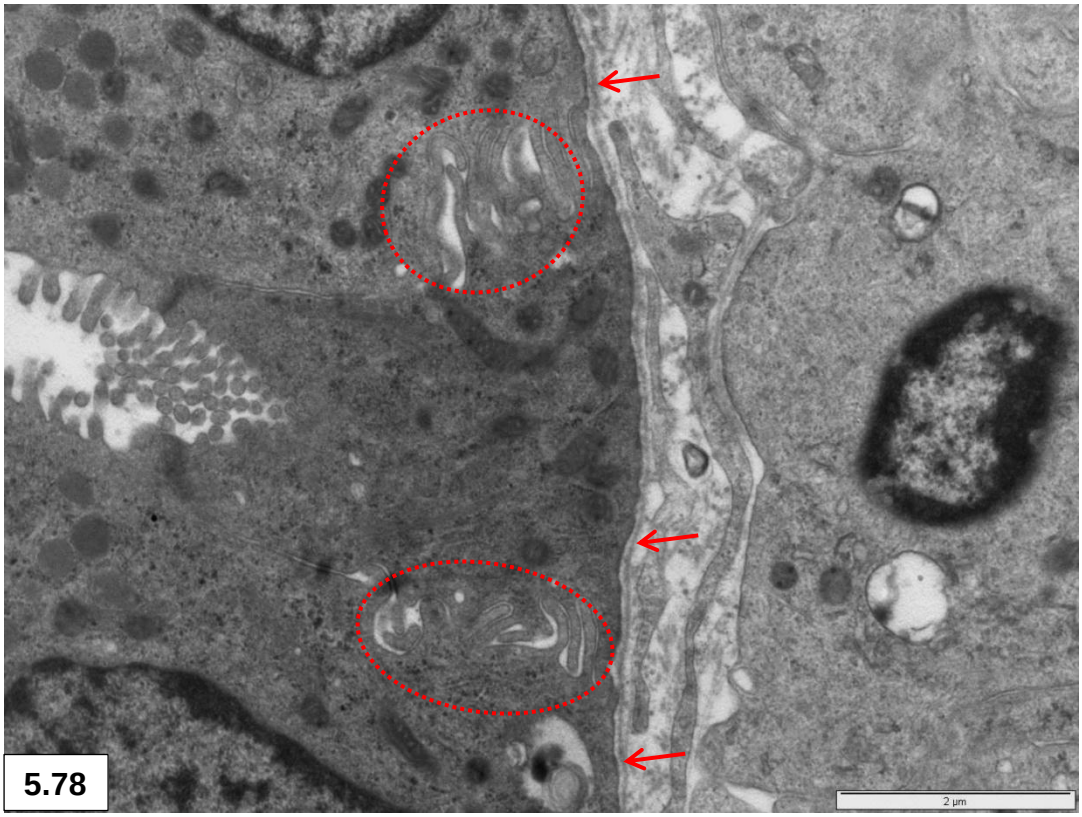

Figure 5.78: Interdigitations (dashed circles) between the lateral membranes of a bile duct. Note basal lamina (arrows).

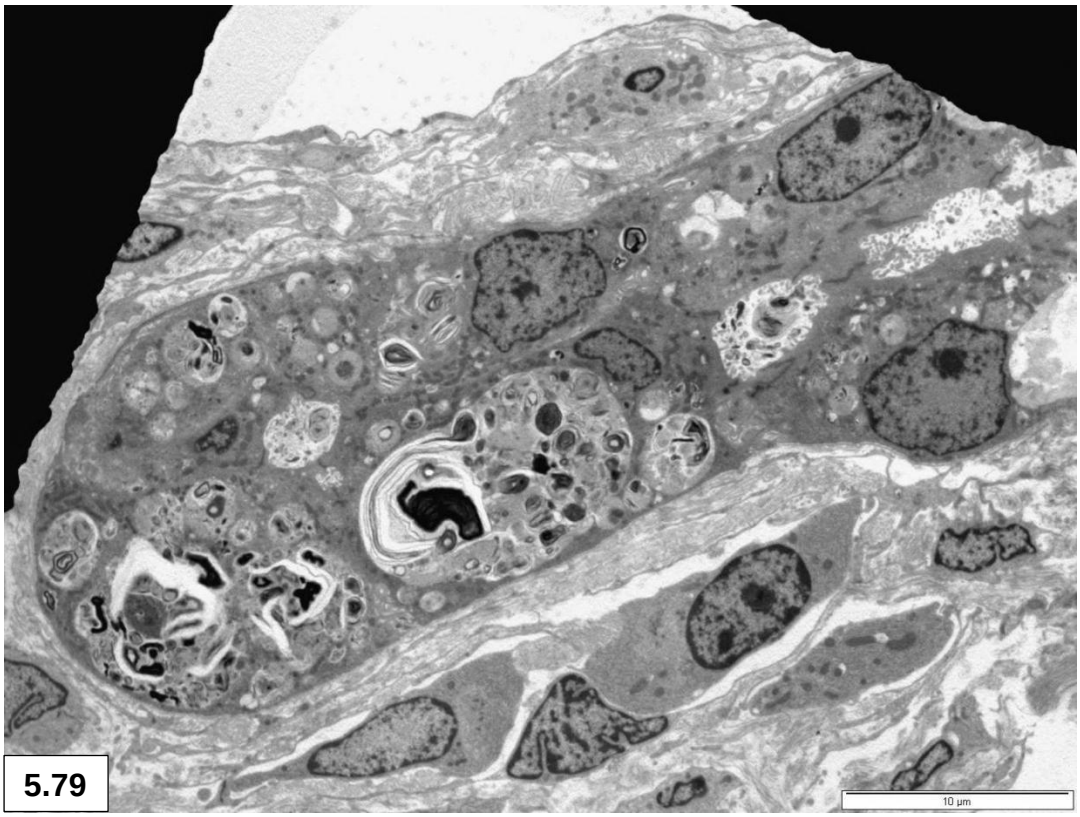

Figure 5.79: Concretions of bile pigment present in biliary cells.

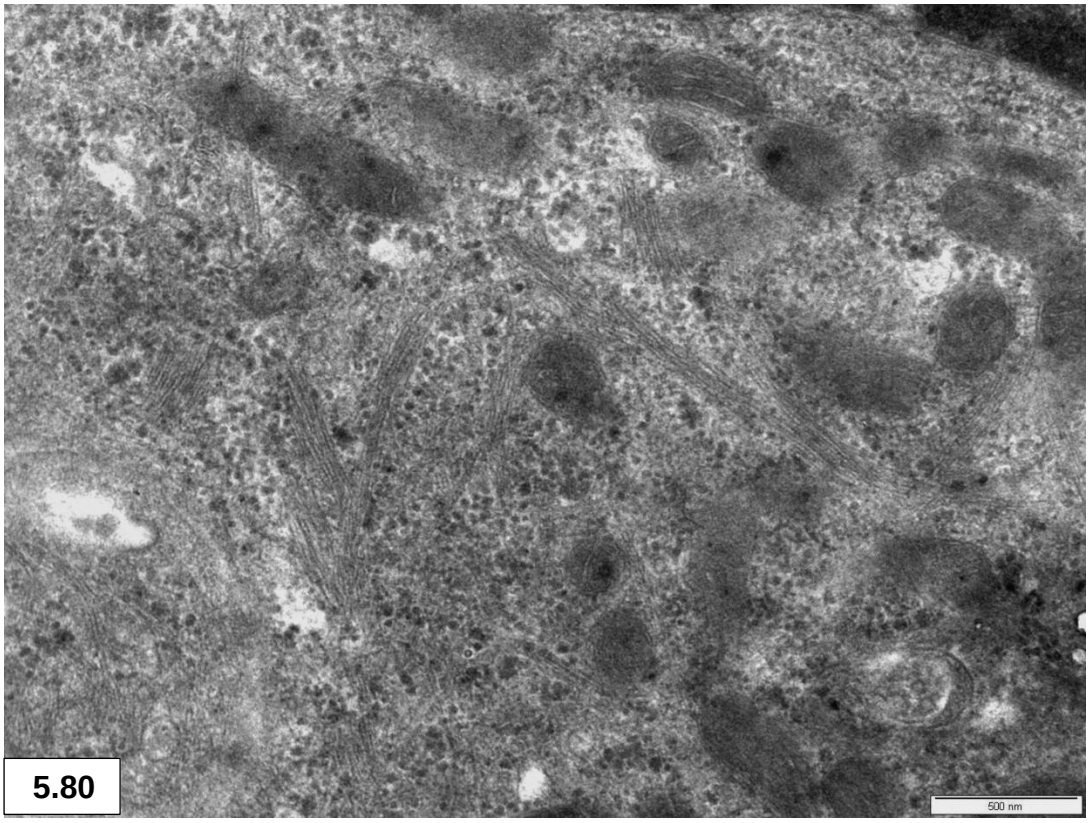

Figure 5.80: Prominent bundles of intermediate filaments in biliary cells.

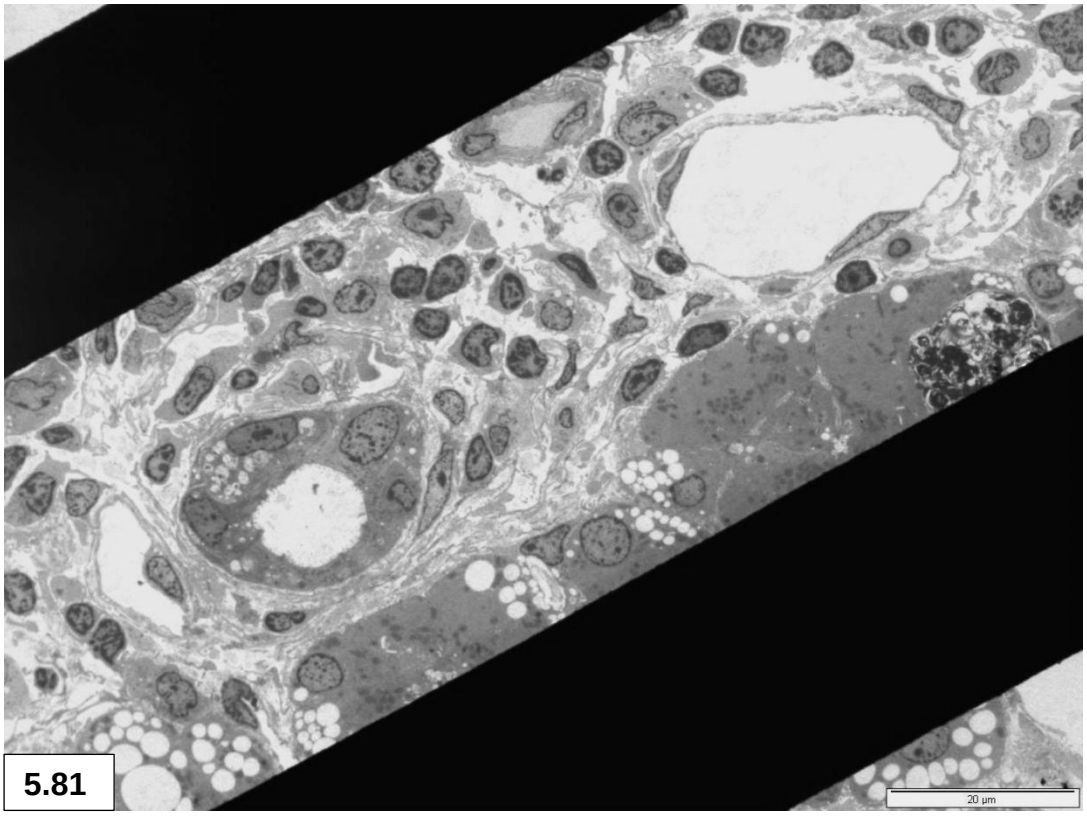

Figure 5.81 & 5.82: Collections of lymphocytes were occasionally seen in the portal areas.

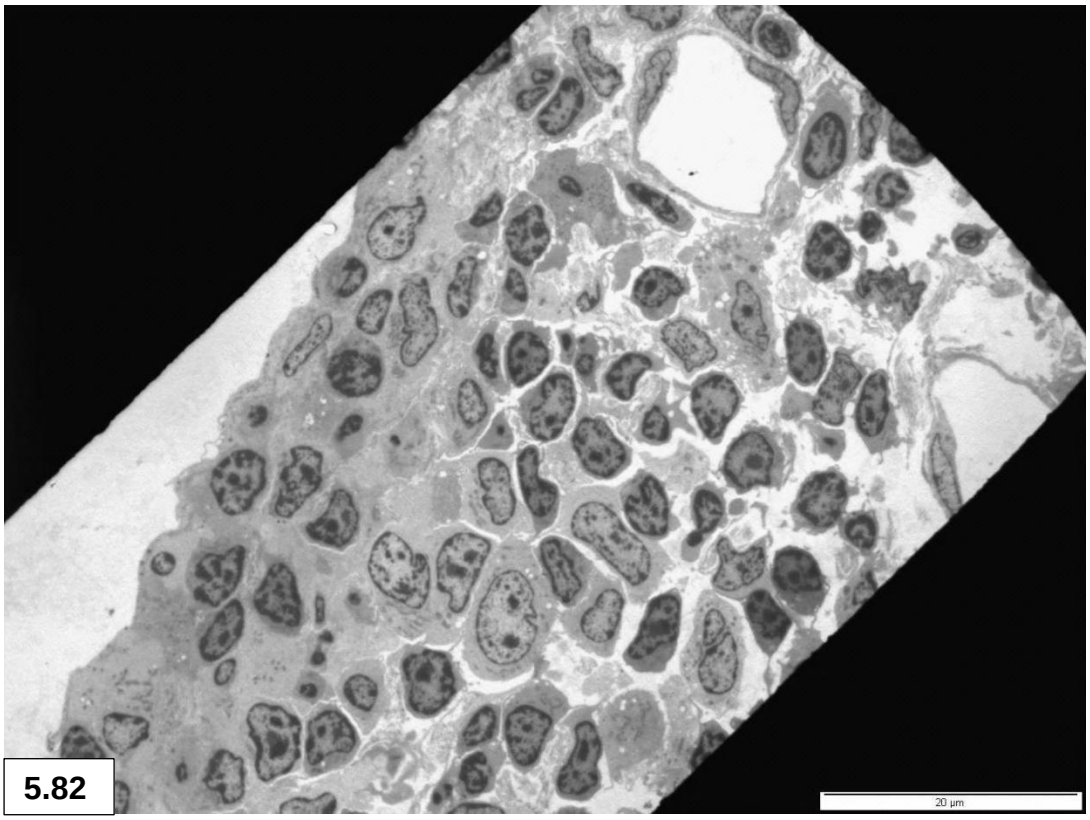

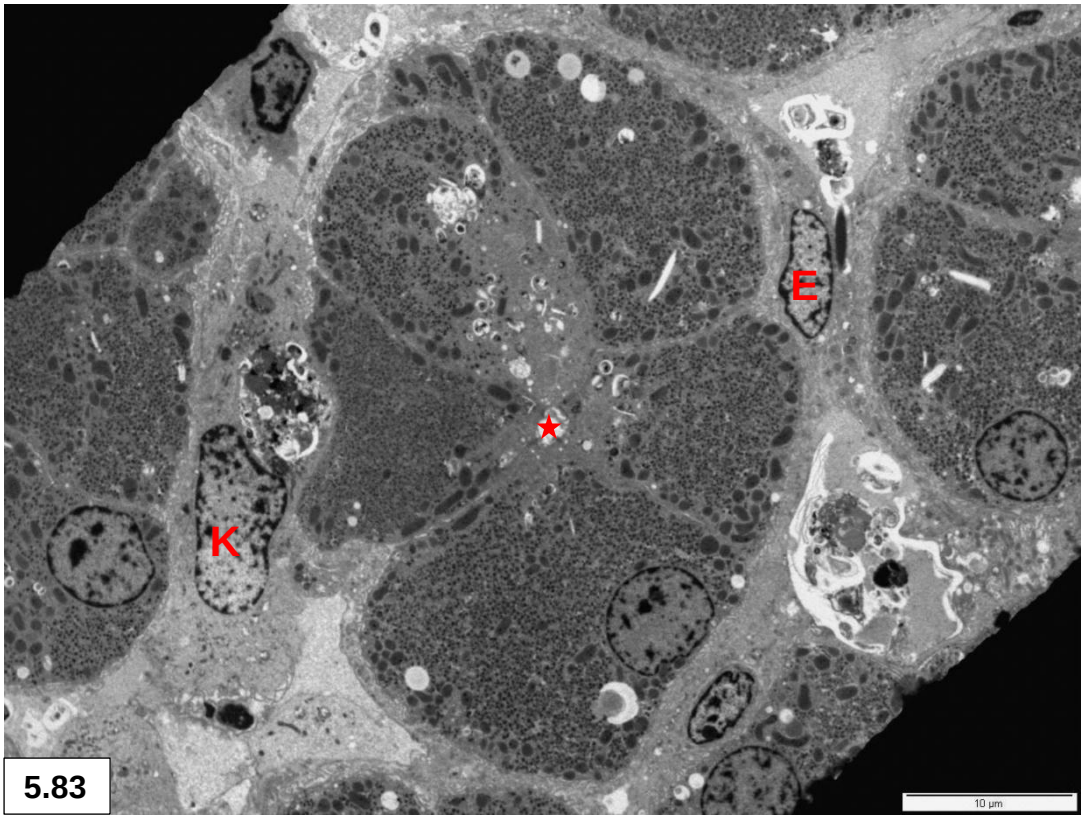

Figure 5.83: Isthmus – A group of hepatocytes with a central bile canaliculus (star) surrounded by a Kupffer cell (**K**) and an endothelial cell (**E**).

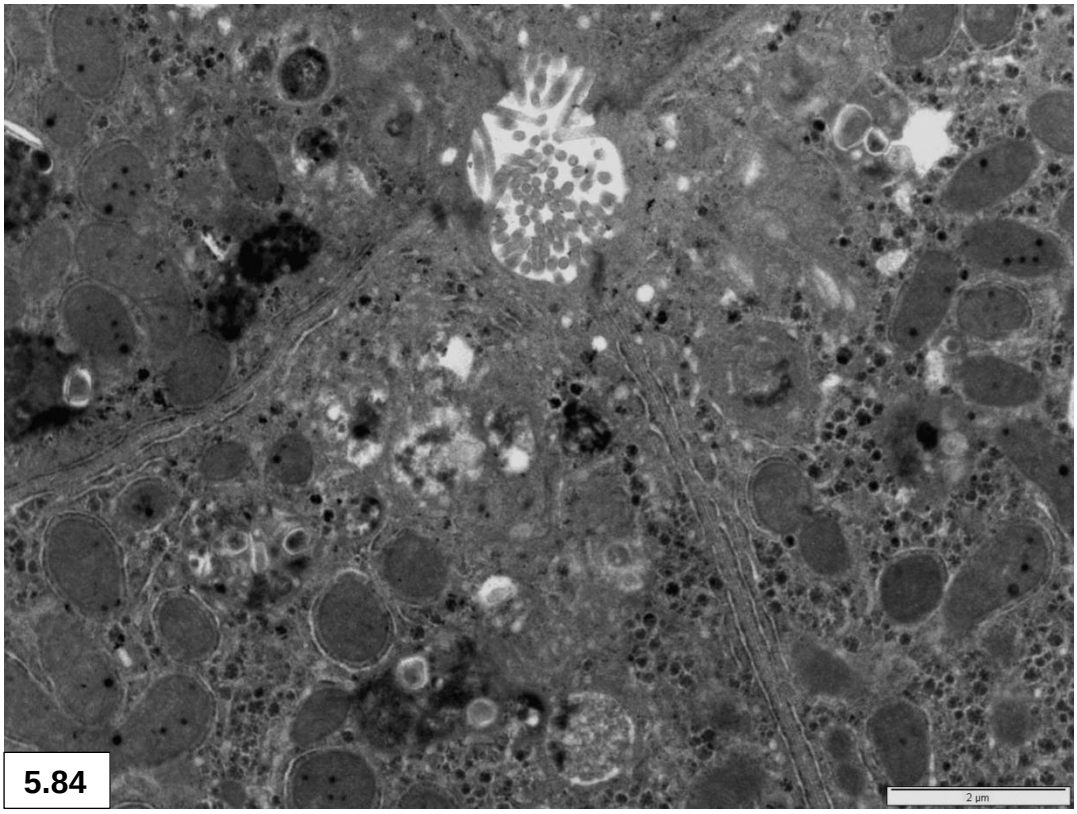

Figure 5.84: Isthmus - Bile canaliculus forming the lumen of the tubular hepatocyte cords.

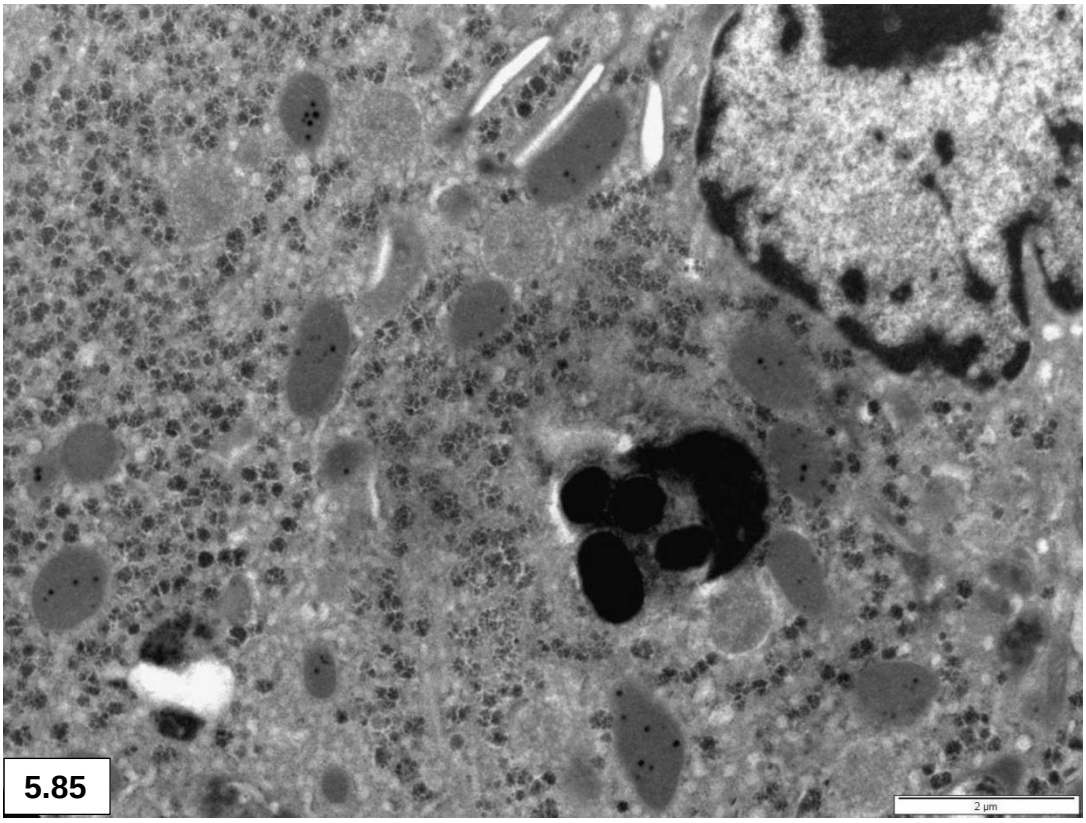

Figure 5.85: Melanin granules in a hepatocyte of the isthmus.

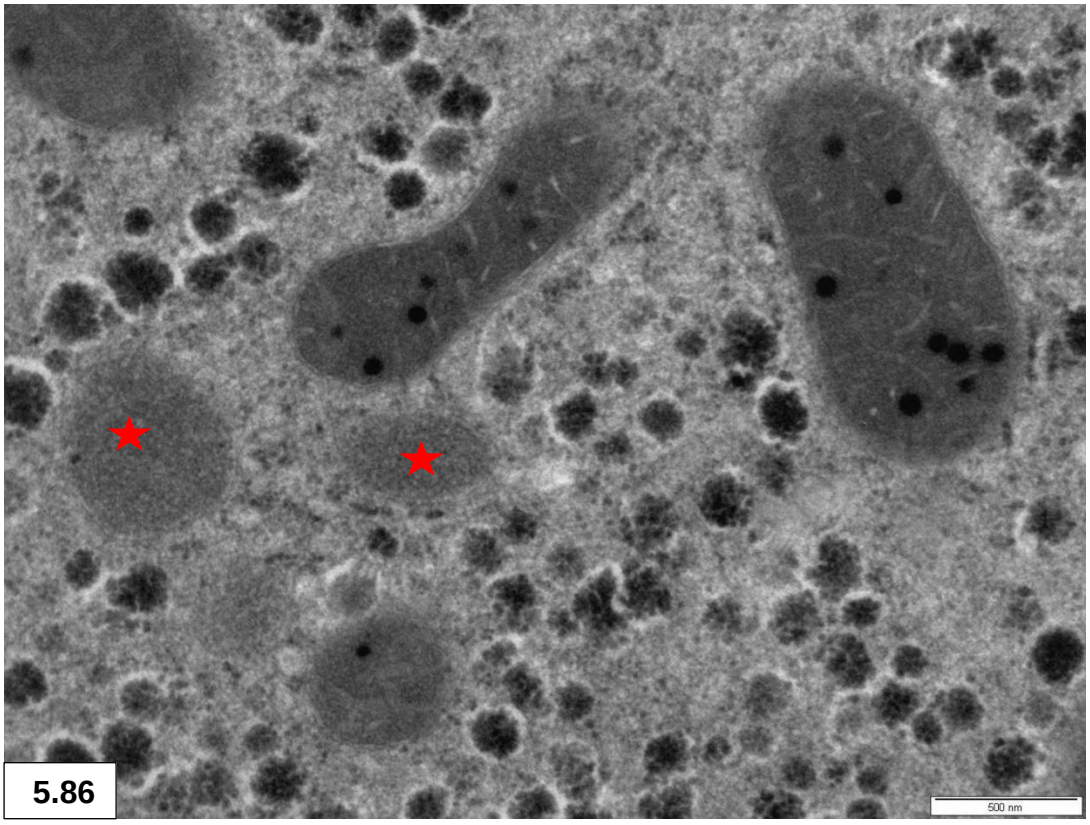

Figure 5.86: Peroxisomes in hepatocyte (stars) of the isthmus. Mitochondria with matrix granules and glycogen rosettes are also present.

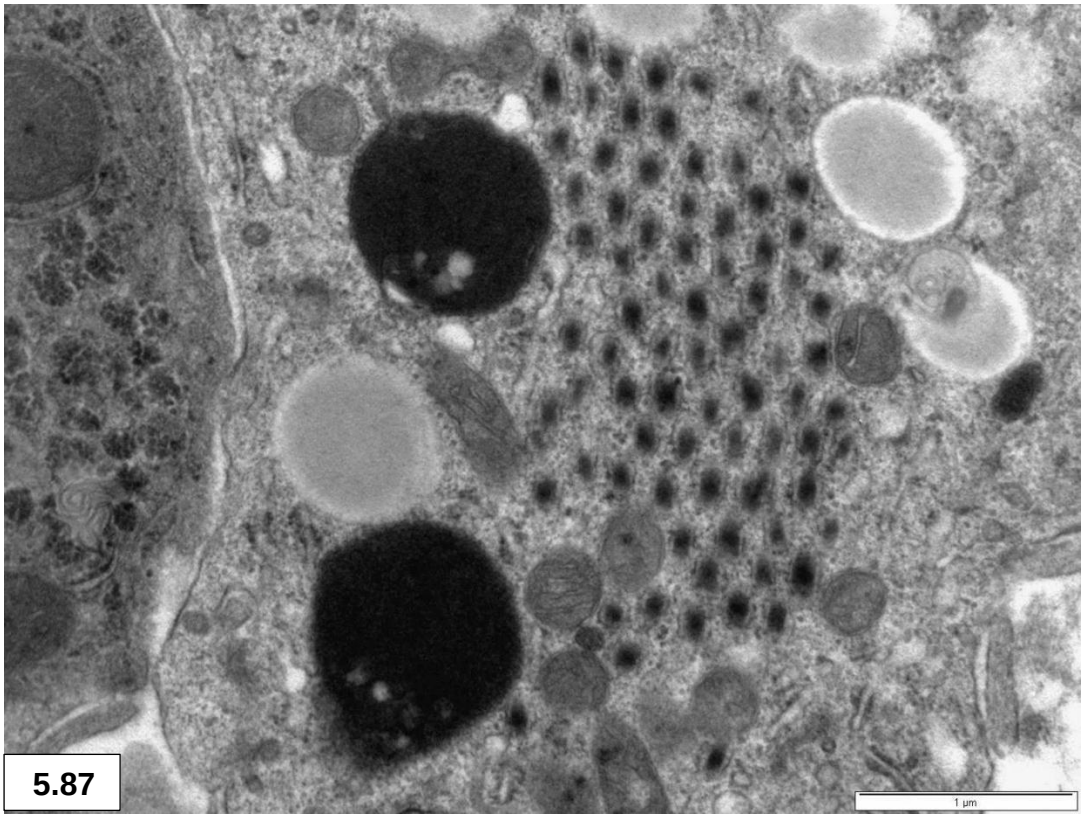

Figure 5.87: A group of tubulosomes in transverse profile in a Kupffer cell of the isthmus.

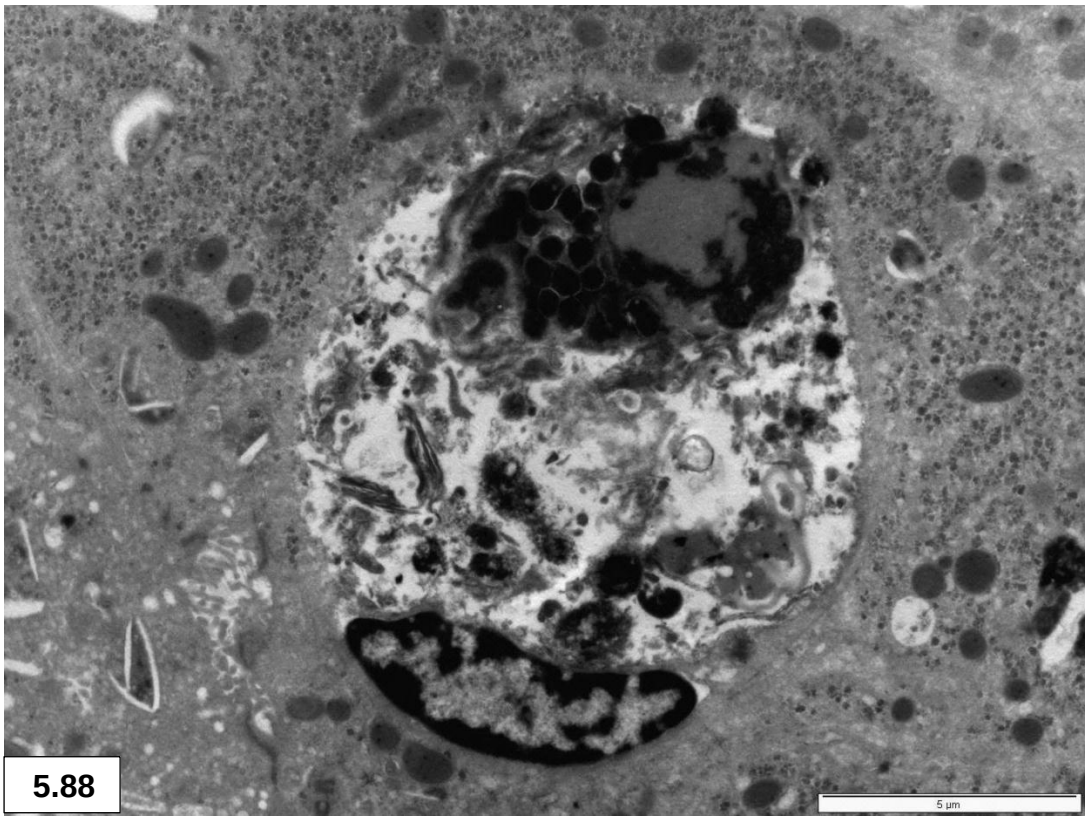

Figure 5.88: A pigmented cell present in a group of hepatocytes of the isthmus.

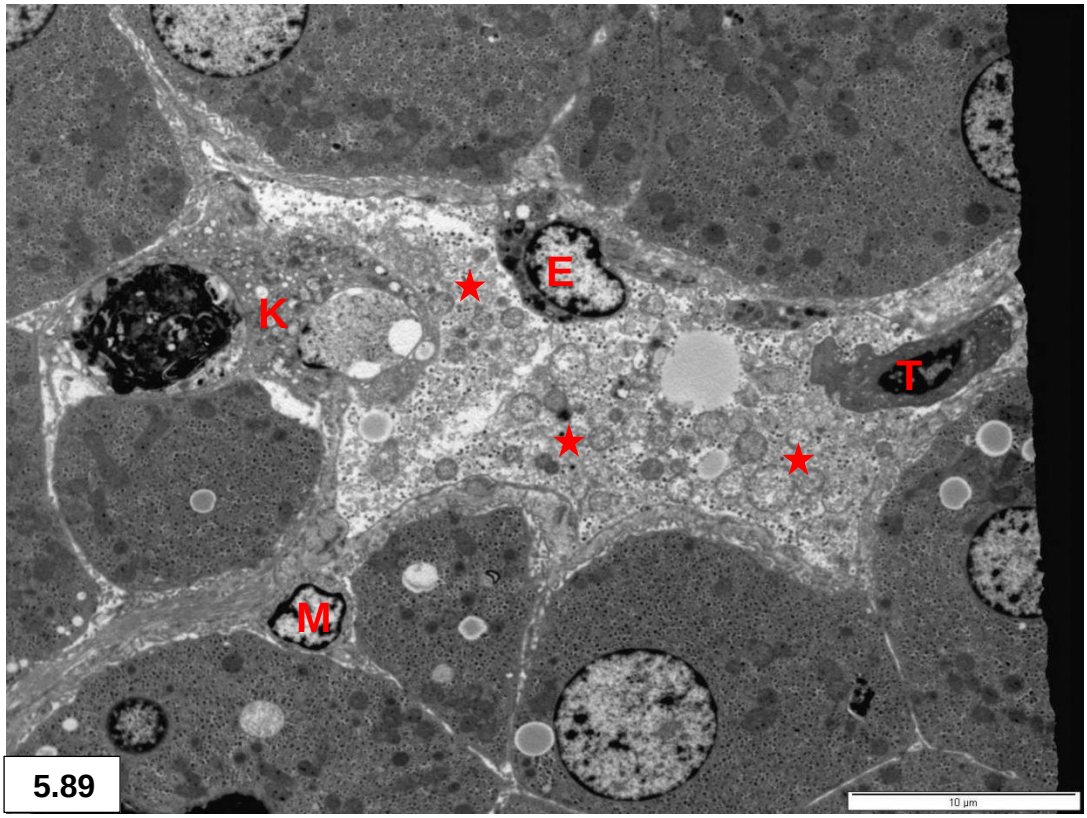

Figure 5.89: Isthmus - sinusoid with a thrombocyte (**T**), Kupffer cell (**K**) and endothelial cell (**E**). Note cellular debris (stars) in lumen. Myofibroblastic cell (**M**).

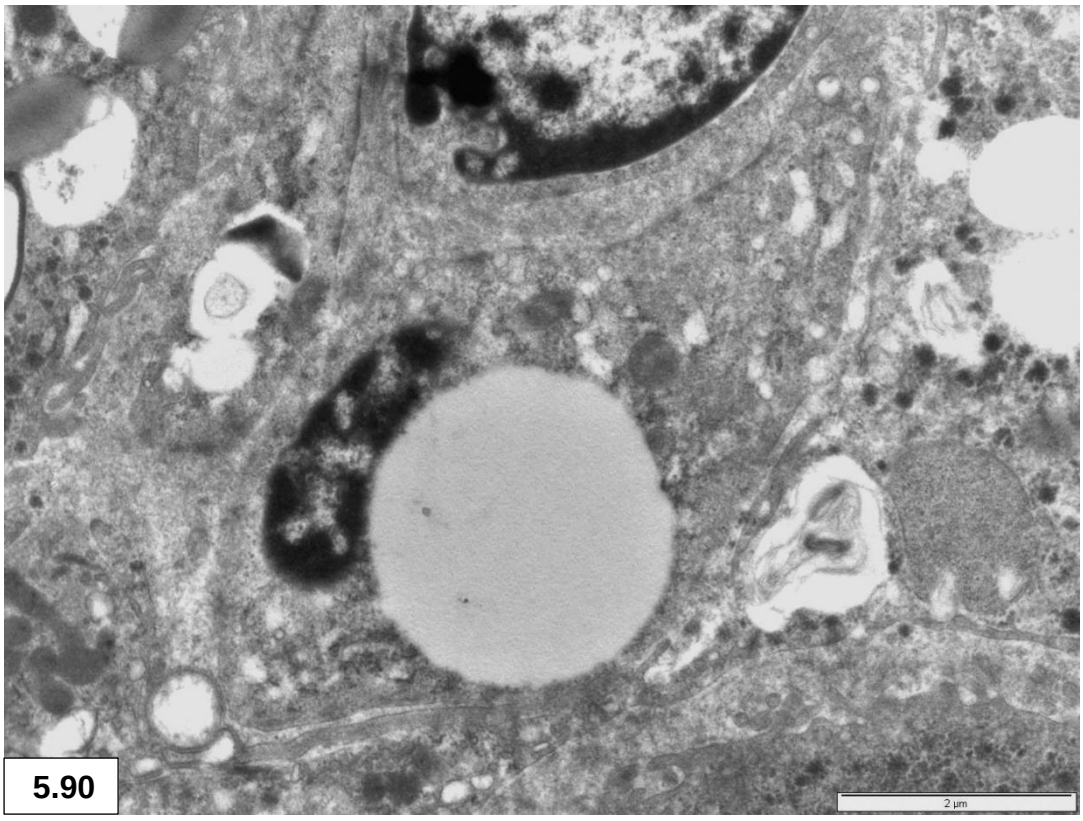

Figure 5.90: Isthmus - stellate cell containing a lipid droplet.

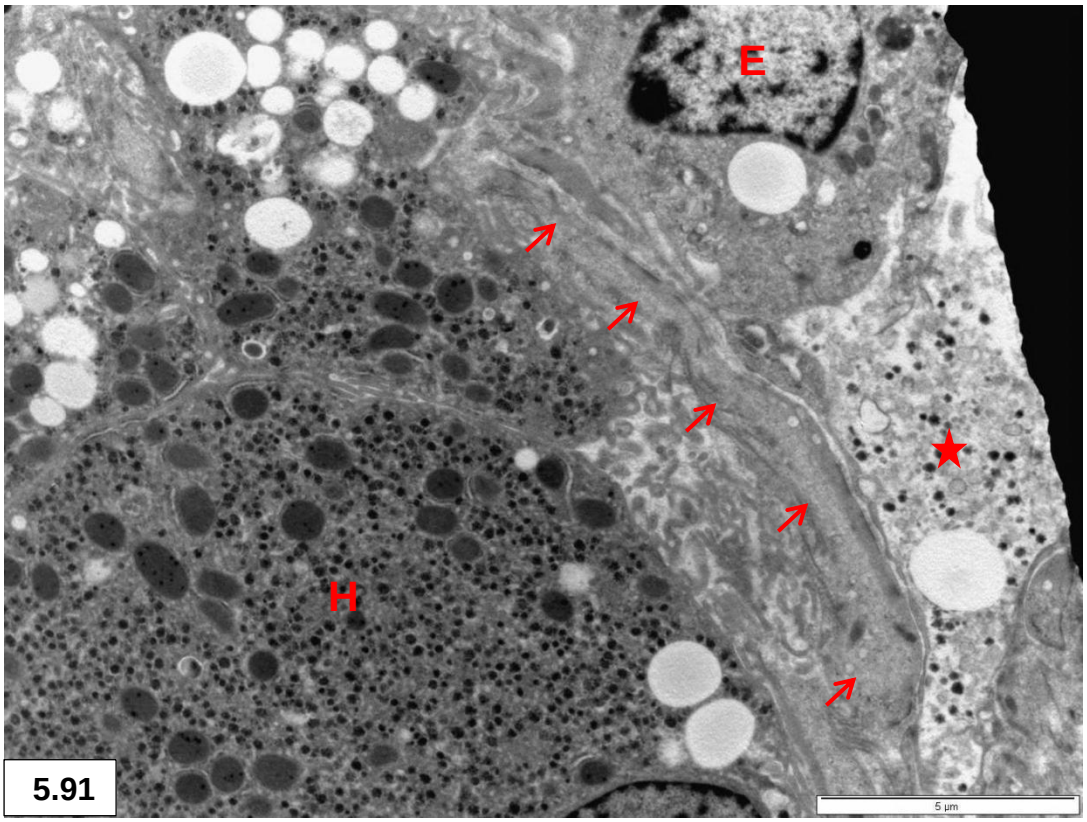

Figure 5.91 & 5.92 : Myofibroblastic cytoplasmic extension (arrows) in the space of Disse. Note cellular debris in lumen (star). Hepatocyte (**H**), endothelial cell (**E**).

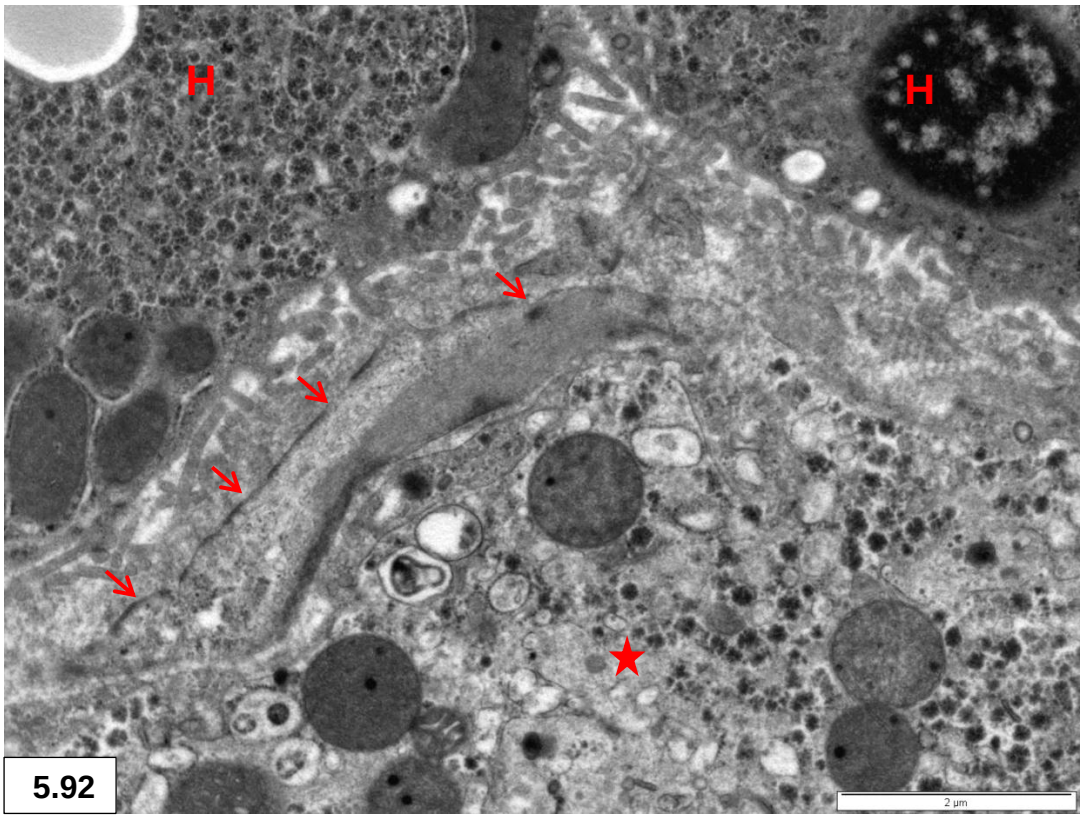

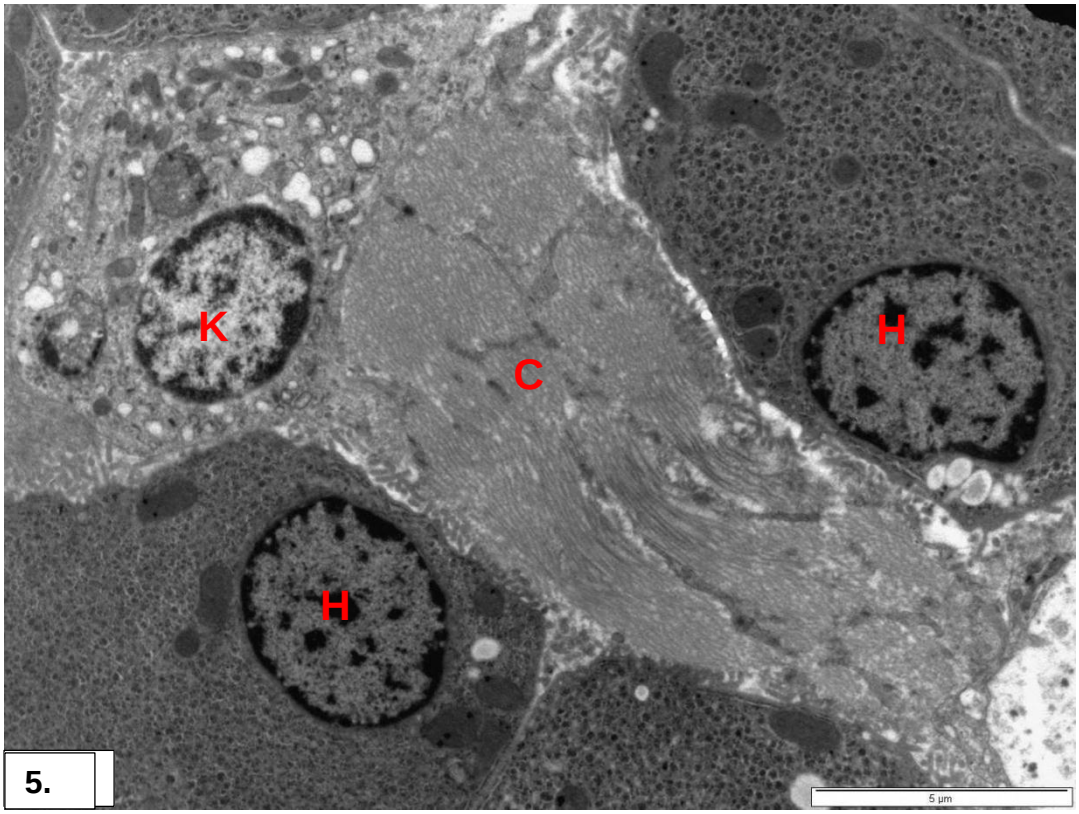

Figure 5.93: Isthmus - collagen trabecula (**C**)between hepatocytes (**H**). Kupffer cell (**K**).

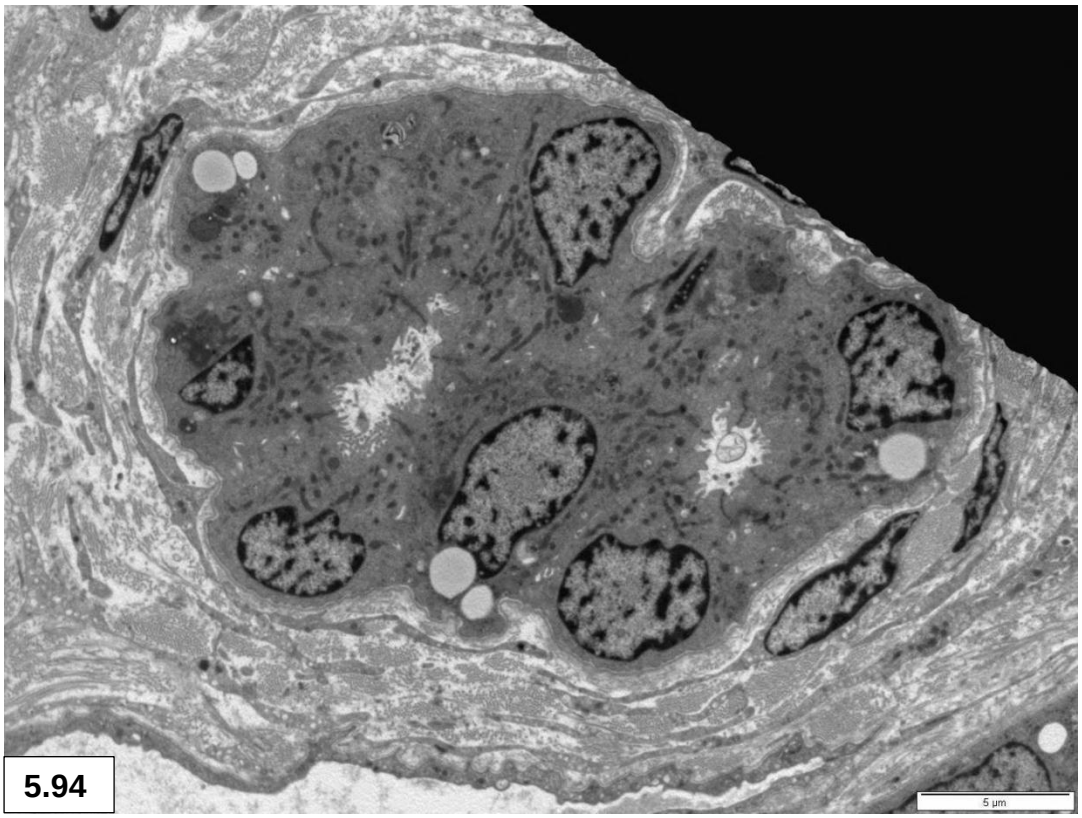

Figure 5.94: Bile duct surrounded by collagenous stroma in the isthmus.